

# Development of an acute excitotoxic model of Huntington's disease in sheep

---

Adam O'Connell

Preclinical, Imaging and Research Laboratories (PIRL), SAHMRI  
Hopwood Centre for Neurobiology, Lifelong Health Theme, SAHMRI  
School of Medical Specialties, University of Adelaide

Thesis submitted for the degree of Doctor of Philosophy  
January 2020

# Declaration

---

I certify that this work contains no material which has been accepted for the award of any other degree or diploma in my name, in any university or other tertiary institution and, to the best of my knowledge and belief, contains no material previously published or written by another person, except where due reference has been made in the text. In addition, I certify that no part of this work will, in the future, be used in a submission in my name, for any other degree or diploma in any university or other tertiary institution without the prior approval of the University of Adelaide and where applicable, any partner institution responsible for the joint-award of this degree.

I acknowledge that copyright of published works contained within this thesis resides with the copyright holder(s) of those works.

I also give permission for the digital version of my thesis to be made available on the web, via the University's digital research repository, the Library Search and also through web search engines, unless permission has been granted by the University to restrict access for a period of time.

I acknowledge the support I have received for my research through the provision of an Australian Government Research Training Program Scholarship.

---

Adam O'Connell

21/01/2020  
Date

*This thesis is dedicated to Dr. Timothy Rex Kuchel AM  
07/06/1951 – 14/12/2019*

# Acknowledgements

---

I would like to acknowledge the following people for their assistance, advice and support during the candidature: My supervisors, Jenny Morton, Kim Hemsley and Cara Fraser who have been exceptionally generous with their time and knowledge and to whom I am incredibly grateful for their involvement: All of the staff at SAHMRI, Gilles Plains where I was very lucky to be based during the candidature, especially Shamika Moore, Raj Perumal, Paul Herde, Robb Muirhead, Loren Matthews, Kevin Neumann, Dan Johns, Chris Seidel, Marianne Keller and Charne Rossouw: Everyone else who contributed during the candidature, including Neil Dear, Jim Manavis and the AHMS histology team, John Finnie, Helen Beard, Daniel Neumann, Vicky Sherwood, Ali Nichols, Paul Trim, Marten Snel, Suzanne Edwards and Tony Blackheart Brown (who did not sabotage the study or stab me in the back, as would be expected, and may even have contributed something useful).

A big thank-you to friends and family who were essential in helping me finish the thesis, especially my magnificent wife, Caroline, who continued to work, look after our kids and keep the household going. I would also like to thank Team Buttercup, Bebop and Rocksteady, you rock my socks.

Apologies to anyone else who contributed and did not get a mention above, it is completely unintentional and your help was very appreciated. I would like to gratefully acknowledge the support of the Rotary Club of Adelaide who provided funding, SAHMRI, Gilles Plains and the National Imaging Facility (NIF, an NCRIS capability) located at SAHMRI, Gilles Plains for in-kind contribution of facilities, consumables, scientific and technical assistance and Adelaide Medical School for a travel award.

Finally, I would like to thank Tim Kuchel who convinced me to undertake the candidature and provided boundless support, advice, opportunity to get side-tracked and infectious enthusiasm. A fellow veterinarian, role model and friend, he was in every sense of the word, my mentor. Thanks Tim, this thesis is dedicated to you.

# Contents

---

<b>Declaration</b>	<b>i</b>
<b>Acknowledgements</b>	<b>iii</b>
<b>Contents</b>	<b>iv</b>
<b>Abstract</b>	<b>vi</b>
<b>Abbreviations</b>	<b>viii</b>
<b>1 Introduction</b>	<b>1</b>
1.1 Background	1
1.2 The striatum	3
1.3 Neuropathology of Huntington's disease	10
1.4 Animal models of Huntington's disease	16
1.5 Phenotype testing in sheep models of disease	25
1.6 Research significance, hypothesis and aims	32
<b>2 Methods</b>	<b>34</b>
2.1 Ethics statement	34
2.2 Animals	34
2.3 Experimental regime	34
2.4 Surgical procedure	37
2.5 Magnetic resonance methodology	39
2.6 Neurological examination procedure	42
2.7 Rotation studies	44
2.8 Two-choice discrimination learning	46
2.9 Histology	49
<b>3 Surgery and neurological examination</b>	<b>52</b>
<b>4 Rotation and discrimination</b>	<b>74</b>
<b>5 Magnetic resonance studies</b>	<b>90</b>
<b>6 Summary</b>	<b>105</b>
6.1 Association between pathology and phenotype	106
6.2 Comparison with large animal quinolinic acid models	108
6.3 Study limitations	111
6.3 Future directions	112
6.4 Conclusion	113

<b>7</b>	<b>Appendix A: Method development</b>	<b>115</b>
<b>8</b>	<b>Appendix B: Activity monitoring</b>	<b>117</b>
<b>9</b>	<b>Appendix C: Cerebrospinal fluid analysis</b>	<b>118</b>
<b>10</b>	<b>References</b>	<b>120</b>

# Abstract

---

Huntington's disease (HD) is an autosomal dominant neurodegenerative disorder. The earliest and most severe neuropathological change in HD occurs within the striatum. Exogenous excitotoxic lesioning of the rodent and non-human primate (NHP) striatum is used to model HD. Apart from NHPs, no other excitotoxic large animal model of HD has been established. Sheep have the potential to be an important species for modelling neurodegenerative disease, primarily because of neuroanatomical similarities between the sheep and human brain. This thesis describes the development of an excitotoxic sheep model of HD using the excitotoxin, quinolinic acid (QA). QA is an N-methyl-D-aspartate (NMDA) glutamate receptor agonist that produces pathological changes within the striatum that resemble those seen in HD.

Sixteen castrated-male, 18 month old, Merino-Border Leicester cross sheep underwent two surgical procedures, four weeks apart, to infuse 75  $\mu$ l of 180 mM QA (experimental group) or 75  $\mu$ l of saline (control group) into the left (first surgery) and then the right (second surgery) caudate nucleus of the striatum. Longitudinal magnetic resonance imaging (MRI), magnetic resonance spectroscopy (MRS) and diffusion tensor imaging (DTI) of the brains of the sheep was performed on a 3-Tesla scanner pre-surgically, one week after the first surgery, five weeks after the first surgery and sixteen weeks after the first surgery to investigate the neuropathological changes that occur *in vivo* after QA lesioning of the sheep striatum. The phenotypic consequences of lesioning the sheep striatum with QA were investigated using a veterinary neurological examination, dopamine agonist induced rotation and a two-choice discrimination task. The author / investigator was blind to the treatment group.

MRI revealed QA-lesion hyperintensity and dilation of the lateral ventricles, consistent with atrophy of the caudate nucleus. MRS and DTI revealed a significant decrease in the neuronal marker N-acetylaspartate (NAA), and in fractional anisotropy (FA) in the acutely-lesioned (one week after

surgery) striatae of the QA-lesioned sheep, followed by recovery in NAA and a significant increase in FA in the chronic (five to sixteen weeks) QA-lesioned striatae. NAA and FA changes are consistent with neuronal loss and structural disruption in the acute lesion, followed by recovery of reversibly impaired neurons, structural reorganisation and gliosis in the chronic lesion. Heterogeneous neuronal loss and damage and gliosis were visible on histological analysis of the QA-lesioned sheep striatae, supporting the *in vivo* MRS and DTI detected changes.

Neurological examination of the sheep revealed evidence of laterality and mild hind limb motor paresis in seven out of eight of the QA-lesioned sheep, however the examination was not informative of lesion characteristics. A directional bias was evident in the QA-lesioned sheep during rotation studies. However, the direction and magnitude of bias in individual sheep at any one timepoint varied markedly, making identification of QA-lesioned individuals difficult. There was no difference between the QA-lesioned and saline-treated sheep in performance of the acquisition and reversal phases of the two-choice discrimination task. The behavioural studies described in this thesis were not suitable for comprehensive identification and characterisation of QA lesions in the striatum of sheep.

This is the first description of the development of an acute excitotoxic sheep model of HD. The experiments demonstrate that longitudinal analysis of the neuropathological changes in the QA-lesioned sheep striatum is possible using advanced magnetic resonance modalities performed on a clinically relevant 3-Tesla scanner and that neuropathological changes are consistent with HD-like pathology in other species. Furthermore, phenotypic investigation of the QA-lesioned sheep is possible, however more refined methods than those described need to be utilised. The excitotoxic sheep model of HD is clinically relevant HD model with potential for use in disease mechanism and therapy investigations.



# Abbreviations

---

Only abbreviations that appear more than once and within the body of the text are shown.

Abbreviations within figures or tables are explained in the corresponding legends.

3-NP	3-nitropropionic acid
CAG	cytosine-adenine-guanine
CSF	cerebrospinal fluid
CED	convection-enhanced delivery
D1	dopamine receptor D1
D2	dopamine receptor D2
DTI	diffusor tensor imaging
EEG	electroencephalography
FA	fractional anisotropy
GABA	gamma-aminobutyric acid
GFAP	glial fibrillary acidic protein
Gln	glutamine
Glu	glutamate
HD	Huntington's disease
<i>HTT</i>	Huntingtin gene
HTT	Huntingtin protein
Iba1	ionised calcium binding adaptor molecule 1
Ins	myo-inositol
mHTT	mutant Huntingtin protein
MR	magnetic resonance
MRI	magnetic resonance imaging
MRS	magnetic resonance spectroscopy
MSN / MSNs	medium spiny neuron(s)
NAA	<i>N</i> -acetylaspartate
NADPH	nicotinamide adenine dinucleotide phosphate
NDS	normal donkey serum
NHP / NHPs	non-human primate(s)

PBS	phosphate buffered saline
PD	Parkinson's disease
QA	quinolinic acid
S+	positively associated novel stimuli
S-	negatively associated novel stimuli
T1-MPRAGE	T1-weighted, magnetisation-prepared, rapid gradient-echo
TE	echo time
TNAA	<i>N</i> -acetylaspartate and <i>N</i> -acetylaspartylglutamate
TR	repetition time

# 1 Introduction

---

## 1.1 Background

Huntington's disease (HD) is an autosomal dominant neurodegenerative disorder caused by a polymorphic trinucleotide repeat within the Huntingtin gene (*HTT*) gene that codes for the Huntingtin protein (HTT). The disease causing gene has an abnormally long cytosine-adenine-guanine repeat (CAG)<sub>n</sub> encoding a polyglutamine tract near the N-terminus of the HTT protein, termed mutant huntingtin protein (mHTT; MacDonald et al. 1993). The CAG repeat is unstable during DNA replication and shows genetic anticipation (Zuhlke et al. 1993, Wheeler et al. 2007, Neto et al. 2017). The length of the repeat correlates inversely with age of onset, with longer CAG repeats predisposing individuals to an earlier age of onset (Wexler et al. 2004, Lee et al. 2012, Lee et al. 2015a). HD is always fatal, with an average of ten to twenty years from onset of clinical symptoms until death (Roos 2010).

HD has a prodromal phase of up to fifteen years before clinical diagnosis. The prodromal phase is characterized by subtle motor, cognitive and behavioural changes (Stout et al. 2011, Mason and Barker 2015). HD was previously known as Huntington's chorea due to the presence of an often dramatic chorea, a form of dyskinesia that results in irregular, involuntary movements (Bhattacharyya 2016). However, the symptomatic profile of patients is variable, with a broad range of intellectual, emotional, behavioural and physical changes, including (but not limited to) involuntary movements, speech and swallowing difficulties, reduced mental concentration, difficulty learning or planning, deteriorating ability to communicate, apathy, anxiety, irritability and depression (Ha and Fung 2012, Ghosh and Tabrizi 2018). Currently, there is no cure or disease-modifying therapy available for HD, only symptomatic treatment (Brett et al. 2014, Kumar et al. 2015, McColgan and Tabrizi 2018).

HD primarily leads to degeneration of the striatum, although a wide range of central nervous system and peripheral tissues are affected (Marques and Humbert 2013, Bates et al. 2015, Rub et al. 2016). Because the striatum is the first region to degenerate in HD, HD research has greatly benefited our knowledge of the functional anatomy and pathology of this structure. Most pre-clinical studies on HD and other neurodegenerative diseases utilise rodent models (Dawson et al. 2018, Fisher and Bannerman 2019). Our knowledge of the striatum in other species is limited, and often relies on extrapolation of knowledge from rodent studies.

The sheep has been proposed as a suitable animal model for HD therapeutic research in a translational capacity between rodent HD models and clinical trials (Morton and Howland 2013). A transgenic sheep model of HD exists (Jacobsen et al. 2010), however it has not developed the full spectrum of neuropathology associated with HD (Morton 2018), a problem that also occurs with transgenic rodent models (Yan et al. 2019). Because of the limited neuropathology that develops in transgenic HD models, excitotoxic lesioning of the striatum is frequently used in HD research to recreate the spectrum of striatal neuropathology associated with HD (Cui et al. 2018, Foucault-Fruchard et al. 2018, Sánchez et al. 2018, Sumathi et al. 2018, Verma et al. 2018, Emerich et al. 2019, Lavisse et al. 2019).

Excitotoxins are conformationally restricted analogues of the excitatory amino acid neurotransmitter, glutamate (Schliebs et al. 1996). Very recently, a non-human primate (NHP) excitotoxic HD model was developed for use in a translational capacity between rodent excitotoxic models and clinical trials (Lavisse, Williams et al. 2019), an indication of the continued relevance of the model. Aside from NHP models (for examples see: Burns et al. 1995, Kendall et al. 2000, Roitberg et al. 2002), no large animal excitotoxic model of HD has been developed.

This study aimed, for the first time, to lesion the striatum of sheep with the excitotoxin quinolinic acid (QA) and examine the QA-lesioned sheep for a phenotype. Magnetic resonance studies were used to investigate the resultant pathology *in vivo*. An excitotoxic sheep model could be used to

validate, in a large-brained animal, results from pre-clinical trials that utilise rodent excitotoxic models. It would also complement the transgenic sheep HD model, improve our knowledge of the role of the striatum in sheep and provide evidence for the suitability of sheep as a model of neurodegenerative disease.

## 1.2 The striatum

Placing an excitotoxic lesion directly within the sheep striatum and understanding the consequences and relationship to HD, requires knowledge of the normal striatum. The striatum is part a group of interconnected subcortical nuclei that form the basal ganglia (Lanciego et al. 2012). Traditionally the striatum was considered to be involved solely in control of motor function (Dudman and Krakauer 2016), a view that arose because of the prominent motor symptoms of basal ganglia disorders like HD (Bates et al. 2015) and Parkinson's disease (PD; Kalia and Lang 2015). Over time, our knowledge of the role of the striatum has been expanded to recognize the striatum's importance in assimilating cognitive, emotive and motor input and monitoring and refining pre-selected actions, therefore having an important role in a diverse range of functions including planning, motivation, action-selection, skill learning, habit formation, reward and modulation of motor behaviour (Burton et al. 2015, Graybiel and Grafton 2015, Provost et al. 2015, Knowlton and Patterson 2018, Le Heron et al. 2018, Robbe 2018). The striatum has an outwardly homogenous appearance that belies a complicated circuitry, which has made determining and understanding its many functions difficult (Benarroch 2016, Yin 2016, Gahm and Shi 2017).

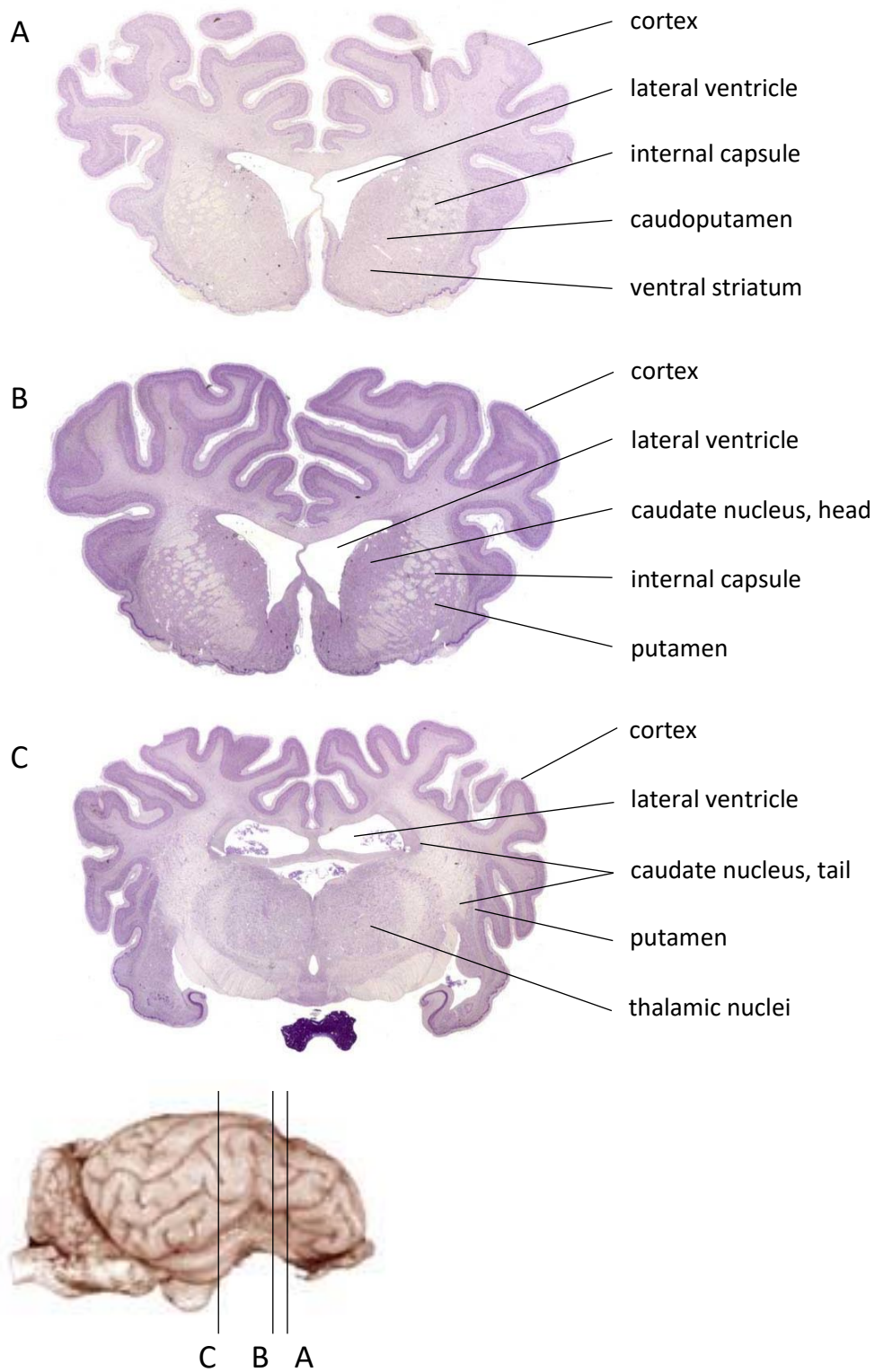
### 1.2.1 The gross anatomy of the striatum

No study has been published that comprehensively compares the gross anatomy of the rodent, primate and sheep striatum. However, the gross anatomy, cellular morphology and neurochemical expression of one region of the ovine basal ganglia that is closely connected to the striatum, the substantia nigra, has been demonstrated to be very similar to the human brain (Murray et al. 2019). Furthermore, the sheep and primate (including human) striatum is comprised of two distinctly

separate structures, the caudate nucleus and putamen, unlike in rodents (Lanciego and Vázquez 2012, Ella et al. 2017, Dong 2019, Johnson et al. 2019, Sudheimer et al. 2019). Articles outlining major differences between the rodent brain and the large animal brain, as well as the anatomical similarities of the primate (including human), sheep and pig brain are available (Morton and Howland 2013, John et al. 2017, McBride and Morton 2018, Morton 2018, Vink 2018, Murray et al. 2019), with the similarity between the human and sheep brain being important for the development of an excitotoxic sheep model of HD. Major similarities and differences are outlined in Sections 1.4.1 and 1.4.2.

The striatum is traditionally divided into two regions, the dorsal and the ventral striatum (Burke et al. 2017). The dorsal striatum is typically referred to as the striatum (corpus striatum or neostriatum; Snell 2010). The dorsal striatum, referred to hereafter as the striatum, is comprised of two sub-cortical nuclei within the basal ganglia of the telencephalon; 1) the caudate nucleus and 2) the putamen (see Fig. 1.1).

In primates (including humans) and sheep, the caudate nucleus is an elongated comma-shaped structure sitting dorsomedial to the larger, ovoid-shaped putamen (Lanciego and Vázquez 2012, Roshchupkin et al. 2016, Ella et al. 2017, Sudheimer et al. 2019). The caudate nucleus has a large head that extends ventrally and progressively narrows in an elongated posterior direction until only a thin tail remains, again extending ventrally (Snell 2010, Johns 2014). The putamen forms a concave ovoid shape intimately and medially bordered by the pallidum (internal and external globus pallidus; Ella et al. 2017, Tang et al. 2018b). The caudate nucleus sits directly beneath the lateral ventricle such that it forms the floor of the lateral ventricle (Snell 2010, Tang et al. 2018a). In effect the putamen sits within the crook of the caudate nucleus, the two structures being separated, in primates (Lanciego and Vázquez 2012, Sudheimer et al. 2019) and sheep (Ella et al. 2017), by a thick band of white matter that forms part of the internal capsule (Gerfen and Bolam 2016). Multiple thin bridges of grey matter, called caudolenticular grey bridges, link the caudate nucleus and putamen.



**Figure 1.1 Selected coronal sections of the sheep brain** showing the gross anatomical features of the striatum at three locations; A) the ventral striatum, B) the head of the caudate nucleus and C) the tail of the caudate nucleus (Johnson et al. 2019).

Whilst the caudate nucleus and putamen are two separate structures, functionally they are considered to be a single unit divided by the internal capsule (Gerfen 1992, Shipp 2016). In rodents, the caudate nucleus and putamen are not distinguishable and are commonly referred to as the caudoputamen (Swanson 2018), a key anatomical difference between rodents and humans. The ventral striatum sits below the striatum and comprises the nucleus accumbens and olfactory tubercle (Burke et al. 2017).

### 1.2.2 The functional anatomy of the striatum

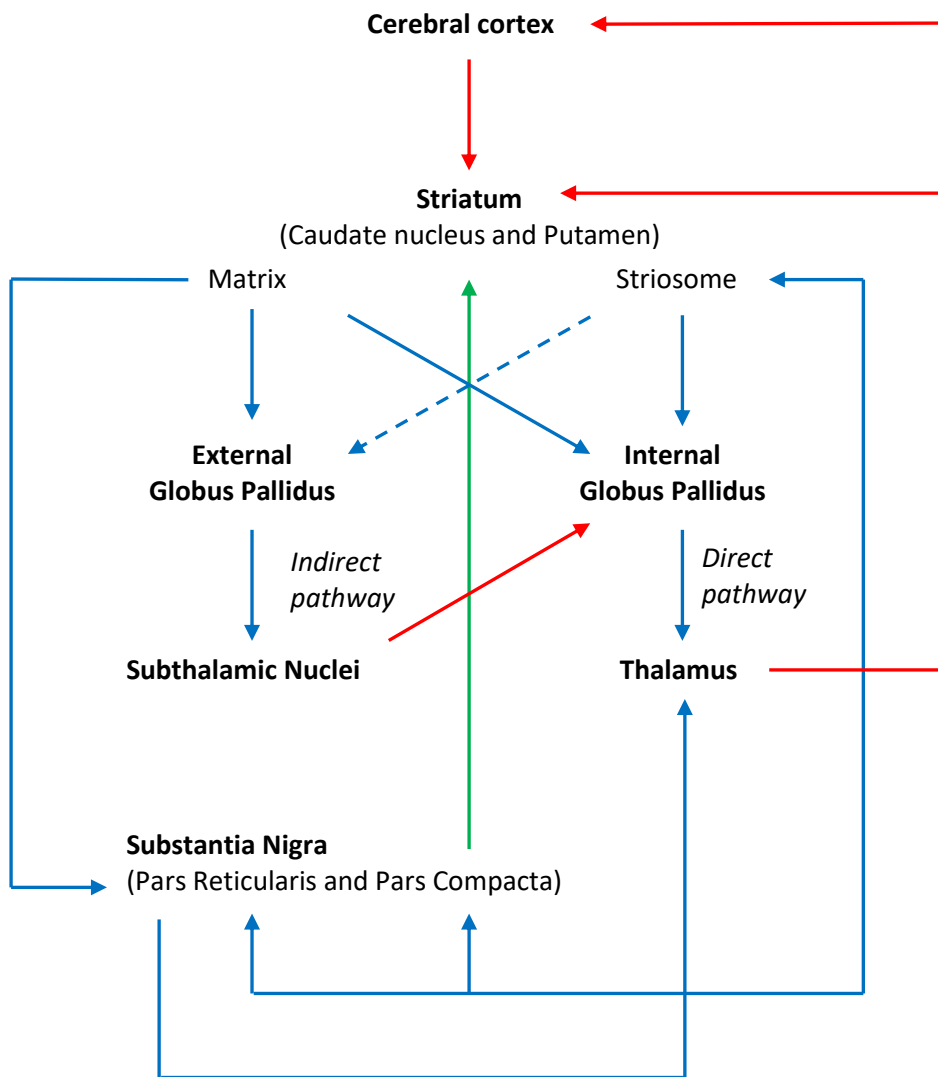
The striatum integrates inputs from, and projects to, many brain regions (Lanciego et al. 2012). In this section of the introduction, an overview of the functional anatomy is given, however it focuses on areas important to QA and HD (QA creates changes within the striatum that resemble HD, discussed in Section 1.4.4) to maintain relevance. The striatum is the primary afferent structure of the basal ganglia (Gerfen 1984, Donoghue and Herkenham 1986, Guo et al. 2015). The striatum receives excitatory inputs from all regions of the cortex, ventral tegmental area and substantia nigra pars compacta and projects inhibitory inputs to the rest of the basal ganglia (Lanciego et al. 2012, Ogawa et al. 2018). Afferent striatal inputs from the cortex can be topographically mapped prescribing a regionality to the striatum, with the caudate nucleus associated with cognitive inputs and the putamen with motor control (Adler et al. 2013, Haber 2016). Because the caudate nucleus is associated with cognition, a two-choice discrimination task was established (see Chapter 4) to determine whether cognitive decline is identifiable in the QA-lesioned sheep.

The striatum consists primarily of inhibitory gamma-aminobutyric acid (GABA) producing (Gonzales et al. 2013) medium sized spiny projection neurons (MSNs; Kita and Kitai 1988, Matamales et al. 2009). The MSNs can be further subdivided by receptor and neuropeptide expression such that two major subtypes of MSN exist (Grillner and Robertson 2016). The two major subtypes of MSN are defined by whether they contain D1 or D2 dopamine receptors (Perez et al. 2017, Yapo et al. 2017), and substance P and enkephalin neuropeptides, respectively (Gerfen et al. 1990, Cazorla et al. 2015).



Within the striatum is a small heterogeneous population of aspiny interneurons that form functional networks with, and modulate, MSN activity (Abudukeyoumu et al. 2018, Aldrin-Kirk et al. 2018, Tepper et al. 2018). The exact proportion of MSNs and interneurons within the striatum vary between species (Graveland and DiFiglia 1985, Wu and Parent 2000). The majority of these interneurons are GABAergic and the different populations can be differentiated by the calcium-binding proteins, parvalbumin and calretinin (Prensa et al. 1998, Wu and Parent 2000, Garas et al. 2018). As well as the GABAergic interneurons, there are also large cholinergic interneurons (Klug et al. 2018) and interneurons that contain neuropeptide Y, somatostatin, nitric oxide synthase and nicotinamide adenine dinucleotide phosphate (NADPH) diaphorase (Waldvogel et al. 2015).

Originating in the striatum and continuing throughout the basal ganglia are two structurally and functionally connected pathways, known as the indirect and direct pathways (Fig. 1.2; Cui et al. 2013, Calabresi et al. 2014, Nonomura et al. 2018, Tinterri et al. 2018). The direct and indirect pathways are simultaneously activated GABAergic MSN inhibitory pathways (Cui et al. 2013), however the direct pathway is functionally facilitatory in nature and the indirect pathway is functionally inhibitory (Lanciego et al. 2012, Nelson and Kreitzer 2014, Bahuguna et al. 2018). The direct pathway is mainly comprised of D1, substance P-expressing MSNs, while the indirect pathway is mainly comprised of D2, enkephalin-expressing MSNs (Albin et al. 1989, Alexander and Crutcher 1990, Smith et al. 1998).



**Figure 1.2 Classic projection neuron pathways within the basal ganglia** (with thalamus and cerebral cortex). Excitatory pathways in red, inhibitory pathways in blue, dopamine pathway in green.

Thalamus activation facilitates movement. Indirect pathway activation is associated with increased inhibition of the thalamus therefore inhibiting movement, direct pathway activation is associated with a reduced inhibition of the thalamus therefore facilitating movement.

As well as direct and indirect pathway organization, the striatum also has a histochemically distinct striosome and matrix compartmental organization based on differential immunoreactivity and protein expression (Olson et al. 1972, Pert et al. 1976, Graybiel and Ragsdale 1978, Graybiel et al. 1981, Herkenham and Pert 1981, Gerfen 1984, Gerfen et al. 1985). Striosomes form a labyrinth or patchwork like structure within the surrounding matrix (Brimblecombe and Cragg 2017). The output projections of the striosome and matrix differ and the pathway specificity of striosome and matrix projections may vary between species (Gerfen 1984, Levesque and Parent 2005, Watabe-Uchida et al. 2012, Crittenden et al. 2016, Reiner and Deng 2018, Fujiyama et al. 2019).

Sensory cortical and limbic structures have also been shown to preferentially target direct pathway neurons and striosomes, while the motor cortex preferentially targets indirect pathway neurons and the matrix (Kincaid and Wilson 1996, Crittenden and Graybiel 2011, Wall et al. 2013). The striatum can be further arranged into a large number of functional and structural subdivisions, functionally connected to cerebrocortical functional networks (Ogawa et al. 2018). The regions and functional subdivisions within the striatum do not form exclusive boundaries, with substantial overlapping of the inputs and divisions associated with the integrative role of the basal ganglia (Mailly et al. 2013, Florio et al. 2018).

### 1.2.3 The role of the wild-type huntingtin protein

HTT is expressed throughout the nervous system and many tissues of the body (Li et al. 1993, Strong et al. 1993, Carroll et al. 2015). Even though there is almost ubiquitous expression of HTT, the specific functions of the protein are still not fully known (Liu and Zeitlin 2017, Selvaraj et al. 2020). HTT has been implicated in multiple processes, including; vesicle transport (Colin et al. 2008, Zala et al. 2013), ciliogenesis regulation (Keryer et al. 2011), endocytosis (Waelter et al. 2001), autophagy (Martin et al. 2015), steroidogenesis (Selvaraj et al. 2020) and transcription regulation (Valor 2015). HTT expression is present early in embryonic development, and disruption of the *HTT* gene is lethal if it occurs early enough in embryonic development (Nasir et al. 1995, Zeitlin et al. 1995). The importance

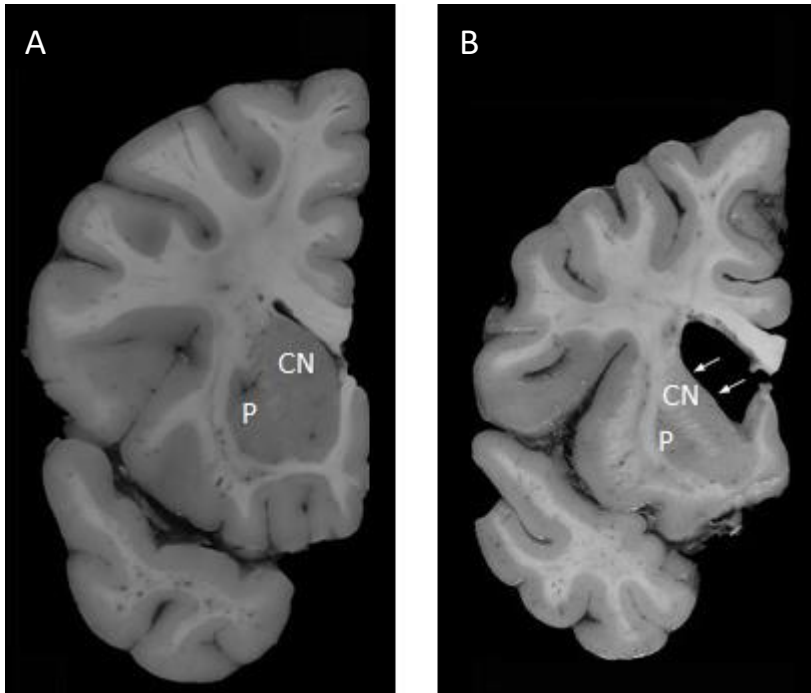
of HTT in the adult is less clear. Disruption of HTT in the nervous system of adults may lead to selective neurodegeneration, with the striatum being particularly vulnerable (Dragatsis et al. 2000), however it has also been shown that neurodegeneration does not occur in adult mice for at least seven months after inactivation of HTT (Wang et al. 2016, Liu and Zeitlin 2017).

### 1.3 Neuropathology of Huntington's disease

The pathophysiology of HD is complex and affects many areas of the brain and body outside of the striatum. In this section, an overview of HD neuropathology is given with a focus on striatal neuropathology that is relevant to a QA model of HD.

HD is caused by an abnormal HTT protein, mHTT. HD results in widespread atrophy of the brain with reduced brain volume, cortical thinning and ventricular enlargement (de la Monte et al. 1988, Mason et al. 2018, Nanetti et al. 2018, Wijeratne et al. 2018). Particular regions of the brain affected in HD include the cerebral cortex, striatum, pallidum, thalamus, brainstem and cerebellum (Rub et al. 2016).

The earliest and most severe neuropathological changes in HD occur within the striatum (Vonsattel et al. 1985). Striatal neuronal loss and reactive gliosis follow a topographic distribution and ordered pattern, with the earliest recognisable changes occurring caudo-dorsally (primarily in the tail of the caudate nucleus and dorsal putamen) before progressively becoming more diffuse throughout the striatum. Severe atrophy of the striatum with concomitant concavity of the ventricular border and enlargement of the ventricle, eventually occurs due to significant neuronal loss (Fig. 1.3; Vonsattel et al. 1985, Waldvogel et al. 2015, Rub et al. 2016). Atrophy is visible in the caudate nucleus before the putamen (Reiner et al. 2011), which influenced the decision to target the caudate nucleus of the sheep with QA in an attempt to replicate early HD neurodegeneration.



**Figure 1.3 Gross striatal pathology in the brain of a human with Huntington's disease.** Coronal sections at the level of the striatum of A) a 35 year old male brain without Huntington's disease, and B) a grade 3/4 Huntington's disease case. Arrows in (B) indicate severe atrophy of the striatum in the Huntington's disease case. The lateral ventricle, which is the space the arrows have been drawn in, is visibly dilated due to the striatal atrophy. There is also atrophy of the cortex. CN = caudate nucleus, P = putamen. Image edited from Figure 2 of the *Neuropathology of Huntington's disease* (2015) (Waldvogel et al. 2015).

Atrophy of the striatum with concomitant lateral ventricle enlargement, evidence of corticostriatal projection neuron degeneration and evidence of other brain pathology is detectable in HD patients up to ten years before the onset of clinically observable symptoms (Tabrizi et al. 2013). The integrative role of the striatum with extensive motor, sensory, emotive and cognitive inputs suggests that pathology of this structure will have a broad clinical symptomology (Florio et al. 2018). As the disease progresses, a heterogeneous pattern of neurodegeneration eventually occurs throughout the basal ganglia and cerebral cortex. The heterogeneous neurodegeneration results in the variable symptomology of HD (Waldvogel et al. 2012a, Waldvogel et al. 2012b, Nana et al. 2014). For example, HD patients with significant striosome loss and preservation of the matrix showed predominantly mood symptoms, while HD patients with primarily matrix loss have a predominance of motor abnormalities (Tippett et al. 2007, Thu et al. 2010).

In HD, widespread pathology eventually occurs in both neural and non-neural tissues (van der Burg et al. 2009, Mielcarek 2015, Rub et al. 2016). The pathological change in non-neural tissues is possibly due to a direct effect of mHTT expression in the tissue affected, as well as an indirect effect of neurodegeneration (van der Burg et al. 2009). The majority of HD patients die of pneumonia, possibly due to dysphagia-associated aspiration (Heemskerk and Roos 2012). Other prominent causes of death include infection, heart failure or suicide (Heemskerk and Roos 2010, Heemskerk and Roos 2012, Rodrigues et al. 2017).

### 1.3.1 The role of the mutant-huntingtin protein in neuron cell death

The relationship between mHTT and clinical disease is not yet understood. The CAG repeat causes a polyglutamine expansion that results in instability and misfolding of mHTT (MacDonald et al. 1993, Labbadia and Morimoto 2013). The misfolded protein forms characteristic aggregates and nuclear inclusions (Davies et al. 1997, DiFiglia et al. 1997). The role of the aggregates in the mechanism of disease is not fully appreciated (Waldvogel et al. 2015, Sahoo et al. 2016) though compromising the ability to clear aggregated proteins in a mouse model of HD was a pathogenic driver (Fox et al. 2019).

Even though a single mutant gene causes HD, the aetiology is complex (Bates et al. 2015). The *HTT* gene interacts with many other genes (Hodges et al. 2006, Dong and Cong 2018) resulting in dysfunction in multiple cellular processes (Waldvogel et al. 2015, Patassini et al. 2016), including; transcriptional dysregulation (Sharma and Taliyan 2015, Le Gras et al. 2017, Joag et al. 2019), axonal transport alterations (Reddy and Shirendeb 2012, Zhao et al. 2016), intracellular signalling defects (Trager et al. 2014), deregulation of the proteasome pathway (Liebelt and Vertegaal 2016, Lin et al. 2016), autophagy (Ashkenazi et al. 2017), loss of calcium homeostasis and excitotoxicity (Bezprozvanny 2007, Glaser et al. 2018), alteration in brain cholesterol homeostasis (Di Pardo et al. 2019) and mitochondrial dysfunction with resultant oxidative stress (Di Cristo et al. 2018). The expression of mHTT leads to disruption of central pathways of energy metabolism including glycolysis, the polyol-pathway, the tricarboxylic acid (TCA) cycle, and the urea cycle (Patassini et al. 2019). Cellular process dysfunction, and possibly loss of wild-type HTT function (Mehler et al. 2019), lead to early changes in corticostriatal connectivity and eventually widespread degeneration.

The predilection of mHTT to cause its most significant deleterious effects within the striatum and cortex is not consistent with the ubiquitous expression of HTT (Marques and Humbert 2013). The reason for the susceptibility of neurons within the striatum and cortex to mHTT is unknown (Morigaki and Goto 2017). Molecular complexity, metabolic rate, loss of wild-type HTT function and blood-brain barrier permeability are all possible factors (Li et al. 1993, Strong et al. 1993, Francelle et al. 2014, Mehler et al. 2019). The regions of the brain susceptible to mHTT are also susceptible to the neurotoxic effects of QA, which has been implicated in HD pathophysiology (see Section 1.4.4; Schwarcz et al. 2010, Rub et al. 2016). Furthermore, contradictory evidence has shown mHTT to both be toxic and protective to cell function (Davies et al. 1997, Saudou et al. 1998, Miller et al. 2010). The significance of the loss of wild-type HTT function versus a disruptive or toxic gain of function of the mHTT protein to the development of HD is still being debated (O'Kusky et al. 1999, Dragatsis et al. 2000, Saudou and Humbert 2016).

### 1.3.2 Cellular changes within the striatum in Huntington's disease

A heterogeneous pattern of neuron loss develops in the striatum during HD. The D2, enkephalin-expressing MSNs of the striatum associated with the indirect pathway appear to degenerate first in the disease, such that the characteristic chorea is possibly a symptom of indirect pathway dysfunction since this pathway normally has an inhibitory effect on movement (Reiner et al. 1988, Deng et al. 2004). Both enkephalin and substance P containing GABAergic MSNs (Marshall et al. 1983) and interneurons containing parvalbumin and choline acetyltransferase are eventually lost from the striatum as HD progresses (Cicchetti and Parent 1996, Reiner et al. 2013), while the interneurons containing somatostatin, neuropeptide Y, NADPH diaphorase, nitric oxide synthase and the medium sized GABAergic calretinin interneurons are relatively spared (Cicchetti et al. 2000, Waldvogel et al. 2015). The large, calretinin-expressing cholinergic interneurons are preserved until later stages of HD (Ferrante et al. 1987, Kowall et al. 1987). Table 1.1 summarises the major neuron populations within the striatum and their vulnerability during HD. Gliosis occurs within the striatum, especially the caudate nucleus, from early in HD, with an increase in oligodendrocytes, astrocytes and microglial (Waldvogel et al. 2015). The cellular changes, along with the gross pathological change of striatal atrophy and concomitant lateral ventricle dilation described earlier in Section 1.3, can be replicated in the striatum using QA, as discussed in Section 1.4.4.



**Table 1.1 Major neuron populations in the striatum and their vulnerability to Huntington's disease**

<b>Neuron Type</b>	<b>Transmitter</b>	<b>Major location - Major projection</b>	<b>Differentiating receptors and neuropeptides</b>	<b>Vulnerability</b>
Medium sized spiny neuron (MSN, projection)	GABA	Matrix - GPe (Indirect pathway)	Dopamine 2 Enkephalin Calbindin (Matrix)	Lost Earliest
Medium sized spiny neuron (MSN, projection)	GABA	Matrix - GPi Matrix - SNr Striosome - SNc (Direct pathway)	Dopamine 1 Substance P Calbindin (Matrix)	Lost Early
Medium sized aspiny neuron (interneuron)	GABA	Matrix - Local	Parvalbumin	Lost Later
Medium sized aspiny neuron (interneuron)	GABA	Matrix - Local	Calretinin	Spared
Medium sized aspiny neuron (interneuron)	GABA	All - Local	Neuropeptide Y Somatostatin NADPH diaphorase Nitric oxide synthase Tyrosine Hydroxylase	Spared
Large sized aspiny cholinergic neuron (interneuron)	ACh	Matrix - Local	Calretinin Substance P	Lost Late

GABA: gamma-aminobutyric acid, Ach: acetylcholine, GPe: external globus pallidus GPi: internal globus pallidus, SNr: substantia nigra pars reticularis, SNc: substantia nigra pars compacta. (Waldvogel et al. 2015)

## 1.4 Animal models of Huntington's disease

This section provides context for why the development of acute, excitotoxic sheep model of HD is important. First, the disadvantages of rodent models and the advantages of large animal models of neurodegenerative disease are discussed. An appreciation of the benefits of a sheep model of HD, compared to NHP models, is also provided. It is important to understand that large animal models can complement rodent models by addressing the disadvantage of rodent models, however large animal models are not envisioned as a replacement for rodent based research. An overview of the limitations of genetic models of HD is also provided in this section to provide context for the relevance of excitotoxic models. Finally, excitotoxic models of HD are discussed, with a focus on the use of QA.

### 1.4.1 The disadvantages of rodent models of neurodegenerative disease

The convenience, low cost and ethical advantages of using a lower order species mean that small animals, particularly rodents, are the first choice model for preclinical studies. Compared to humans, however, there are inherent properties of rodents which need to be carefully considered when drawing conclusions from any rodent HD study, including; the short life span, small brain volume, neuroanatomically dissimilar brain, differences in drug metabolism and the blood-brain barrier, genomic differences and disparate behavioural responses (Morton and Howland 2013, Howland and Munoz-Sanjuan 2014).

The short life span of a mouse does not preclude it from reflecting the progression of a human disease that typically manifests in middle age and has a prolonged duration from diagnosis (average 15 to 20 years; Roos 2010) as life span is relative (Dutta and Sengupta 2016). However, relative age at different developmental stages may influence the progression of a disease, as may the physiological causes of aging such as metabolic rate (Demetrius 2006). Furthermore, comparatively rapid development of a disease in a murine model that is typically of a chronic duration in humans may make an accurate study of the progression of that disease in mouse models more challenging or not

fully portray the disease seen in humans (Demetrius 2005, Demetrius 2006, Dutta and Sengupta 2016).

Significant neuroanatomical differences in rodents, compared to primates, include a different gross organization of the basal ganglia, the lissencephalic cortex in rodents versus the gyrencephalic cortex in primates (Rohlfing et al. 2010, Swanson 2018) and differences in neurogenesis (Lazarov and Marr 2013). However, cell and pathway organization of the human and rodent basal ganglia is similar, which indicates that while gross anatomy varies, functional anatomy is conserved (Brooks and Dunnett 2015). A small brain volume creates disparities in the application of therapeutic modalities when converted to clinical trials and may limit the application of techniques which identify and measure outcomes such as imaging and electroencephalography (EEG; Pouladi et al. 2013).

One advantage of laboratory mice, genetic uniformity, may be a disadvantage when studying chronic progressive later-onset diseases with complicated multifactorial aetiologies (Duty and Jenner 2011, Hugenholtz and de Vos 2018). Genetic and environmental variability in the human population may better enable sub-population manifestations of these diseases which may not be easily reproducible or even be apparent in a murine model with a very specific genotype (Lin 2008, Libby 2015). Furthermore the genetic modification of laboratory mice almost certainly selects for alleles whose presence or effect on a study may not be fully appreciated (Mahajan et al. 2016), while genetic drift may affect reproducibility of a study (Taft et al. 2006).

There is substantial conservation of genes between humans and mice (Monaco et al. 2015). However, homologous genetic and organizational similarity between humans and mice does not mean transcriptional or molecular similarity. For instance, the mouse transcriptional inflammatory and immune responses are very different to that of the human. This may be of particular relevance for complex diseases invoking multi-system responses like neurodegenerative disease (Mestas and Hughes 2004, Seok et al. 2013). Furthermore, dysfunction in homologous genes can manifest differently in different species, for example, a recent study of dysfunction in MPV17 homologs in

humans, mice, zebrafish and yeast found substantial pathological and phenotypic differences across species (Lollgen and Weiher 2015).

#### 1.4.2 Large animal models of neurodegenerative disease

The basis for developing a large animal model of HD is that large animals may anatomically and physiologically align better with humans than do rodents (Morton and Howland 2013, McBride and Morton 2018). For example, because of the difference in size of the substantia nigra pars reticula and internal segment of the globus pallidus in rodents, most direct pathway medium spiny neurons in rodents project to the substantia nigra pars reticula, with a small percentage projecting to the internal segment of the globus pallidus. In primates, including humans, because the two regions are similar in size, an approximately even number of direct pathway medium spiny neurons target both regions (Reiner and Deng 2018). The substantia nigra in sheep has been demonstrated to be very similar to the human substantia nigra, as discussed in Section 1.2.1.

Other advantages include larger brains and a more similar body size (which may assist ‘scaling-up’), a longer life span (which may increase the accuracy of chronic disease models) and greater genetic variability between any two animals (that more closely approximates the human population and helps eliminate unrecognized and disadvantageous genomic effects seen in in-bred rodents; Dai et al. 2018, Herrmann et al. 2019, Murray et al. 2019). With the low correlation between preclinical and clinical trial success, development of a well-characterised large animal model of HD would provide another option for assessing efficacy and safety of a potential treatment that has shown promise in rodent models, prior to costly clinical trials.

NHPs are the obvious large animal model to replicate human disease, with their similar anatomy, physiology and genome. Various excitotoxic and transgenic NHP models have been developed that have provided insights into HD (Ferrante et al. 1993, Brouillet et al. 1995, Burns et al. 1995, Palfi et al. 1996, Kendall et al. 2000, Yang et al. 2008, Lavis et al. 2019). The largest impediments to the development and use of a NHP model of HD are practical factors including the high cost of purchase,

difficulties and cost of adequate management of a NHP with dementia over an extended time period and the reluctance of the public to support NHP models of human disease (Morton and Howland 2013).

Farm animals circumvent some of the practical difficulties associated with the use of NHPs in HD research. In particular, pigs and sheep are easy to source, relatively economical to buy and house, ethically more acceptable to the general public, of a suitable size to be useful and manageable, and have very similar brains to humans, both in terms of size and anatomy (Dai et al. 2018, Morton 2018, Herrmann et al. 2019). For these reasons, transgenic large animal models of HD have been developed in pigs and sheep (Jacobsen et al. 2010, Yang et al. 2010, Baxa et al. 2013).

#### 1.4.3 Genetic models of Huntington's disease

There have been numerous fragment, full length and knock-in transgenic mouse models of HD developed (Mangiarini et al. 1996, Menalled et al. 2003, Slow et al. 2003, Gray et al. 2008, Southwell et al. 2017). Each of the transgenic mouse HD models have well documented advantages and disadvantages, with some excellent reviews detailing these models (Pouladi et al. 2013, Menalled and Brunner 2014, Brooks and Dunnett 2015). The main criticism of the transgenic HD mouse models has been a lack of overt neurodegeneration and full replication of the human pathology, and in particular the very long CAG repeats that are needed to induce pathology (Li and Li 2012).

Large animal models of HD that express the full mHTT protein have been developed in sheep (Jacobsen et al. 2010), pigs (Yan et al. 2018), miniature pigs (Baxa et al. 2013) and NHPs (Yang et al. 2008). The sheep model, OVT73, express a full length mHTT encoding cDNA with 73 polyglutamine repeats (CAG) under the control of the human *HTT* promoter. OVT73 express mHTT in all tissues, not just the brain, and have been shown to develop N-terminal mHTT fragment aggregates in the brain (Reid et al. 2013). Furthermore, immunohistochemistry of brains from OVT73 sheep revealed decreased expression of the spiny neuron marker DARPP-32 (Jacobsen et al. 2010). Circadian abnormalities have also been noted in the sheep model (Morton et al. 2014). Locomotor

abnormalities have been reported in the full length mHTT miniature pig model (Askeland et al. 2018), however OVT73 has not developed any clinical signs of HD. OVT73 sheep express their wildtype HTT as well as the transgenic human mHTT (Jacobsen et al. 2010). The pig model has shown selective neurodegeneration of medium spiny neurons as well as rapid development of behavioural and motor abnormalities and early death (Yan et al. 2018).

The miniature pig and sheep models have the advantage of longevity and reproducibility, with the oldest progeny of the transgenic sheep and miniature pig models currently being nine years old and five years old respectively. None of these models have fully captured the spectrum of neuropathological changes and symptoms seen in HD, which is an important reason why excitotoxic models continue to be relevant, however the miniature pig model is exhibiting gradually progressing neurodegeneration (Ardan et al. 2019) while the transgenic sheep model has increased plasma melatonin which is postulated to be neuroprotective (Morton et al. 2019).

A miniature pig model that expressed an N-terminal mHTT fragment either died antenatally or had poor postnatal survival (Yang et al. 2010). The histological change in the miniature pig model replicated HD, including mHTT aggregates and cell apoptosis. However, the expression of the N-terminal mHTT fragment only, which forms the insoluble aggregates seen in HD-afflicted neurons and is associated with cell malfunction and death, may have replicated an advanced stage of the disease neuropathologically, limiting the lifespan of the model (Li and Li 2015). The N-terminal mHTT fragment miniature pig model did not develop the full spectrum of symptoms seen in HD by life end, with their shortened life span limiting their usefulness (Morton and Howland 2013, Rogers 2016).

The transgenic NHP model (Yang et al. 2008) produced histologic changes consistent with HD but few of the animals survived more than a few months. Disease in the NHP transgenic model progressed rapidly, not accurately replicating the disease (Chan et al. 2015). If the neuropathogenesis of HD is reliant on both a loss of wildtype HTT function as well as the toxic effects of mHTT, then any

transgenic animal, including OVT73, expressing both wildtype HTT and mHTT may not fully replicate the disease or may take longer than predicted to replicate the disease.

#### 1.4.4 Toxic models of Huntington's disease

While the use of toxins to selectively lesion the striatum pre-date transgenic models of HD, toxic models continue to be highly relevant and frequently utilized in preclinical research (Cui et al. 2018, Emerich et al. 2019, Zhang et al. 2019). They can develop characteristic pathology not seen in transgenic models in an acute timeframe (Lelos and Dunnett 2018). However, they only replicate a portion of the neuropathology associated with HD, don't develop characteristic aggregates and because they are acute, do not replicate the slow development and chronic nature of HD (Pouladi et al. 2013). The main toxins that have been used to model HD are the glutamate analogues kainic and ibotenic acid, the N-methyl-D-aspartate (NMDA) receptor agonist QA and mitochondrial toxins 3-nitropropionic acid (3-NP) and malonic acid. Table 1.2 summarises the major advantage and disadvantage for each toxin listed above.

Kainic and ibotenic acid are excitotoxins that cause striatal degeneration and reproduce some of the histological changes seen in HD striatal degeneration (Coyle et al. 1983, Hantraye et al. 1990). Intra-striatal kainic acid produces epileptic activity rarely seen in HD patients and results in neurodegeneration in limbic structures outside of the striatum (Schwarcz et al. 2010, Nam et al. 2017). Ibotenic acid produces circumscribed striatal lesions (compared with kainic acid) following intra-striatal injections and does not result in epileptic activity (Schwarcz et al. 1979, Schwarcz et al. 2010). Neither compound is endogenous (Jorgensen and Olesen 2018, White et al. 2019) and therefore have not been implicated as a part of pathogenesis of HD.

3-NP is an irreversible neurotoxin that inhibits mitochondrial energy production (Albin 2000) and produces spontaneous dose-dependent selective striatal pathology and clinical signs homologous to HD when administered systemically (Beal et al. 1993b, Brouillet et al. 1995). 3-NP replicates one possible mechanism of neuron cell death in HD, deficient oxidative energy metabolism (Borlongan et

al. 1997, Carmo et al. 2018). The reason for the susceptibility of the striatum to 3-NP is not fully known, however MSNs have been shown to be particularly sensitive to mitochondrial dysfunction (Pickrell et al. 2011, Crook and Housman 2013). 3-NP directly inhibits succinate dehydrogenase in the electron transport chain, generating reactive oxygen species that produce mitochondrial DNA damage and alter mitochondrial permeability further affecting the mitochondrial function (Tunez et al. 2010). 3-NP striatal lesions are homogenous to QA in representing HD striatal pathologic change (Kumar et al. 2010, Tunez et al. 2010). Because 3-NP is a mitochondrial inhibitor given systemically, it effects a wide range of tissues and has the potential to have a more deleterious effect on the health and welfare of an animal than QA which primarily causes a localized lesion (Alarcon-Herrera et al. 2017).

A reversible succinate dehydrogenase inhibitor, malonic acid, produces lesions similar to 3-NP when injected into the striatum (Beal et al. 1993a, Bazzett et al. 1995). Malonic acid lesions are less pronounced and more transient in nature compared to 3-NP and malonic acid models have been used to trial potential neuroprotective HD therapeutics (Fancellu et al. 2003, Sagredo et al. 2009, Kumar et al. 2013).

Exogenous lesioning of the rodent and NHPs striatum using QA produces lesions that closely resemble HD pathological changes, with a reduction in GABA-producing spiny neurons and selective sparing of axons of passage, aspiny neurons containing somatostatin and neuropeptide Y and large cholinergic neurons plus a hypertrophy of glial cells, especially astrocytes. Grossly, atrophy of the striatum, with concomitant enlargement of the lateral ventricles occurs (Vonsattel et al. 1985, Beal et al. 1986, Bjorklund et al. 1986, Davies and Roberts 1988, Ferrante et al. 1993, Brickell et al. 1999, Lavisse et al. 2019). The gross and cellular pathological changes caused by QA resemble those of HD, discussed in Section 1.3.



**Table 1.2 Common toxins used to create animal models of Huntington's disease**

<b>Toxin</b>	<b>Action and delivery method</b>	<b>Advantage</b>	<b>Disadvantage</b>
Kainic acid	Glutamate analogue. Acute striatal injection.	Neuronal changes resembling HD.	Large area of necrosis with cystic cavity formation at centre of lesion. Seizures and seizure-induced neuropathology possible.
Ibotenic acid	Glutamate analogue. Acute striatal injection.	HD like neuronal degeneration in well-circumscribed injection region with sparing of transient and terminating fibres.	Large area of necrosis with cystic cavity formation at centre of lesion.
Quinolinic acid (QA)	NMDA receptor agonist. Acute striatal injection.	HD like neuronal changes in transition zone may better model HD than Kainic or Ibotenic acid. Endogenous compound implicated in HD pathogenesis.	Large area of necrosis with cystic cavity formation at centre of lesion.
3-Nitropropionic acid (3-NP)	Irreversible succinate dehydrogenase inhibitor. Chronic systemic injection.	Systemic chronic injections affect all of the striatum and reproduce key characteristic histological and neurochemical HD features	Animals often become very sick or die. Can affect other brain regions, especially thalamus and hippocampus.
Malonic acid	Reversible succinate dehydrogenase inhibitor. Acute striatal injection.	Similar lesions to 3-NP though also spares somatostatin neurons. Can be blocked.	Milder, more transient effects than 3-NP.

QA is an intermediate of the kynurenine pathway which is important for L-tryptophan metabolism and nicotinamide adenine dinucleotide (NAD<sup>+</sup>) synthesis. QA is active in both neuronal and non-neuronal tissues (Hogan-Cann and Anderson 2016). Physiological concentrations of QA in the different parts of the rat brain vary from 0.6 nmol/g in the striatum to 1.8 nmol/g in the cortex (Moroni et al. 1984). Endo- and exogenous elevation of QA is neurotoxic, with chronic exposure of rat striatal tissue to as little as 100 nmol QA capable of inducing excitotoxic damage (Whetsell and Schwarcz 1989).

QA causes toxicity through multiple mechanisms; overactivation of primarily NR2A and NR2B subunit NMDA receptors resulting in massive calcium entry into the affected cells (de Carvalho et al. 1996); increased glutamate release by neurons and inhibition of uptake by astrocytes increasing extracellular glutamate concentration and leading to overstimulation of the glutamatergic system (Tavares et al. 2002); oxidative damage including lipid peroxidation (Rios and Santamaria 1991); hyperphosphorylation of the light neurofilament subunit and glial fibrillary acidic protein resulting in destabilization of the neuronal and astrocytic cytoskeleton (Pierozan et al. 2010); mitochondrial dysfunction and energy depletion (Bordelon et al. 1997); and induction of autophagy and apoptosis (Guillemin et al. 2005, Braidy et al. 2014).

One reason why QA models of HD are relevant is because early in the development of HD, QA is significantly elevated in the striatum and cortex (Guidetti and Schwarcz 2003). It is postulated that QA and other metabolites of the kynurenine pathway are involved in the pathogenesis of HD. Both microglia and macrophages produce QA under pathological conditions, potentiating neurodegenerative disease like HD (Schwarcz et al. 2010). Furthermore, not only does mHTT induce transcription of the kynurenine pathway, but also multiple unrelated genetic suppressors of mHTT toxicity converge on the kynurenine pathway suggesting that kynurenine pathway dysfunction may be an important link between mHTT production and neuron dysfunction and death (Giorgini et al. 2008). The striatum, pallidial formation and hippocampus are vulnerable to the neurotoxic effects of

QA, whilst the cerebellum, substantia nigra, amygdala, medial septum and hypothalamus are more resistant (Schwarcz and Kohler 1983, Nakanishi 1992). The brain regions that are vulnerable to QA are not dissimilar to the brain regions most affected in HD (Rub et al. 2016). The possibility that QA is involved in the pathophysiology of HD influenced the decision to use QA to lesion the sheep striatum in this study.

## 1.5 Phenotype testing in sheep models of disease

Creation of an excitotoxic sheep model of HD requires the ability to phenotype the model. Sheep are ungulated, quadrupedal prey animals who naturally flock and spend approximately 16 hours a day grazing or ruminating. Because of their tendency to follow each other and act unpredictably when isolated, the common impression of sheep is one of stupidity. However, a range of sheep phenotyping studies disprove the orthodoxy on sheep intelligence (for examples, see below), allowing characterization of behavioural responses, cognitive function and motor performance and revealing phenotypic subtleties that were not previously appreciated.

### 1.5.1 Cognition

Sheep have been repeatedly shown to have a good memory and can discriminate between similar objects. Operant testing has shown that sheep are capable of discriminating between similar shapes, hue and brightness (Baldwin 1981, Bazely and Ensor 1989, Morris et al. 2010, Morton and Avanzo 2011, Sugnaseelan et al. 2013, Knolle et al. 2017a) and can inhibit an already-started response (a response that deteriorates in HD patients; Knolle et al. 2017b). Sheep can also remember and perform complex tasks when retested twenty two weeks after initial training (Hunter et al. 2015) and are capable of remembering and discriminating between fifty individual sheep faces for two years (Kendrick et al. 2001).

Sheep have a good spatial memory, with significant improvements in time to traverse and reductions in errors over time when repeatedly traversing a complex maze. They also show a

deterioration in complex maze traversing performance when challenged with a muscarinic receptor agonist, scopolamine hydrobromide, which impairs memory function (Lee et al. 2006). The ability to remember and discriminate reinforces evidence that they have learning and memory neural systems in their frontal and temporal lobes analogous to those in humans, with a good capacity for learning and memory (Kendrick and Baldwin 1987, Kreiman et al. 2000, Kendrick et al. 2001, Ferreira et al. 2004).

Sheep have a high predicted level of cognitive capacity (McBride and Morton 2018). As well as discrimination and memory, sheep are capable of two complex executive decision making processes which are used for testing cognition in neurological disorders; namely reversal learning and attentional set-shifting (Morton and Avanzo 2011). Reversal learning is the ability to switch from a reinforced discriminatory choice to a previously incorrect choice (Izquierdo et al. 2017) while attentional set-shifting is the ability to transfer a reinforced belief to novel stimuli (Brown and Tait 2016). Reversal learning and attentional set-shifting measure the functional capacity of the fronto-striatal regions of the cerebrum and cognitive flexibility in a broader sense (Heisler et al. 2015). Comparatively, sheep are very capable of reversal learning and ranked third in a reversal index that included humans, other primates, pigs, dogs and rodents (McBride and Morton 2018). Executive decision making in the diseased sheep brain has not been previously published. Therefore, the two-choice discrimination task performance of the QA-lesioned sheep, described in Chapter 4, is both novel and potentially very informative, given the reversal learning capability of sheep and the importance of the striatum for the task (Heisler et al. 2015, McBride and Morton 2018).

High-throughput, semi-automated testing cognition in sheep is possible (McBride et al. 2015). However, the design of any operant system for sheep needs to minimise the effects of negative stimuli (Doyle et al. 2014). Minimising the effects of negative stimuli and ensuring high-throughput were key elements of the maze developed for the two-choice discrimination task described in Chapter 2 and Chapter 4.

### 1.5.2 Breed influence

Breed-choice and breed standardization may be an important consideration in cognitive assessment study design in sheep. Welsh-Mountain sheep performed better than Norfolk Horned and Borderdale breeds in a study investigating navigational ability and self-image engagement (McBride et al. 2015) while Blue-Faced Leicester sheep performed significantly worse than Suffolk, Texel or Beulah breeds at reversal acquisition (McBride and Morton 2018). As well as breed considerations when selecting sheep for cognitive assessment studies, adverse in-utero and lamb conditions can affect cognitive capacity, including undernutrition and handling, as well as age and previous experience, highlighting the need for careful consideration of inclusion criteria for studies assessing cognitive functionality in sheep (Erhard et al. 2004, Coulon et al. 2015). Obtaining sheep from one property that were the same breed and from the same cohort, as described in Section 2.2, ensured that breed, age, gender, environment and management differences between properties, did not influence the results in the two-choice discrimination task. However, the performance of the Merino-Border Leicester cross sheep in cognitive assessment studies, in comparison to other breeds, is unknown.

### 1.5.3 Circadian rhythms and activity monitoring

Circadian rhythms and sleep homeostasis can be measured in sheep. Disruption of the sleep-wake cycle is a symptom of many neurodegenerative diseases (Homolak et al. 2018) (Askenasy 2001, Diago et al. 2018). Disturbances in sleep homeostasis and circadian abnormalities have been identified in the CLN5 Batten disease-affected sheep and the transgenic HD sheep through the use of EEG and activity monitoring (Morton et al. 2014, Perentos et al. 2016). An activity monitoring study was performed in the present study, as described in Appendix B.

### 1.5.4 Motor phenotyping and rotation

Motor changes are a well-defined part of the spectrum of clinical signs that occur in HD (Bates et al. 2015), with the basal ganglia having an essential role in motor control (Dudman and Krakauer 2016). Motor performance in sheep can be evaluated using a variety of techniques including a veterinary

neurological examination, which is discussed in Section 1.5.5 and utilised in Chapter 3. Other techniques for motor analysis that have been utilised in sheep include kinematic performance analysis, using treadmill locomotion and motion capture technology, with analysis of fore- and hind limb gait analysis in healthy and experimentally injured sheep assessed (Faria et al. 2014, Safayi et al. 2015, Safayi et al. 2016). The ability to identify motor changes in sheep is an important component of the development of a sheep HD model.

Dopamine agonists, especially apomorphine, are frequently used in rodent and NHP studies to investigate if a striatal lesion is functional and unmask a motor phenotype in otherwise normal appearing animals (Giorgetto et al. 2015, Lavisse et al. 2019). Apomorphine is a non-selective dopamine receptor agonist with a rapid onset of action that stimulates locomotor activity (Beninger 1983, Boyle and Ondo 2015). Rodent studies have shown that imbalance in dopamine signalling between the left and right striatum results in a side preference (Glick et al. 1977), measurable as a directional bias following administration of dopamine agonists in rodents and NHPs with striatal lesions (Molochnikov and Cohen 2014). Selective direct and indirect pathway activation within the unilateral striatum can also cause rotation, with direct pathway activation causing contralateral rotation and indirect pathway activation resulting in ipsilateral rotation (Kravitz et al. 2010). In NHPs, dystonia, dyskinesia and abnormal posture is often observed and measured in response to dopamine agonists, while rotation can be inconsistent (Brownell et al. 1994, Storey et al. 1994, Burns et al. 1995, Kendall et al. 2000). Based on NHP studies (for examples, see references above), it was predicted that the QA-lesioned sheep would appear normal after initial surgical recovery. Therefore, dopamine agonist-induced rotation of the QA-lesioned sheep was investigated (described in Chapter 4), as a technique for unmasking a phenotype in the functionally normal animals.

### 1.5.5 The neurological examination of sheep

There have been some comprehensive descriptions of the general neurological examination process for ruminants (Constable 2004, Finnie et al. 2011, Crilly et al. 2015). No sheep specific neurological

examination has been described previously, however. Descriptions that generalize a neurological examination for use in a range of species that vary from a 30kg goat to a 500kg cow need to be refined for each species if a veterinary neurological examination is going to be a useful research technique. The general neurological examination of ruminants is similar to humans and other species in that it is a process that integrates signalment (age, gender, breed), history, distance examination, general physical examination, and a systematic evaluation of the peripheral and central nervous system to identify and localize neurological deficits and in some cases allow a specific disease entity to be diagnosed (Constable 2004). Typically, once clinical signs are localized, additional tests, either *ante-* or *post mortem*, are required to allow an accurate disease diagnosis with the *post mortem* examination of the nervous system an important part of the ruminant neurological exam (Nagy 2017, Wasle et al. 2017).

The major clinical signs, pathology and basic mechanism of disease for sheep neurological conditions of veterinary importance are well described (see for an example an excellent review series of ruminant neurological disease in Australia by JW Finnie, PA Windsor and AE Kessell (2011)). Typically, the primary motivation of a neurological examination in sheep in a veterinary environment is to diagnose the presence or absence of a disease, not to grade the severity of that disease (Constable 2004). Characterisation of the clinical signs of neurological disease in sheep therefore emphasizes easily recognizable nerve deficit, motor, mentation and behavioural changes (Fecteau et al. 2017). Emotional, cognitive or social changes in sheep with neurological diseases are less recognized, as are the subtle pre-symptomatic and early clinical signs.

There is no rating scale for any neurological diseases in sheep that quantify specific clinical signs and align those clinical signs with specific pathological changes to assess the severity and progression of a neurological condition in sheep. Recently a clinical examination protocol was developed to detect Scrapie in sheep (Konold and Phelan 2014). The examination protocol was a short protocol to

assist quick identification of possible scrapie affected animals in a suspect flock and was not intended to allow detailed grading of the disease in a single animal.

### 1.5.6 Additional diagnostic techniques

A wide range of techniques are utilized to diagnose and evaluate neurological conditions in ruminants (Nagy 2017). Apart from a clinical examination, standard veterinary diagnostic techniques for neurological conditions in ruminants include haematological and biochemical analysis, gross- and histo- pathology, microbiology, radiography (Lin et al. 2015) and ultrasonography (Guilbaud et al. 2014).

Additional diagnostic techniques to those described above, are typically performed in a research context. There are numerous examples of naturally occurring and experimentally induced sheep models of human neurological disease (see Table 1.3 for examples). Additional diagnostic techniques include; cerebrospinal fluid sampling (CSF; Scott 1995: See Appendix C), myelography (Mageed et al. 2014), computerized tomography (CT; Birch et al. 2015), magnetic resonance imaging (MRI; Ertelt et al. 2016, Ella et al. 2017), electromyography (Bergmeister et al. 2016), electroretinography (Regnier et al. 2011), brainstem auditory-evoked potentials (Pierson et al. 1995, Griffiths et al. 1996), deep brain stimulation (Lentz et al. 2015) and EEG (Perentos et al. 2015, Oxley et al. 2016).

Many of these additional diagnostic techniques, for example magnetic resonance (MR) modalities like MRI, magnetic resonance spectroscopy (MRS) and diffusion tensor imaging (DTI) have a paucity of published information specific to sheep. MRS and DTI investigation of the lesioned sheep brain, discussed in Chapter 5, is novel and will help build a foundation of literature for sheep-based MR studies.



**Table 1.3 Sheep models of human neurological disease**

<b>Naturally occurring sheep diseases</b>	<b>Mechanism of disease</b>
Neuronal ceroid lipofuscinosis (Batten disease)	Lysosomal storage disease. CLN5 <sup>1</sup> , CLN6 <sup>2</sup> or cathepsin D mutation. <sup>3</sup>
Gaucher disease	Lysosomal storage disease. Mutation in the $\beta$ -glucocerebrosidase gene. <sup>4</sup>
Tay-Sachs disease	Lysosomal storage disease. Deficiency of lysosomal enzyme $\beta$ -N-acetylhexosaminidase A (Hex A). <sup>5</sup>
Hereditary lissencephally	31-bp deletion in the RELN gene results in cerebellar hypoplasia and disorganisation of the cerebral cortex and hippocampus. <sup>6</sup>
Scrapie	A transmissible spongiform encephalopathy caused by infective distorted prion proteins. <sup>7</sup>
Alexander disease	Astrocytic disorder. <sup>8</sup>
Hereditary cerebellar abiotrophy	Loss of purkinje cells in the cerebellum and glial cell accumulation. <sup>9</sup>
<b>Experimentally induced diseases</b>	<b>Mechanism of disease</b>
Stroke	Proximal middle cerebral artery occlusion. <sup>10</sup>
Foetal alcohol syndrome	Maternal intravenous alcohol infusion during pregnancy. <sup>11</sup>
Non-accidental infant head injury (shaken baby syndrome)	Manual shaking of anaesthetised lambs. <sup>12</sup>
Schizophrenia	Lipopolysaccharide infection during pregnancy. <sup>13</sup>
Foetal hypoxic brain damage	Pregnant ewes housed in isobaric hypoxic chambers. <sup>14</sup>

<sup>1</sup>(Jolly et al. 2002) <sup>2</sup>(Jolly and West 1976) <sup>3</sup>(Tynnela et al. 2001) <sup>4</sup>(Karageorgos et al. 2011) <sup>5</sup>(Torres et al. 2010) <sup>6</sup>(Perez et al. 2013) <sup>7</sup>(Das and Zou 2016) <sup>8</sup>(Kessell et al. 2012) <sup>9</sup>(Harper et al. 1986) <sup>10</sup>(Wells et al. 2012) <sup>11</sup>(Birch et al. 2015) <sup>12</sup>(Finnie et al. 2012) <sup>13</sup>(Gantert et al. 2012) <sup>14</sup>(Brain et al. 2015)

## 1.6 Research significance, hypothesis and aims

The value of large animal neurodegenerative disease models as an intermediary step in the therapeutic development process is well established (Morton and Howland 2013). The sheep offers numerous advantages as a large animal neurodegenerative disease model, including; large brain, anatomically and physiologically similar brain to humans, genetic diversity, relatively low cost, amenable to handling, easy to control and maintain and more acceptable to society as a medical research model than NHPs (Dai et al. 2018, Morton 2018). Sheep can reproduce human neurological disease, with multiple examples published (see Table 1.3).

There is a need for excitotoxic large animal models of HD to be developed for use in validating pre-clinical research undertaken in excitotoxic rodent models of HD. The first step in developing an excitotoxic large animal model of disease is to describe a technique for lesioning the striatum and assess if there is detectable pathology and phenotypic change.

The hypotheses tested here were that:

- 1) The sheep striatum can be lesioned with QA to create an excitotoxic sheep model of HD.
- 2) Pathological change in sheep with QA lesions of the striatum will be detectable using MRI.
- 3) Sheep with QA lesions of the striatum will have a detectable phenotype.

Using techniques validated in rodents and NHPs, QA was injected into the striatum of sheep to create excitotoxic pathology. Sheep are ungulated quadrupedal ruminants with very different social and behavioural responses to rodents or primates. As such the motor, behavioural and cognitive symptomology that results from striatal lesioning likely manifests differently in sheep than NHPs or rodents.

Therefore, the aims for the thesis were to:

- 1) Describe a protocol for inducing QA lesions in the caudate nucleus of the striatum of sheep.
- 2) Use a clinically relevant 3-Tesla MR scanner to identify lesion development and gross pathological change in the QA-lesioned sheep.

- 3) Render a standard veterinary neurological examination suitable for sheep and characterise the clinical manifestation of striatal lesions in the QA-lesioned sheep using the examination.
- 4) Evaluate the usefulness of a neurological examination of sheep for diagnosing and characterising the phenotype of sheep with QA lesions of the striatum.
- 5) Describe a technique for performing dopamine agonist mediated rotation studies in sheep.
- 6) Investigate the ability of rotation studies to identify and characterise striatal pathology in QA-lesioned sheep.
- 7) Establish a two-choice discrimination task to determine whether QA-lesioned sheep have cognitive decline.

## 2 Methods

---

### 2.1 Ethics statement

The experiment was conducted in accordance with the Australian Code of Practice for the Care and Use of Animals for Scientific Purposes (2013) and approved by the South Australian Health and Medical Research Institute (SAHMRI) (ethics approval: SAM161) and University of Adelaide Animal Ethics Committees (ethics approval: M-2015-106).

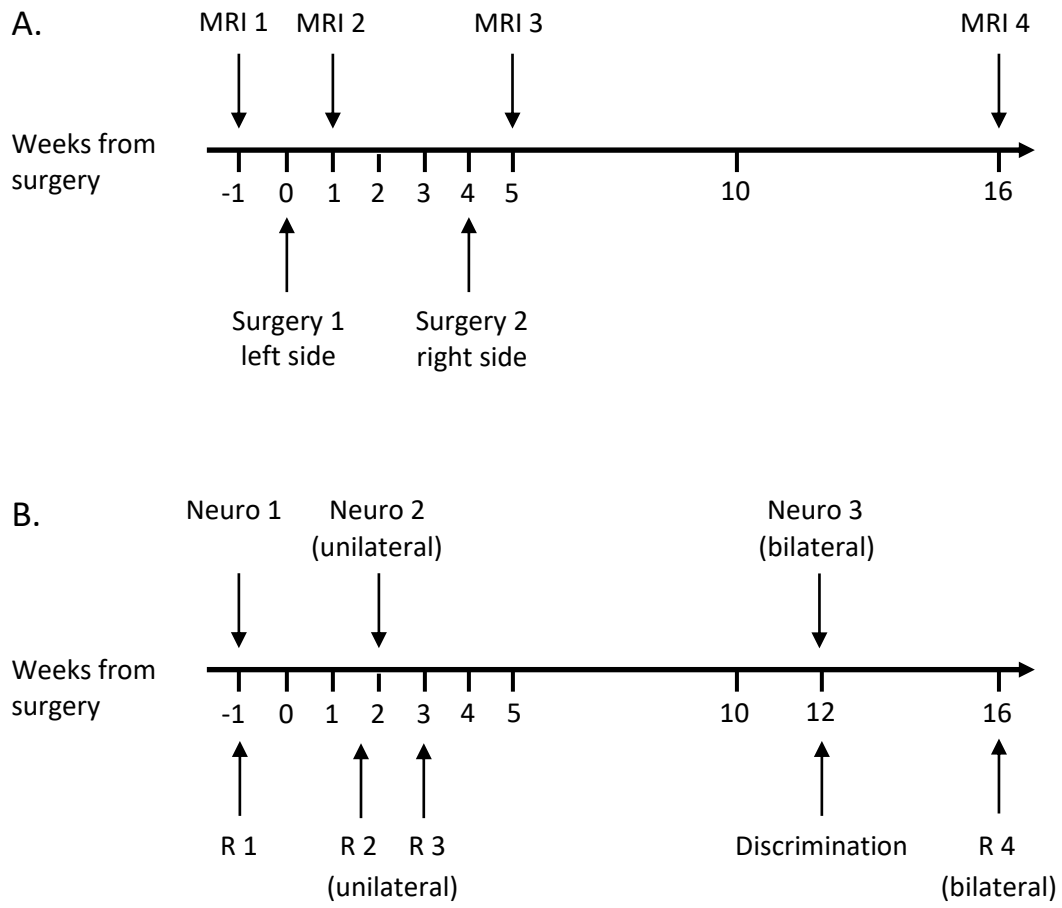
### 2.2 Animals

Sixteen castrated-male, 18 month old, Merino-Border Leicester cross sheep (*Ovis aries*, weight 58 – 65 kg) were obtained from an approved source in South Australia and housed at SAHMRI, Gilles Plains, where all experimental procedures were conducted. Castrated-male sheep were used due to availability of these animals. The sheep were maintained as a flock in a single paddock prior to surgery and in groups of three animals in large outdoor group pens after surgery. Three days prior to surgery, the sheep were penned individually in an indoor facility where they remained until they had fully recovered from the surgery. An evaluation of demeanour, behaviour and ambulation of each sheep was performed at least twice daily for the entire experiment by experienced sheep handlers, with veterinary investigation performed if required. Sheep were fed meadow and lucerne hay once a day, with unlimited access to water and additional grain and Lauke Feedlot pellets (Lauke Mills, SA, Australia) when penned. Sheep were randomly assigned to either experimental or control groups.

### 2.3 Experimental regime

Six weeks prior to the first surgery, the sheep were habituated to facility staff and researchers. Sheep were randomly assigned to either an experimental or control animal group, with eight sheep in each group. The experiments were conducted by a single handler (AO'C) who was blind to the identity of

sheep in each treatment group. Two surgical procedures were performed on each sheep, four weeks apart. QA (experimental group) or saline (control group) was infused into the left caudate nucleus (first surgery) and then the right caudate nucleus (second surgery). MRI scans were performed on the left and the right striatae of each sheep. These were conducted (1) prior to the first surgery, (2) one week after the first surgery, (3) five weeks after the first surgery and (4) sixteen weeks after the first surgery (Fig. 2.1A). Three neurological examinations were performed on the sheep; prior to the first surgery, two weeks after the first surgery and twelve weeks after the first surgery. Sheep underwent rotation studies pre-surgically and ten days, three weeks and sixteen weeks after the first surgery. Discrimination learning testing was performed twelve weeks after the first surgery (Fig. 2.1B). The sheep were euthanised at the end of the sixteenth week. After death, the brains were perfusion fixed and removed from the head for histology.



**Figure 2.1 Diagram indicating the timeline of the study.** Timeline of (A) surgical and MRI procedures and (B) phenotyping studies; neurological examinations (Neuro 1,2,3), rotation studies (R 1,2,3,4) and the two-choice discrimination task (Discrimination); ‘unilateral’ indicates the sheep only have a lesion in the left striatum, ‘bilateral’ indicates the sheep have a lesion in the left and right striatum.

## 2.4 Surgical procedure

The surgery was based on a similar surgical procedure published in a study that injected an AAV9 vector into the brain of transgenic HD sheep (Pfister et al. 2018). Experimental sheep had QA infused into the caudate nucleus during each surgery. Control sheep received saline infusions *in lieu* of QA. The surgeon (AO'C) was blinded to the treatment group of the sheep. Determination of the dose was based on the dose range used in rodent and primate studies (Popoli et al. 1994, Storey et al. 1994, Burns et al. 1995, Shear et al. 1998). A pilot study was performed to assess the effect of the chosen dose of QA in sheep (Appendix A).

Immediately prior to surgery, QA (Sigma-Aldrich Co. LLC, St. Louis, MO, USA) was dissolved in 1 M sodium hydroxide (NaOH) and neutralised to pH 7 with 0.1 M phosphate buffered saline (PBS). A contrast agent, dimeglumine gadopentetate (Magnevist, Bayer, Germany), was combined with the QA to make a QA solution (QA 180 mM, gadolinium 2 mM), stored in a BD 1 mL tuberculin syringe. The syringe was placed on ice in a lightproof polystyrene container until required during the surgery.

During the first surgery, QA (180 mM, 75  $\mu$ l) or saline (75  $\mu$ l) was infused into the head of the left caudate nucleus to create a unilateral (experimental) or sham lesion (control). During the second surgery QA or saline (at the same concentration and / or volume as previous) was infused into the head of the right caudate nucleus to create a bilateral striatal or sham lesion. Initial rostral, lateral and ventral stereotaxic coordinates for targeting the caudate nucleus were based on cadaver surgeries with the coordinates being progressively refined after each stereotaxic surgical procedure. The stereotaxic coordinate range for targeting the head of the caudate nucleus was taken with bregma as 0,0,0: rostral 19 – 24 mm, lateral 4 – 6 mm, ventral 22 – 24 mm. General anaesthesia was induced in the sheep using 5 mg/kg of 100 mg/mL ketamine hydrochloride (Ceva Animal Health Pty Ltd, Australia) and 0.4 mg/kg of 5 mg/mL diazepam (Pamlin, Ceva Animal Health Pty Ltd, Australia) administered via the jugular vein. Endotracheal intubation allowed sheep to be mechanically ventilated and anaesthesia maintained using 2 – 2.5% isoflurane. A 114.3 mm 16-gauge catheter was

inserted into the jugular vein and lactated Ringers solution (Hartmann's, Baxter Healthcare Pty Ltd, Australia) was administered at a rate of 10 mL/kg/hour. Sheep received 2 mg/kg of 50mg/mL carprofen (Carprieve, Norbrook Laboratories Australia Pty Ltd) before being positioned in a stereotaxic frame (Kopf, model number 1630; Tujunga, CA, USA). Sheep were given 3 g of 1 g cefazolin sodium (Cefazolin-AFT, AFT Pharmaceuticals, New Zealand) intravenously during surgery. Post-surgery, 22 mg/kg of 300 mg/mL procaine penicillin (Depocillin, MSD Animal Health, Australia) was administered daily for three days.

Sheep were placed in the sphinx position on a large elevated cylindrical pad; the ventrum of the sheep rested on top of the pad and the limbs extended down each side of the cylindrical pad, minimising risk of pressure neuropathy or myopathy. The head was placed in a large animal stereotaxic frame. Ear bars and orbital notch prongs were adjusted such that a line between the ventral orbital rim and the horizontal canal of the external auditory meatus was parallel to the horizontal plane and perpendicular to the manipulator apparatus. The cranium was shaved and aseptically prepared. Sterile surgical techniques were maintained throughout the surgical procedure. A monopolar electrocautery was used to create a 3 cm curvilinear incision through the dermal and subcutaneous layers just caudal to the poll of the sheep's head. A rostral 3 cm incision was extended perpendicular to the curvilinear incision. The dermal, subcutaneous and periosteal layers were reflected to expose the skull. Bregma was identified and marked as a reference point using a surgical pen. A 3 – 4 mm burr hole craniotomy was performed to expose the dura using a Dremel 8220 drill (Dremel, Racine, WI, USA) at appropriate coordinates rostral to bregma and lateral to the midline. The manipulator was mounted on the Kopf stereotaxic frame at the predefined rostral and lateral coordinates and a convection-enhanced delivery (CED) cannula (MRI Interventions, Irvine, CA, USA) secured to the manipulator. The CED cannula was attached to a 25 cm luer lock extension set that was secured to the syringe that contained the QA or saline. An infusion pump (New Era Pump Systems Syringe Pump NE-1000, Farmingdale, NY, USA) was used to purge air from the CED cannula



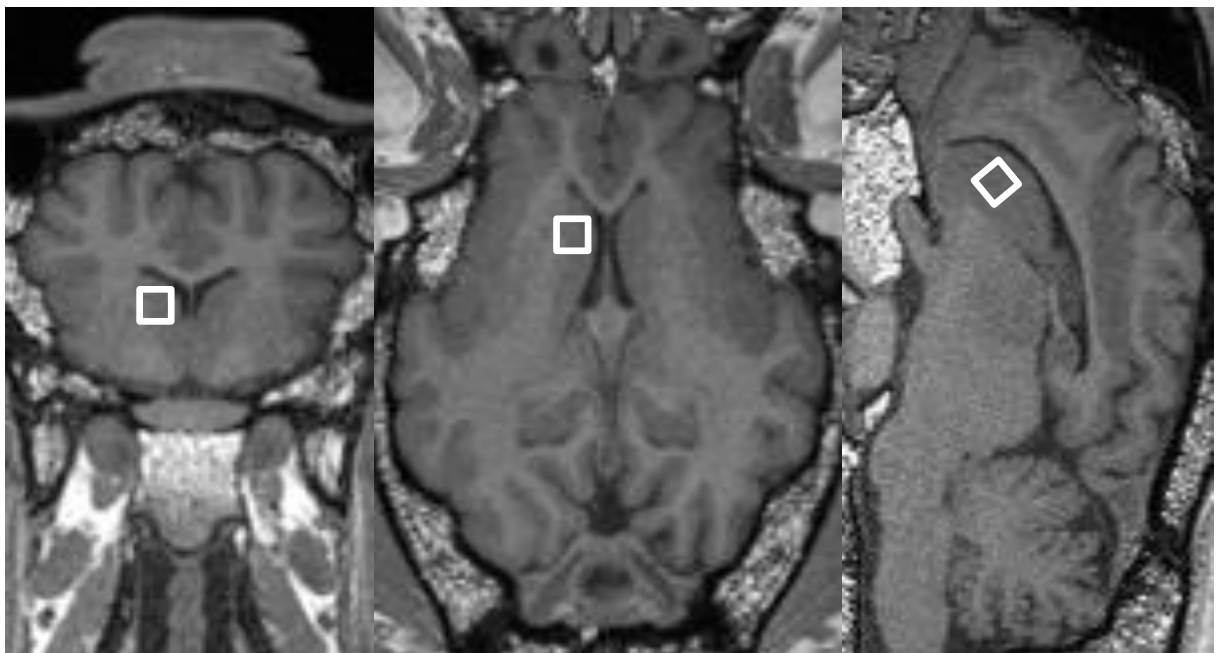
and extension line. A 1.5 mm incision was made through the dura permitting the CED cannula to traverse the dura, while ensuring the dura closely adhered to the cannula to minimise CSF leakage.

A micro-manipulator was used to lower the CED cannula to the predefined ventral coordinate from the dural surface and the exposed skull covered with saline-soaked gauze. QA or saline infusion was started five minutes after the CED cannula was lowered to the ventral coordinate to allow tissue disrupted by the CED cannula to stabilise. QA or saline was infused at a rate of 2  $\mu$ l/minute until the desired volume was completed. The CED cannula was left *in situ* for ten minutes after the infusion ended before being slowly withdrawn over ten minutes. Bone wax (Ethicon, NJ, USA) was used to seal the craniotomy after CED cannula removal. The wound was irrigated with saline and closed using monofilament absorbable suture (PDS, Ethicon, NJ, USA). The sheep was removed from the stereotaxic frame and recovered from the anaesthetic.

## 2.5 Magnetic resonance methodology

Sheep were anaesthetised during each MRI. Anaesthesia was induced with 20 mg/kg of 1000 mg/g thiopentone sodium (Ilium, Troy Laboratories, Australia), administered to effect in the jugular vein and maintained using 2% isoflurane. T1-weighted, magnetisation-prepared, rapid gradient-echo (T1-MPRAGE) sequences were performed on a 48 channel 3-Tesla Siemens Skyra (Siemens AG, Erlangen, Germany) MR scanner with posterior 20 channel head coil and 18 channel surface body coil. DTI was performed using a bipolar scheme, resolution = 2.1 mm<sup>3</sup>; repetition time (TR) / echo time (TE) = 3000 / 100 ms, field of view = 240 mm, base matrix = 112, simultaneous multi-slice factor 2, 256 diffusion directions, b = 0, 1000 s / mm<sup>2</sup>. Diffusion weighted imaging was performed with a readout segmentation of long variable echo-trains monopolar scheme, 4-scan trace, resolution = 1.3 × 1.3 × 1.5 mm; TR / TE 1 / TE 2 = 7870 / 69 / 115 ms, field of view = 220 mm, base matrix = 164, generalised auto-calibrating partial parallel acquisition / 2, b = 50, 500, 1000 s / mm<sup>2</sup>. Single voxel spectroscopy was performed using a point resolved spectroscopy sequence, TR / TE = 2170 / 30 ms, 144 averages, acquisition time (TA) = 5:26 min, using a 5 × 5 × 10 mm voxel located in the striatum, principally in

the head of the caudate nucleus (Fig. 2.2). Voxel size was optimised to maximise signal-to-noise ratio whilst preventing inclusion of anatomical structures outside of the area of interest. Spectra were assessed for variance from the study mean before inclusion into the study, with spectra 1.0 or greater below the study mean excluded. An inline frequency correction was used to compensate for any drift in the spectra due to motion. A water-unsuppressed acquisition was also acquired to provide a concentration reference.



**Figure 2.2 Region of interest placement for single voxel spectroscopy.** Representative example of region of interest placement (white box) in A) coronal, B) axial and C) sagittal orientation, superimposed on a T1-MPRAGE image.

### 2.5.1 Magnetic resonance spectroscopy data processing

Automatic time-domain signal processing was performed using Tarquin (Wilson et al. 2011). Tarquin uses a constrained least-squares approach to estimate signal amplitudes for metabolites in the time-domain. Tarquin has been previously used to process ovine MRS data from pre-term lambs with ventilator induced brain injuries (Skiold et al. 2014). The water peak of the unsuppressed spectrum was used as an internal reference to calculate concentrations of the following metabolites: glutamine (Gln), glutamate (Glu), myo-inositol (Ins), *N*-acetylaspartate (NAA), *N*-acetylaspartate and *N*-acetylaspartylglutamate (TNAA), glycerophosphocholine and phosphocholine (total choline) and creatine and phosphocreatine (total creatine).

### 2.5.2 Anatomical and diffusion tensor imaging data processing

DTI data processing was performed using vendor software (Siemens AG, Erlangen, Germany), measured as fractional anisotropy (FA). Tensors were reconstructed and inspected visually. FA maps were produced inline on the scanner, and were analysed using ITK-Snap software (Yushkevich et al. 2006). Using the trace weighted images, spherical 67.5 mm<sup>3</sup> regions of interest were drawn over the middle of the lesion in the head of the caudate nucleus, if visible, or the middle of the head of the caudate nucleus if no lesion was visible. These regions were then translated to the FA maps for quantification. ITK-Snap software was also used to visualise and segment lesions visible on the T1-MPRAGE images and calculate lesion volumes.

### 2.5.3 Magnetic resonance spectroscopy and diffusion tensor imaging statistics

Statistical analysis of MRS and DTI data was performed using SPSS-25 (IBM, Armonk, New York, United States). Acute (one week after surgery), and chronic (five to sixteen weeks after surgery) changes in metabolite concentrations and FA were compared between QA-lesioned and saline-treated striatae and with unlesioned striatae using a linear mixed-effects model with  $p < 0.05$  considered significant. The linear mixed-effects model had a repeated covariance based on the

lowest Akaike's information criterion. Model assumptions and normality were ascertained using a residual value histogram and scatter-dot plots.

## 2.6 Neurological examination procedure

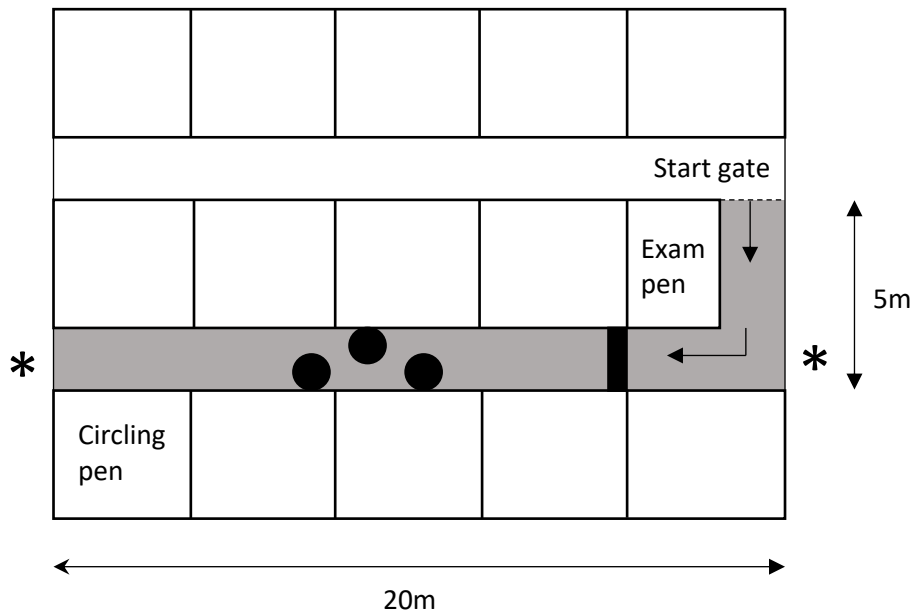
Two experienced veterinarians (AO'C and one other) performed each examination. Both neurological examiners were blinded to whether a sheep was an experimental or control animal and did not see diagnostic MRI, however one veterinarian (AO'C) assumed primary responsibility for the sheep and therefore was not blind to the planned proportion of sheep that received QA lesions or the surgical recovery. The surgical recovery was not discussed by the two veterinarians.

### 2.6.1 Neurological examination protocol

Neurological examinations were based on a standard canine veterinary neurological examination (de Lahunta and Glass 2009), modified to be suitable for sheep. Neurological examinations were performed using a systematic, repeatable method for consistency between examinations and sheep. All sheep recovered fully from surgery and appeared functionally normal prior to post-surgical neurological examinations. The day before the neurological examination, the sheep were housed in individual pens in the testing area (Fig. 2.3) to give them time to acclimatize to the testing area. Sheep were examined individually.

Initially a distance examination was performed with demeanour, behaviour, gait (without exerting pressure to move) and posture of each sheep assessed in their individual pen. Gait was further evaluated using a twenty five metre 'L' shaped race that led into a four metre by four metre square pen. The race contained a 30 cm high, 40 cm wide obstacle that traversed the race at the start of the long arm of the 'L' forcing the sheep to jump. Three cylindrical bins, 100 cm high by 60 cm wide were placed five metres past the jump in a pattern that forced the sheep to zig-zag. One examiner was placed at each end of the race to allow gait assessment from the front and back of each sheep as the sheep moved in a straight line and negotiated obstacles. The square pen was used to assess gait

while circling the sheep clockwise and anticlockwise. Examination of the gait was used to detect evidence of paresis, ataxia, and hypo- or hypermetria.



**Figure 2.3 Diagram of the neurological examination facility.** The solid black rectangle represents a 30cm high, 40cm wide step. The three solid black circles represent three 100cm high, 60cm wide bins. The \* symbols indicate where observers stood as sheep navigated the L-shaped race, shaded grey, that began at the start gate (dashed line) and finished at the circling pen.

After the distance examination was performed, each sheep was brought into a smaller three metre by three metre pen for the rest of the neurological examination. Pupil size and location, menace reflex, palpebral reflex, dazzle response, direct and indirect pupillary light reflex, nystagmus (presence of physiologic, absence of spontaneous), facial and pinnae sensation and response, facial symmetry, swallowing and tongue movement were evaluated to assess cranial nerves: II (optic), III (oculomotor), IV (trochlear), V (trigeminal), VI (abducens), VII (facial), VIII (vestibulocochlear), IX (glossopharyngeal), X (vagus) and XII (hypoglossal). Each cranial nerve assessment was described as either normal, decreased or absent.

Muscular tone and evidence of atrophy was evaluated by palpating the sheep while standing and exerting appropriate pressure over the front and hind limbs. Muscle tone was described as hyper, normal or decreased. Cutaneous trunci, tail and anal tone and the perineal reflex were also assessed while the sheep was standing and described as normal, decreased or absent.

Postural reactions were assessed with both examiners handling the sheep. Postural reactions were described as either normal, decreased or absent. The sheep were lightly restrained and not allowed to lean on the examiner or any object. Knuckling of the distal limb, crossover of fore and hind limbs, bilateral side-hopping and wheelbarrowing of fore and hind limbs was assessed. For the side-hopping assessment, one examiner supported the hind limb and abdomen while the other examiner supported the front limb and elevated the head and neck to the level of the horizontal plane. For the wheelbarrowing, the elevated limbs were held at the horizontal plane with one examiner holding each limb.

After assessment of postural reactions, the sheep was placed in lateral recumbency. Fore- and hindlimb flexor withdrawal and hindlimb patellar reflexes were evaluated as hyper, normal, decreased or absent. Presence or absence of a crossed extensor response was noted. The sheep was then allowed to stand with coordination of the standing process and time to stand evaluated as normal or decreased. At the end of all the individual neurological examinations, the sheep were group housed in a four metre by four metre pen and behaviour in a flock evaluated as either appropriate or inappropriate with any inappropriate behaviour described.

## 2.7 Rotation studies

Rotation studies were performed with sheep placed individually into animal pens. Pens (2.0 metres wide by 3.0 metres long by 1.5 metres high) were under cover, with compacted clay floors and a black corflute (Bunnings, Australia) lining on three sides, leaving an entrance on the fourth side unlined. During each rotation study, sheep were put into the rotation pen the day before recording, with companion sheep housed in the pens on either side to prevent flock separation anxiety. All

rotation recordings were performed in the morning (between 0900 and 1200). A Logitech C920 HD Pro Webcam (Logitech, Switzerland) mounted on a Libec TC-6 camera tripod (Heiwa Seiki Kogyo Co., Ltd, Japan) was placed in front of the rotation pen on the morning of the recording. The camera was positioned so that it captured all activity in the pen. Prior to the start of recording, sheep were given thirty minutes after camera set-up to become accustomed to the camera. Sheep movement was recorded for sixty minutes, and then each sheep was given a subcutaneous 0.1 mg/kg apomorphine hydrochloride (Sigma-Aldrich Co. LLC, St. Louis, MO, USA) injection, dorsally at the midline base of the neck. The injection area had previously been shaved to allow visualization of the injection site. The activity of the sheep was then recorded for a further sixty minutes. Sheep were undisturbed during each sixty minute recording period. During each rotation study, the investigator (AO'C) remained within hearing distance, but not visual contact, of the sheep.

### 2.7.1 Rotation data analysis

Rotation was quantified from video recordings. Only full 360° rotations were counted. For each rotation, the time that had elapsed since the commencement of the study and the direction of rotation was recorded. Net rotational activity was the difference between total rotation in a direction ipsilateral to the side of the first surgery and total rotation in a direction contralateral to the side of the first surgery. Since the investigator (AO'C) knew which side had been injected, he, while remaining blinded to experimental group, made a prediction of which sheep belonged to which experimental group, based on rotational data. Sheep were labelled as 'likely to be QA-lesioned', 'likely to be saline-treated' or 'unsure' (if the data were equivocal for a sheep).

### 2.7.2 Rotation statistics

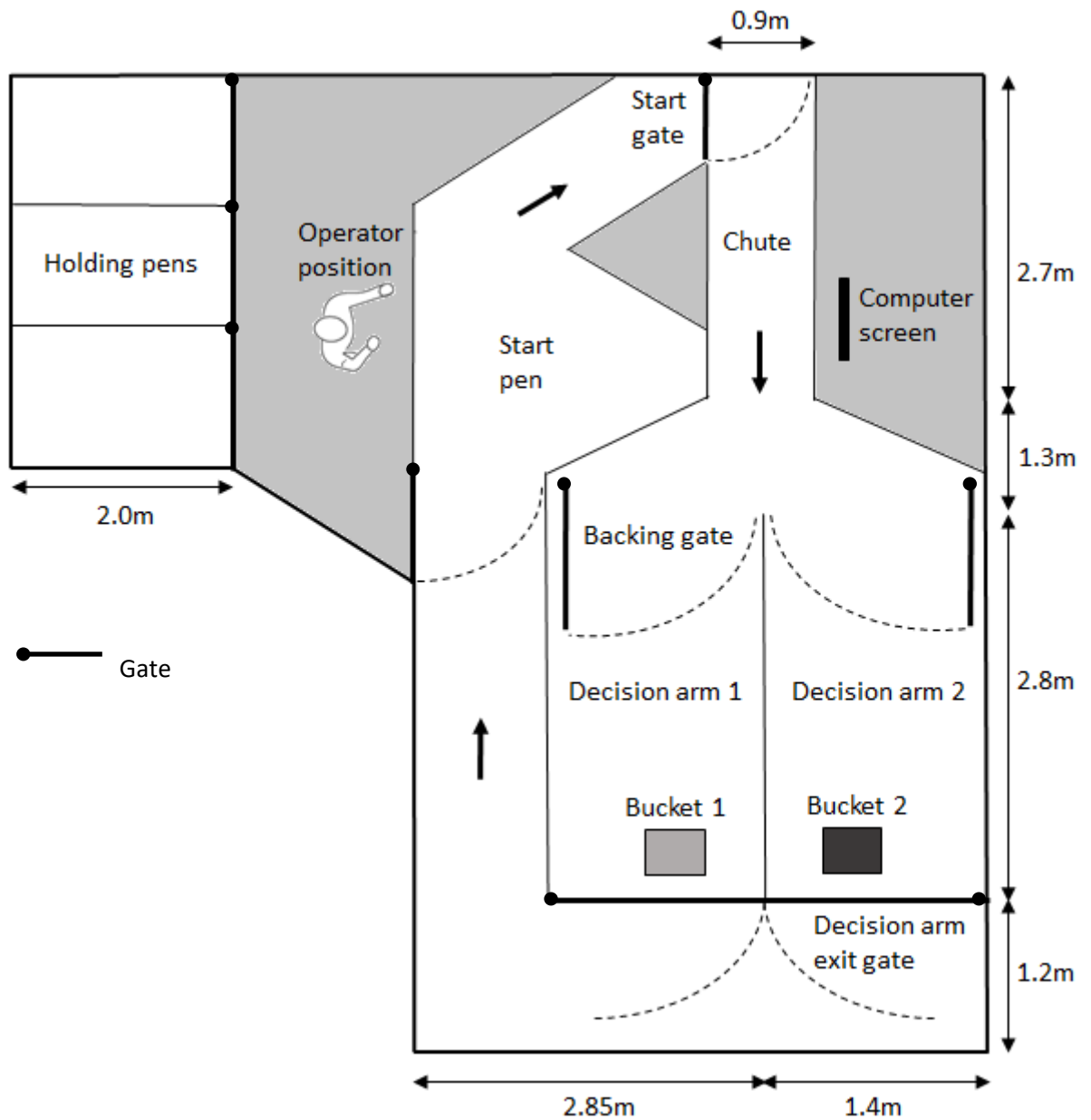
SPSS 25 (IBM, Armonk, New York, United States) was used to perform statistical modelling. Net rotation data was analysed using an unpaired t-test for comparisons between saline-treated and QA-lesioned sheep and a paired t-test for self-control comparisons. For all statistical comparisons,  $p < 0.05$  was considered to be significant.

## 2.8 Two-choice discrimination learning

### 2.8.1 Test apparatus

A novel apparatus was designed, based on a previously published apparatus (Morton and Avanzo 2011). An 8.0 metre by 4.25 metre test apparatus was constructed inside a raised barn with wooden slat floors (Fig. 2.4). The test apparatus comprised of a central corflute-lined chute that opened into a corflute-lined, longitudinally divided decision pen. A single square plastic bucket (Award Storeaway 27 L, Award Brands, Australia) was placed in a pre-marked central position at the end of each decision arm immediately in front of the decision arm exit gate. One of the two buckets was yellow and the other was blue. A race connected the decision pen back to the starting pen. Gates situated at the start point and entry and exit of each arm of the decision pen controlled sheep flow through the apparatus. Gates were operated using a cable-pulley system by the operator. This was situated to the left of the apparatus, so that the operator was able to manipulate all of the gates from one location. A Logitech C920 HD Pro Webcam was mounted above the decision pen with a HP Compaq LA2306x computer screen orientated out of view of the sheep to allow the operator to monitor sheep progress via the screen, without looking at the sheep. Individual holding pens were located to the left of the return race at the level of the starting point.





**Figure 2.4 Plan of the discrimination testing apparatus.** Arrows indicate direction of sheep movement. Individual sheep were moved from the holding pen into the start pen. Sheep were unable to enter the chute and see the buckets until the start gate was opened. When sheep made a decision, the backing gate was closed behind them. The sheep would exit past the bucket in the decision arm and return to the start position or holding pens as appropriate. The start pen gate could be closed behind the sheep at the starting position forming a pen when the start gate was closed. Note, the drawing is not to scale.

## 2.8.2 Habituation and training

Sheep were habituated as a single large group to the test apparatus, including direction of flow and gate movements, daily during the week, for one month prior to their initial surgery. Two weeks prior to the start of testing, sheep were split into groups of two to three animals and housed in group pens. Each group of sheep underwent sixty to ninety minutes of training per day. The order that each group came in for training rotated each day. Individual sheep were progressively introduced to the various operating elements of the test apparatus and acclimatized to the test protocol. Black buckets were used during training. The end of training was when an individual animal was completing the test protocol in a calm manner. The operator always wore a white lab coat when habituating and training sheep and conducting sheep movements associated with the test apparatus.

## 2.8.3 Test protocol

The test protocol utilised a food reward to drive sheep behaviour. Simple two-choice discrimination learning was tested. During the acquisition phase of the two-choice discrimination learning task, the sheep learnt to discriminate between positively (S+) and negatively (S-) associated novel stimuli. During the reversal phase of the two-choice discrimination learning task, S+ and S- were switched, so the previous S+ becomes the S-. Half of the sheep were each assigned the yellow or blue bucket as S+ for the acquisition. The S+ bucket contained a five gram grain reward placed so that it could not be viewed until the head of the sheep was immediately over the bucket, while the S- bucket containing no grain. Small open packets of grain were taped behind each decision arm exit gate to reduce olfactory assistance arising from the grain reward. The operator opened the start gate allowing the sheep to exit the starting pen and enter the central chute. The central chute allowed the sheep to see both S+ and S- and to select the decision arm down which to progress. The sheep was deemed to have made a choice when it reached a point where the backing gate on each decision arm could be closed, restraining the sheep in the decision arm. The sheep were unable to visualise grain in the S+ bucket at the decision point. The sheep were allowed to self-correct for the first five discrimination

trials of the first session for acquisition and reversal. If the sheep selected S+, they were able to eat the grain reward. The exit gate of the decision arm was opened after the animal had eaten the grain if they selected S+ or after a time out of twenty seconds if they selected S-. The decision arm in which S+ / S- was presented in each trial was randomised, with a random sequence prepared prior to the session using a Microsoft Excel (Microsoft Corporation, Redmond, WA, USA) random function. Sheep performed ten discrimination trials per session. After the tenth repeat, they were returned to their holding pen. Sheep were considered to have learned a discrimination when they achieved 8 / 10 correct (80%) or greater in two consecutive sessions. Only the operator was present during testing.

#### 2.8.4 Discrimination data analysis and statistics

SPSS 25 (IBM, Armonk, New York, United States) was used to perform statistical modelling.

Acquisition and reversal performance were compared between experimental groups using the number of sessions required to reach a criterion of two consecutive sessions of 80% or greater correct. The data were also reanalysed, comparing the number of trials required to achieve six correct choices-in-a-row. Discrimination data was analysed using an unpaired t-test and the mean  $\pm$  SD were reported. For all statistical comparisons,  $p < 0.05$  was considered to be significant.

## 2.9 Histology

At the conclusion of the study, sheep were killed humanely with an intravenous injection of 0.5 mL/kg of 325 mg/mL pentobarbitone sodium (Lethabarb, Virbac, Australia). After death the heads were perfusion-fixed with 10% neutral buffered formalin and the brains were removed and placed in 10% neutral buffered formalin. A midline sagittal incision split the brain into two halves. A coronal slice was made through the optic chiasm, which extended up through the head of the caudate nucleus, transecting the QA-lesion site visible on MRI. Sequential coronal blocks (5 mm) were cut rostrally and caudally from the initial incision. Each block was paraffin embedded. Sections (5  $\mu$ m) were cut from the face of each block using a microtome. Light microscopy was performed to examine the sections after staining.

### 2.9.1 Haematoxylin and eosin staining for paraffin sections

Sections were mounted on charged glass microscope slides (Superfrost Plus microscope slides, Lomb Menzel-Glaser, USA) and heated at 60°C for twenty minutes. The sections were then dewaxed in two changes of xylene (two minutes each change), followed by three changes of absolute alcohol (two minutes each change) and then gently washed in running tap water for three minutes. After a brief rinse in distilled water, the sections were stained with freshly filtered Lillie-Mayers haematoxylin (POCD Healthcare, Australia) for three minutes, rinsed in running tap water for one minute, differentiated by quickly dipping ten times in 1% acid alcohol, washed in running tap water until clear, blued in saturated aqueous carbonate solution for one minute, washed in running tap water for thirty seconds, counterstained in filtered 1% alcoholic eosin for one minute, dehydrated in 3x three minute changes of absolute ethanol, cleared in 2x three minute changes of xylene, mounted in DePex mounting medium and cover slipped.

### 2.9.2 Immunohistochemistry

The primary antibodies used were; rabbit anti-glial fibrillary acidic protein (GFAP, #Z0334, Dako, Denmark) diluted 1/13,000 and rabbit anti-ionised calcium binding adaptor molecule 1 (Iba1, #016-20001, Wako, USA) diluted 1/500 in 2% normal donkey serum (NDS). The secondary antibody used was biotinylated donkey anti-rabbit (#715-065-152, Jackson ImmunoResearch, USA) diluted 1/1000 in PBS.

Sections were mounted on charged glass microscope slides (Superfrost Plus microscope slides, Lomb Menzel-Glaser, USA) and heated at 60°C for twenty minutes. The sections were then dewaxed in two changes of xylene (two minutes each change), followed by three changes of absolute alcohol (two minutes each change), and then gently washed in running tap water (three minutes). After a brief rinse in distilled water, antigen retrieval was performed by microwave heating the sections to a gentle boil in 10 mM sodium citrate buffer, pH 6 for ten (GFAP) or twenty (Iba1) minutes. Slides were removed from the microwave and once the buffer cooled to 50°C, they were gently washed in

running tap water (three minutes). All subsequent steps were performed at room temperature in a humidified chamber. Sections were circled with a peroxidase-antiperoxidase pen (DAKO, Denmark), rinsed in two changes of PBS (five minutes each) and then incubated in 10% NDS (Jackson ImmunoResearch, USA) in PBS for sixty minutes. The NDS was drained from the slides and the sections were incubated with the primary antibody overnight. The following day, the sections were rinsed in three changes of PBS (five minutes each) prior to blocking endogenous peroxidase by incubating sections in 0.3% hydrogen peroxide in PBS for thirty minutes. Slides were rinsed in three changes of PBS (five minutes each), and then incubated in the secondary antibody for sixty minutes. Slides were rinsed in three changes of PBS (five minutes each), incubated in Vector Avidin-Biotin Complex (ABC) reagent (Vector Laboratories, USA) for sixty minutes and rinsed again in three changes of PBS (five minutes each). The antibody reaction was visualised using diaminobenzidine. Sections were then rinsed in running tap water for five minutes, dehydrated in three changes of absolute ethanol (three minutes each), cleared in two changes of xylene (three minutes each), mounted in DePex mounting medium (Sigma Life Science, Spain) and cover slipped.

### 3 Surgery and neurological examination

---

Supporting publication:

O’Connell A, Sinnott B, Kuchel TR, Perumal SR, Fraser CK, Hemsley KM, Morton, AJ. 2019.

Neurological examination of sheep (*Ovis aries*) with unilateral and bilateral quinolinic acid lesions of the striatum assessed by magnetic resonance imaging. *J Neurol Exp Neurosci* 5(2): 56-67.

#### Statement of authorship

Title of Paper	Neurological examination of sheep ( <i>Ovis aries</i> ) with unilateral and bilateral quinolinic acid lesions of the striatum assessed by magnetic resonance imaging
Publication Status	<input checked="" type="checkbox"/> Published <input type="checkbox"/> Accepted for Publication <input type="checkbox"/> Submitted for Publication <input type="checkbox"/> Unpublished and Unsubmitted work written in manuscript style
Publication Details	<u>O’Connell A</u> , Sinnott B, Kuchel TR, Perumal SR, Fraser CK, Hemsley KM, Morton, AJ. 2019. Neurological examination of sheep ( <i>Ovis aries</i> ) with unilateral and bilateral quinolinic acid lesions of the striatum assessed by magnetic resonance imaging. <i>J Neurol Exp Neurosci</i> 5(2): 56-67.

#### Principal author

Name of Principal Author (Candidate)	Adam O’Connell		
Contribution to the Paper	Concept, planning, methodological development, experimental work, analysis, writing, article submission		
Overall percentage (%)	90%		
Certification:	This paper reports on original research I conducted during the period of my Higher Degree by Research candidature and is not subject to any obligations or contractual agreements with a third party that would constrain its inclusion in this thesis. I am the primary author of this paper.		
Signature		Date	15/01/2020

#### Co-author contributions

By signing the Statement of Authorship, each author certifies that the candidate’s stated contribution to the publication is accurate (as detailed above); and permission is granted for the candidate to include the publication in the thesis; and the sum of all co-author contributions is equal to 100% less the candidate’s stated contribution.

Name of Co-Author	Brendan Sinnott		
Contribution to the Paper	Surgical assistant, assisted with veterinary neurological examinations as second veterinarian.		
Signature		Date	18/1/2020

Name of Co-Author	Tim Kuchel		
Contribution to the Paper	General advice, support and funding.  <i>This is a correct record of Dr Kuchel's contribution. He has (sadly) passed away.</i>		
Signature		Date	17/1/20

Name of Co-Author	Raj Perumal		
Contribution to the Paper	Performed MR scans.		
Signature		Date	15/1/2020

Name of Co-Author	Cara Fraser		
Contribution to the Paper	Co-supervisor. General advice and support.		
Signature		Date	18 Jan 20

Name of Co-Author	Kim Hemsley		
Contribution to the Paper	Supervision, advice on all facets of the experiment, manuscript review.		
Signature		Date	17/1/20

Name of Co-Author	Jenny Morton		
Contribution to the Paper	Supervision, advice on all facets of the experiment, manuscript review, assistance with article submission.		
Signature		Date	14/1/20

### 3.1 Summary

This chapter describes the surgery used to create an acute QA model of HD in sheep (*Ovis aries*). It also describes the use of a sheep specific veterinary neurological examination to investigate the clinical signs of ovine striatum pathology. The value of the veterinary neurological examination in the symptomology investigation is assessed. Sixteen sheep underwent two surgeries, four weeks apart, in which either QA or saline was infused into the left (unilateral) and then the right (bilateral) caudate nucleus. Neurological examinations were performed pre-surgically, two weeks after the unilateral surgery and eight weeks after the bilateral surgery. Examining veterinarians were blind to treatment group. Evidence of laterality and hind limb motor dysfunction was identified in the QA-lesioned sheep. The neurological examination identified clinical signs in two out of eight saline control sheep and four out of eight QA-lesioned sheep after the unilateral surgery and three out of eight saline control sheep and seven out of eight QA-lesioned sheep after the bilateral lesion surgery. There was no association between clinical profile and lesion size or location. While the neurological examination was moderately useful for identification of QA-lesioned sheep, it was not informative about lesion characteristics.

### 3.2 Background

Sheep have basal ganglia and other brain structures anatomically similar to primates (including humans) and are increasingly being recognised as an important species for translational neurodegeneration research (Morton and Howland 2013). Functional anatomy of the basal ganglia and their outputs, however, is poorly characterised in sheep. As sheep are ungulate ruminant quadrupeds, their pyramidal and extrapyramidal pathways are likely to be different to those of rodents and primates, which utilise fine motor control to reach, grasp and climb. It thus seems unlikely that ruminants with striatal dysfunction will have a clinical presentation similar to that of rodents or primates.



A standard veterinary neurological assessment has never been developed for rodents and is not possible in NHP neurodegenerative models for reasons of safety. Rather, a battery of specific neurological tests are used to identify and characterise striatal dysfunction in these species, e.g. forelimb movement patterns, elevated body swing test and grip strength test in excitotoxin lesioned rats (Antunes et al. 2013, Klein et al. 2013, Gill et al. 2017), or staircase based and object retrieval-detour tasks in NHPs (Kendall et al. 2000, Roitberg et al. 2002). A standard veterinary neurological examination has been developed for canines (de Lahunta and Glass 2009). The canine neurological examination was adapted for sheep in this study.

The first aim of this study was to describe a technique to inject QA into the caudate nucleus of sheep. The second aim of this study was to identify gross pathological change in the QA-lesioned sheep using anatomical MRI. The third aim of this study was to characterise the clinical manifestation of striatal lesions in sheep using a standard veterinary neurological examination that was rendered suitable for sheep. The fourth aim of this study was to evaluate the usefulness of a neurological examination of sheep for diagnosing and characterising the phenotype of sheep with QA lesions of the striatum. By performing a standard veterinary neurological examination on sheep with QA-induced striatal lesions, it is possible to determine the value of the examination as part of a toolkit for assessing neurological function in ruminant models of neurodegenerative disease. The data obtained enabled construction of a symptom profile for sheep with significant striatal damage.

### 3.3 Results

#### 3.3.1 Surgical recovery

After the left side (unilateral) surgery, one control and five QA-lesioned sheep developed hindlimb paresis and proprioceptive deficits. In four of the eight QA-lesioned sheep, clinical signs were mild, with a narrow, slightly crouched hindlimb posture and crossing over of the hind limbs when standing or turning. One QA-lesioned sheep (QA8) developed mild to moderate hindlimb paresis with ambulatory deficits when pressured to move, a slightly crouched hindlimb posture and an inability to

resist pressure over the hindlimbs. Two QA-lesioned sheep with hindlimb dysfunction (QA7, QA8), showed handling-induced orofacial dyskinesia and temporary inappetence. One of the QA-lesioned sheep with mild hind limb dysfunction (QA4) developed intermittent spontaneous anticlockwise circling, which was exacerbated by handling. Two other QA-lesioned sheep had reduced left pinna tone (QA4, QA5). All observable clinical signs resolved completely within one week, with sheep appearing normal under observation thereafter.

After the second surgery, one control (Control 8) and one QA-lesioned sheep (QA4) developed mild hindlimb paresis and mild proprioceptive deficits. Two QA-lesioned sheep developed handling-induced orofacial dyskinesia and temporary inappetence (QA5, QA6), with one of the two sheep developing mild hindlimb paresis and the other sheep developing a narrow hindlimb stance with upright fetlocks, a wide-based forelimb stance, a very mild intention tremor and a tendency to circle left. All observable clinical signs resolved completely within one and a half weeks.

### 3.3.2 Neurological examination

Table 3.1 provides a summary of findings from the neurological examinations of the control and QA-lesioned sheep. There were no abnormalities detected during the pre-surgical neurological examinations of the sheep. Clinical signs were identified in two out of eight unilateral saline-treated (control) sheep and three out of eight bilateral saline-treated sheep during the post-surgical neurological examinations. Two control sheep had possible or very mild hindlimb dysfunction identified during the unilateral examination, with one of those two sheep having a side preference during the bilateral examination. Two different control sheep had possible or very mild hindlimb dysfunction identified during the bilateral examination. Per examination, clinical signs identified in control sheep were mild and limited in number, compared to the identification of multiple clinical signs in QA-lesioned sheep.

Three out of eight QA-lesioned sheep had evidence of hind limb dysfunction including reduced muscle tone, gait abnormalities and postural deficits during the unilateral examination, with one of

those three sheep spontaneously circling to the right. The sheep that developed mild to moderate hindlimb paresis and orofacial dyskinesia following unilateral surgery (QA8) was the most clinically affected sheep with evidence of hindlimb paresis during examination. Interestingly, the other sheep with post-surgical orofacial dyskinesia and hind limb dysfunction (QA7) had no clinical findings during the unilateral examination.

Seven out of eight QA-lesioned sheep had evidence of hind limb dysfunction and laterality during the bilateral examination, including circling, gait abnormalities, postural deficits and decreased hind limb tone. The most clinically affected sheep during the bilateral neurological examination was also the most clinically affected sheep during the unilateral neurological examination (QA8). The two sheep with the most severe clinical signs during surgical recovery after the second surgery were the least affected during the bilateral neurological examination. During the bilateral neurological examination, the sheep with upright hindlimb fetlocks during surgical recovery (QA5) successfully jumped out of a holding pen when initially approached and only had a mildly abnormal narrow stance and a slow yet coordinated rise from lateral recumbency, while the other sheep with orofacial dyskinesia (QA6) had no clinical findings during the bilateral neurological examination.

**Table 1. Neurological examination results for individual sheep**

<b>Animal ID</b>	<b>Pre-surgical</b>	<b>Two weeks after the first surgery (unilateral)</b>	<b>Twelve weeks after the first surgery (bilateral)</b>
QA1	nad <sup>1</sup>	nad	Spontaneous slow moderately tight circling left Narrow hindlimb stance Hind foot placement frequently rotated when standing Occasional overextension left-hind when circling Side-hopping mild delay left hind Slow coordinated rise from lateral recumbency
QA2	nad	nad	Reluctant to circle to left Mild decreased muscle tone left hind
QA3	nad	Occasional right hind limb scuff and knuckling- when circling Narrow hind limb stance	Reluctant to circle to left Occasional overextension right-hind when circling Incorrect correction of cross over right hind Slow hindlimb wheelbarrow Collapsed once on forelimb wheelbarrow Slow coordinated rise from lateral recumbency Mild right hind muscle atrophy Mild decreased muscle tone both hindlimbs
QA4	nad	Spontaneous moderately-fast tight circling right Reluctant to circle left Narrow hind limb stance Hind foot placement frequently rotated when standing Failure to correct left or right hind limb crossover placement	Spontaneous moderately fast tight circling right Very reluctant to circle to left Side-hopping mild delay left and right hind Decreased hind limb muscle tone
QA5	nad	Decreased left ear tone and sensation	Mild narrow hind limb stance Slow coordinated rise from lateral recumbency
QA6	nad	nad	nad

QA7	nad	nad	Spontaneous moderately tight circling right Reluctance to circle left Narrow hind limb stance Hind foot placement frequently rotated when standing Failure to correct hind limb crossover placement
QA8	nad	Narrow hind limb stance Slightly crouched in hind limbs Occasional crossing over of hind limbs when circling Slow coordinated rise from lateral recumbency Very mild reduced muscle tone hind limbs Repeatable collapse on hindlimb wheelbarrow Failure to correct hind limb crossover placement	Spontaneous moderately tight circling right Narrow hind limb stance Hind foot placement frequently rotated when standing Occasional crossing over of hind limbs when turning Occasional overextension of hind and stepping on forelimbs Side-hopping mild delay left and right hind Decreased hind limb muscle tone
Control 1	nad	nad	nad
Control 2	nad	nad	nad
Control 3	nad	nad	nad
Control 4	nad	Slightly crouched in hind limbs	Reluctant to circle to left
Control 5	nad	Occasional mild hind limb bunny hop gait	nad
Control 6	nad	nad	Very mild upright hindlimb posture
Control 7	nad	nad	Possible / very mild left and right hind side-hop delay Possible / very mild hind limb wheelbarrow delay Left fore flexor withdrawal decreased response
Control 8	nad	nad	nad

<sup>1</sup> nad = No abnormalities detected

### 3.3.3 Lesion location and volume

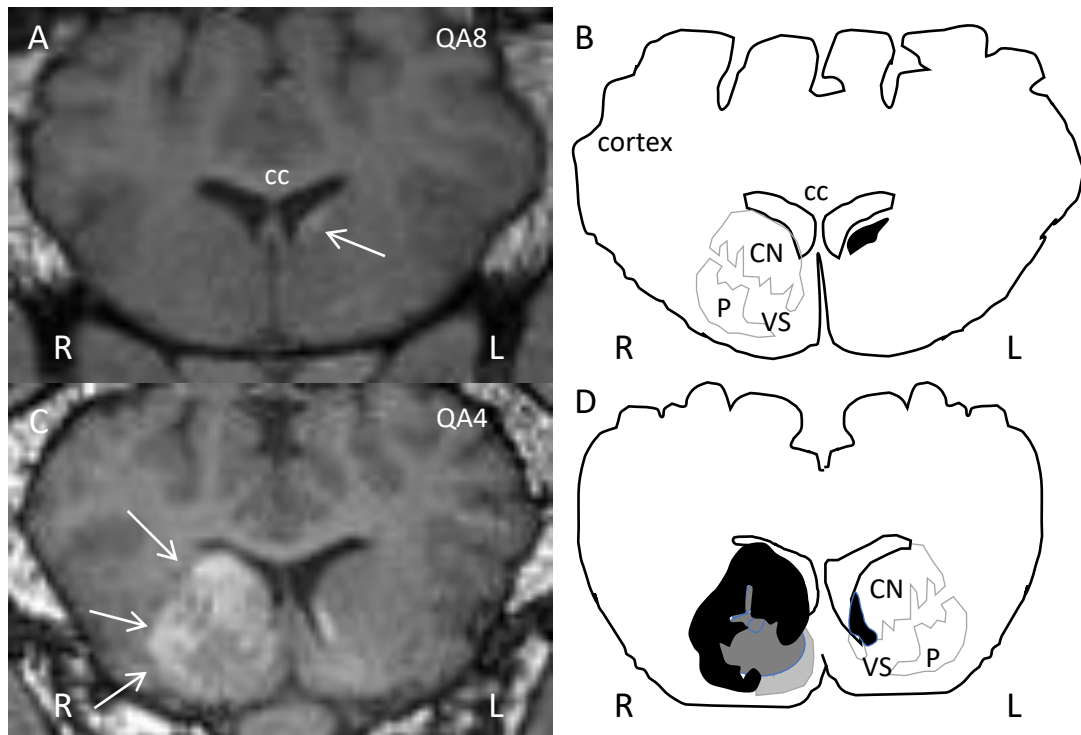
No lesions or evidence of sub-cortical structural abnormalities were visible on the MRI scan of any of the sheep prior to surgery or on any of the scans of the eight control sheep after surgery. Of the eight QA-lesioned sheep, five had clearly visible bilateral striatal lesions, one had a large lesion in the right caudate nucleus and a small lesion in the left caudate nucleus, one had a large right caudate nucleus lesion only and one sheep had a small lesion in the left caudate nucleus. Five of the eight sheep (QA1, QA5 – QA8) also exhibited cortical hyperintensity with minor accompanying histological pathology. In all cases this appeared ipsilateral to the QA-induced striatal lesions and principally in the anterior insular cortex with inconsistent involvement of other structures in the frontal and temporal lobe.

The head of the caudate nucleus was the predominant structure lesioned in all sheep, with inconsistent involvement of the putamen, ventral striatum and cortex. Table 3.2 shows lesion volume and location for individual sheep identified by MRI. Fig. 3.1 shows MRI images of the sheep with the largest striatal lesion visible on MRI (QA4), compared to that with the smallest striatal visible lesion (QA8). Atrophy of the affected caudate nucleus with concomitant enlargement of the lateral ventricle is evident on the final MRI in all lesioned sheep with the morphology of the lateral ventricles in control sheep unchanged (Fig. 3.2 and Fig. 3.3).

**Table 3.2 Location and volume of striatal lesions visible in QA-lesioned sheep using magnetic resonance imaging**

ID	Side	Location <sup>1</sup>	Volume of striatal lesion visible on MRI (mm <sup>3</sup> )		
			1 week	5 weeks	16 weeks
QA1	Left	VS, IC, GR, Ci	0	0	0
	Right	CN, P, GR, Ci		985	166
QA2	Left	CN	149	523	6
	Right	CN		290	31
QA3	Left	CN	199	528	16
	Right	CN		146	19
QA4	Left	CN, P, VS	484	672	48
	Right	CN, P, VS		1559	270
QA5	Left	CN, P, VS, IC, GR	861	910	353
	Right	CN, P, VS, IC		1527	491
QA6	Left	CN	14	40	10
	Right	CN, P, VS, IC, GR, OF, Sy, Si		522	166
QA7	Left	CN, P, VS, IC	377	761	118
	Right	CN, P		830	210
QA8	Left	CN, VS, IC	10	11	0
	Right	-		0	0

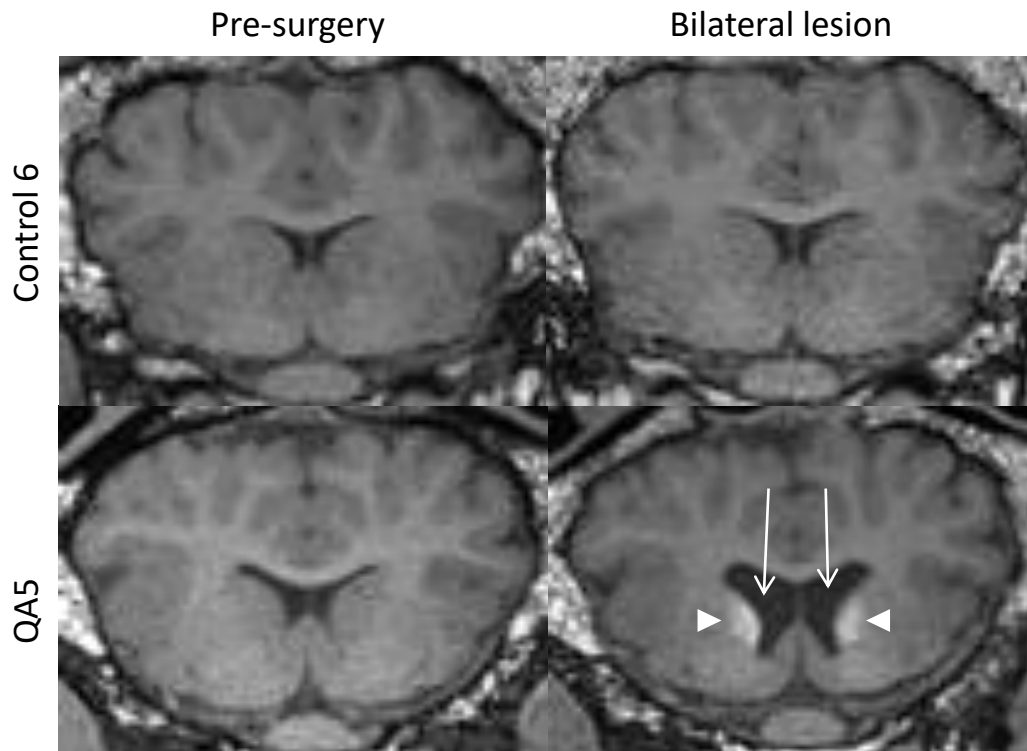
<sup>1</sup>CN: caudate nucleus, P: putamen, VS: ventral striatum, O: olfactory tract and bulb, IC: insular cortex, GR: gyrus rectus, Ci: cingulate gyrus, OF: orbital-frontal gyrus, Sy: sylvian gyrus, Si: sygmoideus gyrus.



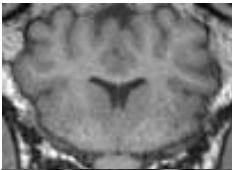

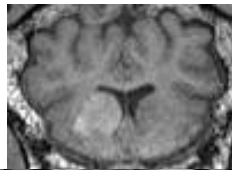
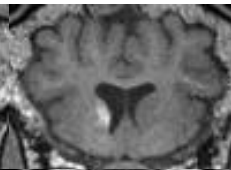


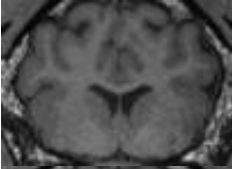
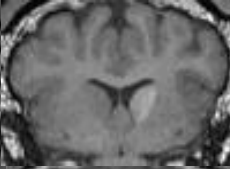
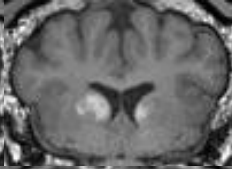
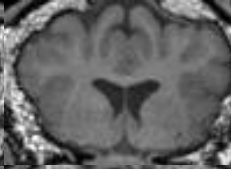


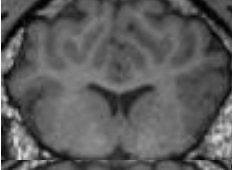
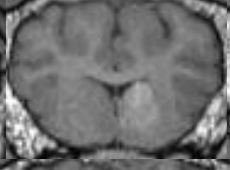
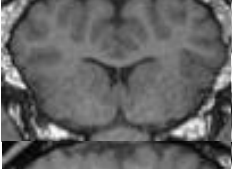
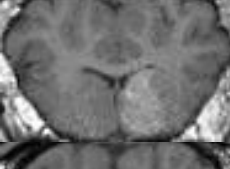
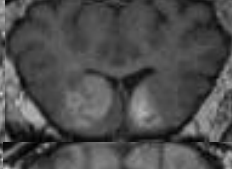
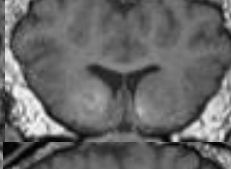


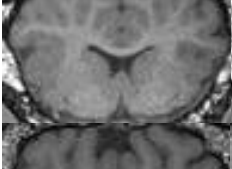
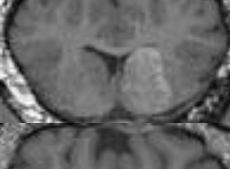
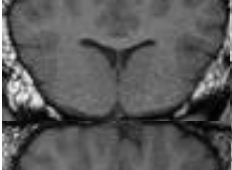
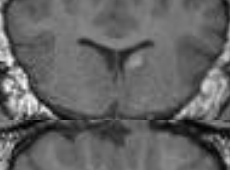
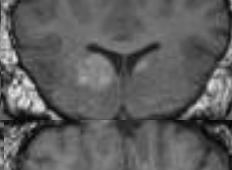
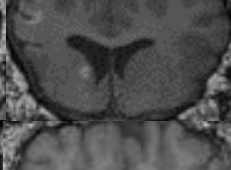


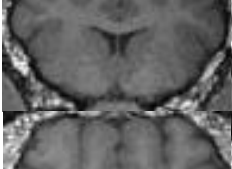
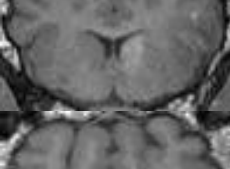
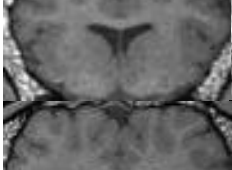

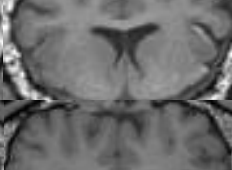



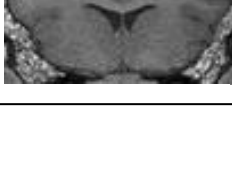
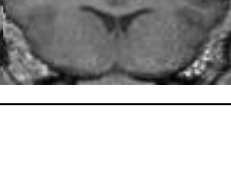














**Figure 3.1 Comparison of the smallest and largest QA lesion by MRI one week after surgery.**

Coronal slice comparing the smallest (A,B, top row, first lesion in the left striatum) with the largest QA lesion (C,D, second lesion in the right striatum) one week after lesion surgery. Images in A and C are from T1-MPRAGE MRI scans; White arrows point to the hyperintensity of the QA lesion. B and D are stylized cartoons of the sections in A and B with the lesions shaded in black / grey. Approximate locations of caudate nucleus (CN), putamen (P) and ventral striatum (VS) are indicated in the cartoons. The lesion is confined to the CN in the QA8. In QA4, the lesion is visible in the CN, P and VS on the right side. There is also some hyperintensity visible in the CN and VS on the left side from the first lesion in this sheep. cc = corpus callosum





**Figure 3.2 Ventricular enlargement is seen after QA lesions.** Examples of MRI T1MPRAGE coronal slices showing enlargement of the lateral ventricles (white arrows) and corresponding atrophy of the caudate nucleus in a QA-lesioned sheep (QA5) with bilateral lesions. Lesions are visible as hyperintensity in the caudate nucleus (white arrow heads in lower right image). No change in ventricle volume is seen in the matched control saline-treated (Control 6) sheep. Images are taken from scans conducted at two time points, pre-surgery and sixteen weeks after the first surgery (bilateral lesion).

Sheep ID	Pre-Surgery		One week (unilateral)		Five weeks (bilateral)		Sixteen weeks (bilateral)	
	R	L	R	L	R	L	R	L
QA1			No MRI					
QA2								
QA3								
QA4								
QA5								
QA6								
QA7								
QA8								
Control 1								

**Figure 3.3 Morphological change in the caudate nuclei and lateral ventricles of sheep with quinolinic acid lesions of the striatum.** MRI T1-MPRAGE mid-lesion coronal slice showing morphology of the lateral ventricles and caudate nucleus in the sheep with QA lesions of the caudate nucleus at four time points: Pre-surgery, one week after the first surgery (left caudate nucleus lesioned), five weeks after first surgery (one week after right caudate nucleus lesioned) and sixteen weeks after the first surgery. Note that sheep QA1 did not have a MR scan after the first surgery. QA lesions are visible as regions of white hyperintensity. Central black regions in each image are the lateral ventricles. A representative control sheep is included for comparison. No region of hyperintensity or enlargement of the ventricles were visible in any of the control sheep at any time point.

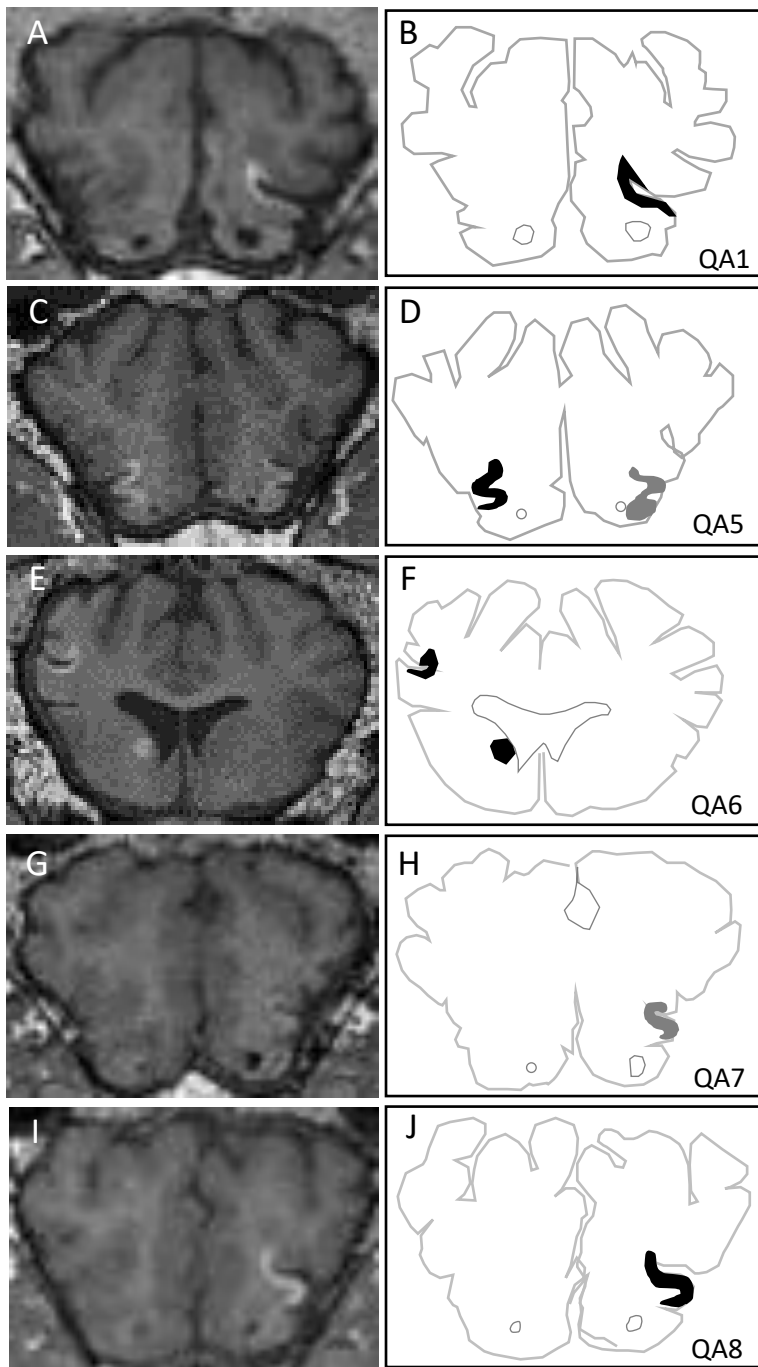
There was no clear relationship between the neurological examination findings and striatal lesion size. One sheep with comparatively severe hindlimb dysfunction, evident during both post-surgical neurological examinations, had only a small lesion evident on MRI (QA8; Figure 3.1). The sheep with upright fetlocks during surgical recovery had the largest bilateral lesions evident on MRI (QA5; Figure 3.2), yet was one of the least clinically affected sheep on neurological examination. Table 3.3 provides a subjective ranking of striatal lesion volume per sheep and neurological examination findings. There was also no relationship between neurological examination findings and striatal lesion location. Two sheep (QA4, QA5) had large bilateral lesions affecting the caudate nucleus, putamen and ventral striatum. Despite lesioning of similar structures, their clinical presentation was different, with one of the two sheep (QA4) presenting with milder clinical signs during surgical recovery yet significantly more clinical findings during the neurological examination. Two sheep (QA2, QA3) had caudate nucleus-only lesions on both sides with only one of the two sheep (QA3) displaying clinical signs during the unilateral neurological examination. Of the two sheep, the same sheep (QA3) displayed significantly more clinical findings during the third neurological examination (after both sides had been lesioned).

**Table 3.3 Subjective ranking of QA lesion volume and neurological examination severity for comparison**

Sheep ID	Subjective ranking <sup>1</sup>	
	Combined lesion volume <sup>2</sup>	Neurological exams
QA1	2	4
QA2	5	2=
QA3	4	6
QA4	7	5
QA5	8	2=
QA6	3	1
QA7	6	7
QA8	1	8

<sup>1</sup> Subjective ranking: combined lesion volume, 1= smallest, 8=largest; neurological exam, 1=least affected, 8=most affected. <sup>2</sup>Based on data in Table 3.2.

Finally, the veterinary neurological examinations were unable to identify a phenotype associated with the cerebral cortex pathology (Fig. 3.4). Lesioning of the striatum was the most important factor for the development of clinical signs detectable using a veterinary neurological examination. During the neurological examination conducted after the first surgery, four QA-lesioned animals had clinical signs detected, with hindlimb dysfunction identified in three of those four animals (QA2, QA3, QA4), and decreased ear tone and sensation identified in one animal (QA5). None of the three sheep with hind-limb dysfunction had cortical pathology in addition to striatal pathology. QA5 had additional cortical pathology, however the clinical signs exhibited by QA5 are consistent with a recognised stereotactic frame complication due to the ear bar-induced facial nerve inflammation rather than cortical dysfunction. During the neurological examination conducted after the second surgery, clinical signs were found in seven out of eight sheep. Three of the five sheep with pathology of the cerebral cortex (QA6, QA8, QA5) incurred the lesions during the second surgery (QA5 developed cortical pathology after both surgeries, ipsilateral to the surgeries). No clinical signs were detected during the neurological examination of QA6. QA8 and QA5 had evidence of hindlimb dysfunction, as seen prior to the cortical pathology and also in sheep without cortical lesions.



**Figure 3.4 Pathology of the cerebral cortex seen in addition to QA lesions of the striatum.** Examples of MRI T1MPRAGE coronal slices (A,C,E,G,I) from each animal showing hyperintensity of the cerebral cortex. Hyperintensity was on the side ipsilateral to the striatal injection site (that is not necessarily in the section). The section from each animal were chosen to show the highest intensity of cortical hyperintensity. B,D,F,H and are stylized cartoons of the sections with regions of hyperintensity shaded in black / grey.

### 3.4 Discussion

This study evaluated the usefulness of a veterinary neurological examination for identifying and characterising clinical signs in sheep with striatal lesions, principally affecting the caudate nucleus. All animals had lesions of the striatum while a smaller number showed additional hyperintensity of the cerebral cortex. The results suggest that a neurological examination is a reasonable method for detection of sheep with bilateral striatal lesions, though it is unreliable for identification of sheep with unilateral striatal lesions. The neurological examination was poor at identifying behavioural changes relating to rostroventral and rostralateral cortical pathology and poor at characterising the magnitude or extent of striatal or cortical pathology.

Therapeutic research ideally targets pre-clinical or early-clinical disease phases. We created a degree of striatal and cortical pathology that produces a normal-appearing phenotype, unless the sheep was interrogated or provoked. Careful neurological evaluation identified a characteristic phenotype associated with bilateral striatal lesions. This consisted of mild hindlimb paresis, mild hindlimb proprioceptive deficits and evidence of laterality with either spontaneous or handling-induced rotation in one direction or reluctance to turn in one direction.

There were a number of clinical signs identified in control sheep, which may be due to pathology associated with the saline infusion or may (more likely) reflect the subjective nature of the veterinary neurological examination. Clinically evident unilateral QA-lesioned and bilateral QA-lesioned sheep had the same characteristic phenotype, with the phenotype being more pronounced in bilateral-lesioned sheep. Four sheep frequently rotated one or both hindlimbs when standing. The rotation occurred without muscle contracture and appeared to be proprioceptive rather than dystonic. There was no evidence of the spontaneous chorea, dyskinesia or dystonia that has been reported in primates (Kanazawa et al. 1986, Burns et al. 1995). Spontaneous chorea, dyskinesia and dystonia in primates typically resolved over time. Failure to identify these motor abnormalities in sheep during the neurological examinations may reflect the delay between surgical lesioning and neurological

examination. Lack of spontaneous chorea, dystonia or dyskinesia in our study may also reflect our choice of dose of QA. The investigator (AO'C) selected a dose that would produce sheep with subtle symptomology reflecting an early stage of HD (as outlined in Chapter 2.4 and Appendix A), and this may not be large enough to cause chorea, dystonia or dyskinesia.

Two sheep had mild cranial nerve deficits after the unilateral surgery, specifically reduced pinna tone. CNVII (the facial nerve) disease can result in reduced pinna tone and can occur secondary to middle ear inflammation (de Lahunta and Glass 2009). Pinna tone was normal in these sheep at the final neurological examination. The author (AO'C) believes the cranial nerve deficits were a surgical complication resulting from ear bar placement and not part of the pathological striatum phenotype in sheep.

Laterality can result from differences in dopamine levels between the two striatae of an individual (Zimmerberg et al. 1974). Laterality, either spontaneous or induced, is a variable clinical feature in rodents and primates with excitotoxic lesioning of the striatum (Rothman and Glick 1976, Hantraye et al. 1990, Kendall et al. 2000). Lower limb motor dysfunction, especially dystonia, has been identified in primates with excitotoxic lesions of the striatum (Brouillet et al. 1995, Palfi et al. 1996) however paresis of the lower limbs has not been reported previously. Postural deficits are consistent with lesions of the extrapyramidal tract and are common in basal ganglia disorders like HD and PD (Salomonczyk et al. 2010, Erro and Stamelou 2017).

The neurological examination was an unreliable modality for detection of unilateral striatal lesions with clinical signs detected in only four out of eight sheep after unilateral surgery, despite lesions being evident on MRI. The difficulty of unilateral striatal lesion detection in sheep is consistent with other species: NHPs typically appeared unaffected or display mild, transient clinical signs following unilateral excitotoxic lesioning (Kanazawa et al. 1986, Hantraye et al. 1990, Burns et al. 1995) necessitating the use of dopaminergic agonists to induce clinical signs; while rodents with



unilateral QA lesions of the striatum required sophisticated quantitative behavioural tests principally involving complex reaching tasks (Whishaw et al. 2007, Klein et al. 2013) for reliable detection.

Rodents and primates display bilaterality in their extrapyramidal pathways with approximately 10-20% of basal ganglia output neurons projecting to the contralateral thalamus (Hazrati and Parent 1991, Christensen et al. 1999). The crossover of basal ganglia output neurons allows the unaffected basal ganglia to compensate for and mask clinical symptomology following a unilateral striatum lesion (Kellinghaus et al. 2003). While the bilaterality of extrapyramidal pathways in sheep is unknown, the assumption of crossover in the efferent pathways of the basal ganglia of sheep, as in rodents and primates, would mean the unaffected basal ganglia could compensate for and mask unilateral striatal lesions, potentially necessitating a more sensitive method of detection of striatally related neurological dysfunction than allowed by the veterinary neurological examination used in this study. The neurological examination detected all sheep with well developed bilateral lesions evident on MRI, though no clinical signs were detected in the sheep that had a large lesion in the right caudate nucleus and a small lesion in the left caudate nucleus. The ability of the neurological clinical examination to detect bilateral striatum lesions likely reflects a loss of bilateral pathway compensation.

Due to the difficulty associated with stereotactic placement in the sheep brain (van der Bom et al. 2013), delivery of QA to and pathology of extra-striatal sites was anticipated, as occurs in similar primate studies (Burns et al. 1995, Kendall et al. 2000, Clarke et al. 2008). The inability of the neurological examination to detect cortical pathology in the QA-lesioned sheep likely reflects the exact structures lesioned, the mainly unilateral nature of the cortical pathology, associated plasticity of the brain following injury (Kou and Irajji 2014, Dall'Acqua et al. 2017) and the motor bias of the veterinary neurological examination. The anterior insular cortex was the principal cortical structure lesioned in those sheep with cortical pathology, with variable lesioning of the gyrus rectus, orbital-frontal cortex, anterior cingulate gyrus, lateroventral sygmoideal cortices and lateroventral sylvian

cortex. These cortices have a wide range of prescribed functions (Meyer et al. 2005, Apps and Ramnani 2014, Leonard et al. 2016, Gogolla 2017, Rudebeck et al. 2017, Schneider and Koenigs 2017), however they tend to be non-motor functions. The primary motor cortex is located within the frontal lobe, medial and posterior to the structures lesioned (Johnson et al. 2019).

The relationship between the proportion of a sheep's total striatal area that was-lesioned and the associated symptomology was poor, even in bilaterally-lesioned sheep. For example, one sheep had the largest lesion in both the left and right striatum yet was one of the least clinically affected of the bilaterally-lesioned sheep, while another sheep with similar sized lesions displayed marked laterality and evidence of hind limb paresis. NHP studies have found that the association between lesion size and clinical signs is also not straightforward and that very large lesions involving 60% of the striatum or greater can paradoxically be associated with less choreic movement than smaller lesions (Kanazawa et al. 1990). The four week delay between the left and right striatal lesions may have allowed resolution of acute reversible neuropathology on one side at the time of second lesion and the opportunity for brain plasticity mechanisms to reduce symptomology (Chen et al. 2010, Buch et al. 2017).

The region of the striatum consistently lesioned was the head of the caudate nucleus, with inconsistent involvement of the putamen and ventral striatum. No association was identified between lesion location and the clinical profile. NHP studies have found that lesion location is important for the development of dyskinesia and rotational behaviour in primates, with putamen lesions associated with motor dysfunction (Burns et al. 1995, Kendall et al. 2000). Assuming sheep display similar topographical regionality as primates, more extensive lesioning of the sheep putamen may result in a greater range and severity of clinical signs detectable by neurological examination. Notably, the topography of the striatum is heterogeneous and includes a large number of functional subdivisions (Ogawa et al. 2018). Thus, even slight variation in lesion placement or size between

striatae may impact different functional sub-divisions, potentially resulting in different symptomology.

### 3.5 Conclusion

In summary, this study evaluated the use of a veterinary neurological examination as a method of phenotype identification and pathology characterisation in sheep with significant excitotoxic lesions of the striatum and cortex, principally affecting the caudate nucleus of the striatum. A phenotype was identified consisting of mild hindlimb motor dysfunction and laterality, however the diagnostic sensitivity of the veterinary neurological examination was moderate. The phenotype appeared to be associated with the striatal lesions, with it being more evident after bilateral striatal lesioning.

Characterisation of the proportion or region of the striatum and cortex lesioned was not possible in this study using a standard veterinary neurological examination. To ensure we can comprehensively evaluate striatal symptomology and pathology in sheep, more specific neurological tests of striatal dysfunction need to be developed.

## 4 Rotation and discrimination

---

Chapter 4 is based on a manuscript currently under peer-review:

O'Connell A, Sinnott B, Kuchel TR, Perumal SR, Hemsley KM, Morton, AJ. 2019. Rotation and discrimination learning studies in sheep (*Ovis aries*) with quinolinic acid lesions of the neostriatum. Submitted to Brain Research Bulletin 19<sup>th</sup> December 2019.

### Statement of authorship

Title of Paper	Rotation and discrimination learning studies in sheep ( <i>Ovis aries</i> ) with quinolinic acid lesions of the neostriatum.
Publication Status	<input type="checkbox"/> Published <input type="checkbox"/> Accepted for Publication <input checked="" type="checkbox"/> Submitted for Publication <input type="checkbox"/> Unpublished and Unsubmitted work written in manuscript style
Publication Details	<u>O'Connell A</u> , Sinnott B, Kuchel TR, Perumal SR, Hemsley KM, Morton, AJ. 2019. Rotation and discrimination learning studies in sheep ( <i>Ovis aries</i> ) with quinolinic acid lesions of the neostriatum. Submitted to Brain Research Bulletin 19 <sup>th</sup> December 2019.

### Principal author

Name of Principal Author (Candidate)	Adam O'Connell		
Contribution to the Paper	Concept, planning, methodological development, experimental work, analysis, writing, article submission		
Overall percentage (%)	90%		
Certification:	This paper reports on original research I conducted during the period of my Higher Degree by Research candidature and is not subject to any obligations or contractual agreements with a third party that would constrain its inclusion in this thesis. I am the primary author of this paper.		
Signature		Date	15/01/2020

## Co-author contributions

By signing the Statement of Authorship, each author certifies that the candidate's stated contribution to the publication is accurate (as detailed above); and permission is granted for the candidate to include the publication in the thesis; and the sum of all co-author contributions is equal to 100% less the candidate's stated contribution.

Name of Co-Author	Brendan Sinnott		
Contribution to the Paper	Surgical assistant.		
Signature		Date	18/1/2020

Name of Co-Author	Tim Kuchel		
Contribution to the Paper	General advice, support and funding. <i>Dr Kuchel has passed away</i> <i>* This contribution is correct</i>		
Signature		Date	17/1/20

Name of Co-Author	Raj Perumal		
Contribution to the Paper	Performed MR scans (MR data from this manuscript was included in Chapter 3: Surgery and neurological examination, not Chapter 4: Rotation and discrimination).		
Signature		Date	15/01/2020

Name of Co-Author	Kim Hemsley		
Contribution to the Paper	Supervision, advice on all facets of the experiment, manuscript review.		
Signature		Date	17/1/20

Name of Co-Author	Jenny Morton		
Contribution to the Paper	Supervision, advice on all facets of the experiment, manuscript review.		
Signature		Date	14/1/20

## 4.1 Summary

This chapter investigates the consequences of QA-induced striatal pathology in sheep on rotational behaviour and performance in discrimination learning tasks. Two surgeries were performed, four weeks apart, on sixteen sheep. During the first surgery, QA (180 mM in 75 $\mu$ l) or the same volume of saline was infused into the left striatum; during the second surgery, the same treatment (QA or saline) was infused into the right striatum. Rotation studies were performed pre-surgically, ten days, three weeks and sixteen weeks after the first surgery. Two-choice discrimination learning was assessed in a novel apparatus twelve weeks after the first surgery. A directional bias was evident three weeks (unilateral lesion) and sixteen weeks (bilateral lesions) after the first surgery in the QA-lesioned sheep, when compared to the saline-treated sheep. However, the direction and magnitude of bias in individual sheep at any one timepoint varied markedly, making identification of QA-lesioned individuals difficult. No association was observed between net rotation and lesion characteristics. There was no difference between saline-treated and QA-lesioned sheep in their ability to learn the acquisition and reversal phases of the two-choice discrimination learning task. These results indicate that rotation studies are a more sensitive technique than two-choice discrimination learning tasks for identification of striatal lesions in sheep. However, alternative techniques to those investigated in this study are required in sheep to identify and characterise striatal lesions comprehensively. Excitotoxic lesioning of the sheep striatum produces a variable phenotype, consistent with HD patient symptomology. Further research is required to establish the relationship between lesion characteristics and phenotype.

## 4.2 Background

Locomotor activity abnormalities and discrimination task deficits have been demonstrated in QA-lesioned rodents (Ayalon et al. 2004, Giorgetto et al. 2015, Morales-Martinez et al. 2017) and NHPs (Clarke et al. 2008). Measuring the magnitude and direction of net rotation, or directional bias, in response to dopamine agonists has been shown to be an effective method for identifying and

characterising striatal lesions in rodents (Ungerstedt and Arbuthnott 1970, Hudson et al. 1993) although lesion size and location is important (Norman et al. 1992, Fricker et al. 1996) and results are variable in NHPs (Kendall et al. 2000). Sheep are capable of striatal dependent two-choice discrimination tasks (Morton and Avanzo 2011), however the effect of brain lesion(s) on discrimination learning in sheep has not been determined previously.

The first aim of this study was to describe a technique for performing dopamine agonist mediated rotation studies in sheep. The second aim of this study was to investigate the ability of dopamine agonist mediated rotation studies to identify and characterise striatal pathology in QA-lesioned sheep. The third aim was to perform two-choice discrimination tasks in the QA-lesioned sheep to determine if they have cognitive decline. The studies expand our understanding of the phenotypic consequences of lesioning the sheep striatum with QA and further develop the toolkit for assessing striatal lesions in sheep.

## 4.3 Results

### 4.3.1 Rotation

At three weeks after the first surgery, net rotation in response to apomorphine was significantly greater in QA-lesioned than in saline-treated ( $p = 0.04$ ; Fig. 4.1C) or pre-surgical control sheep ( $p < 0.01$ ; Fig. 4.2B), indicating that the QA-lesioned sheep showed a propensity to rotate more in one direction. Table 4.1 shows the mean rotation for the QA-lesioned and saline-treated sheep at each timepoint. There was no difference in apomorphine-induced net rotation between QA-lesioned, saline-treated or pre-surgical control sheep ten days after the first surgery ( $p = 0.11$ ; Fig. 4.1A,B and Fig. 4.2).

However, there was an appreciable increase in the spread of QA-lesioned individual sheep responses after apomorphine, compared to saline-treated sheep (Fig. 4.1B). Interestingly, apomorphine-induced net rotation was significantly increased in QA-lesioned sheep sixteen weeks after the first surgery, compared to the saline-treated ( $p = 0.04$ ; Fig. 4.1D) and the pre-surgical

control ( $p < 0.01$ ; Fig. 4.2B) sheep, indicating that, despite a lesion in the contralateral striatum, a directional bias still existed in the QA-lesioned sheep with mature lesions.

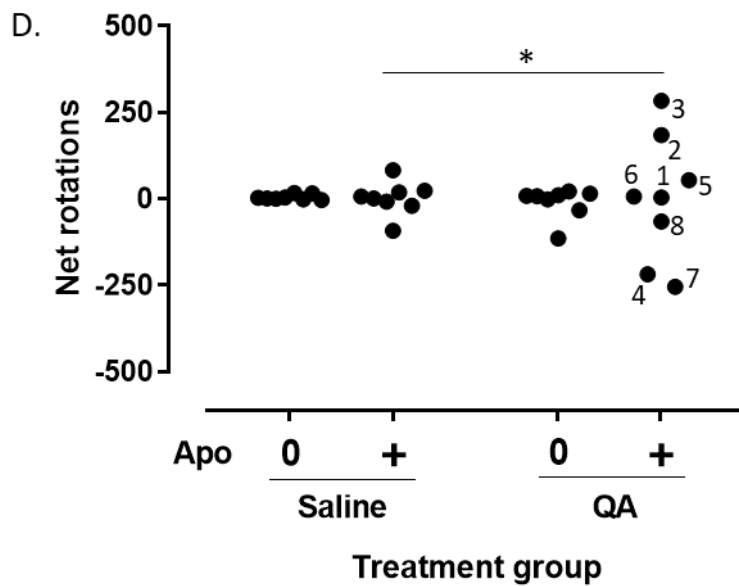
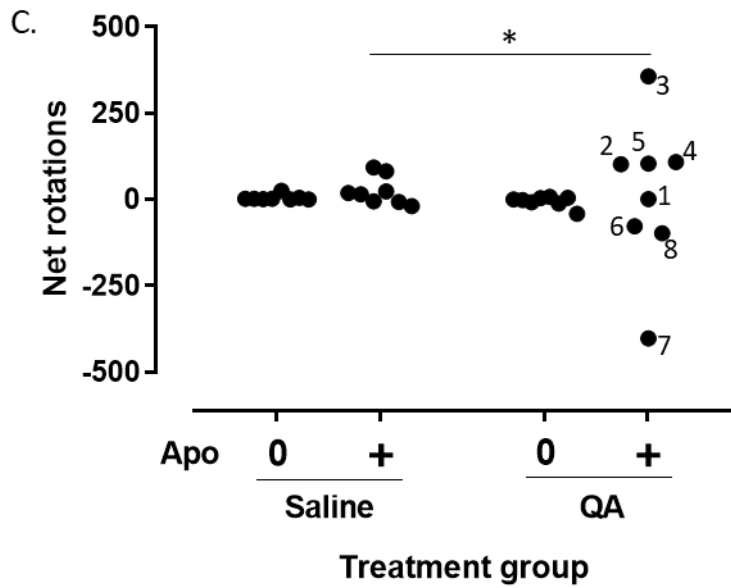
**Table 4.1 Mean net rotation for each time period for saline-treated and QA-lesioned sheep**

Treatment Group	Time Period	Number of rotations (Mean $\pm$ SEM)	95% Confidence Interval	
			Lower Bound	Upper Bound
Saline-treated	Pre-surgical	16 $\pm$ 10	-6	38
	Ten days	31 $\pm$ 28	-28	91
	Three weeks	28 $\pm$ 37	-51	108
	Three months	26 $\pm$ 26	-30	82
QA-lesioned	Pre-surgical	27 $\pm$ 10	5	49
	Ten days	99 $\pm$ 28	39	158
	Three weeks	146 $\pm$ 37	67	226
	Three months	107 $\pm$ 26	51	163

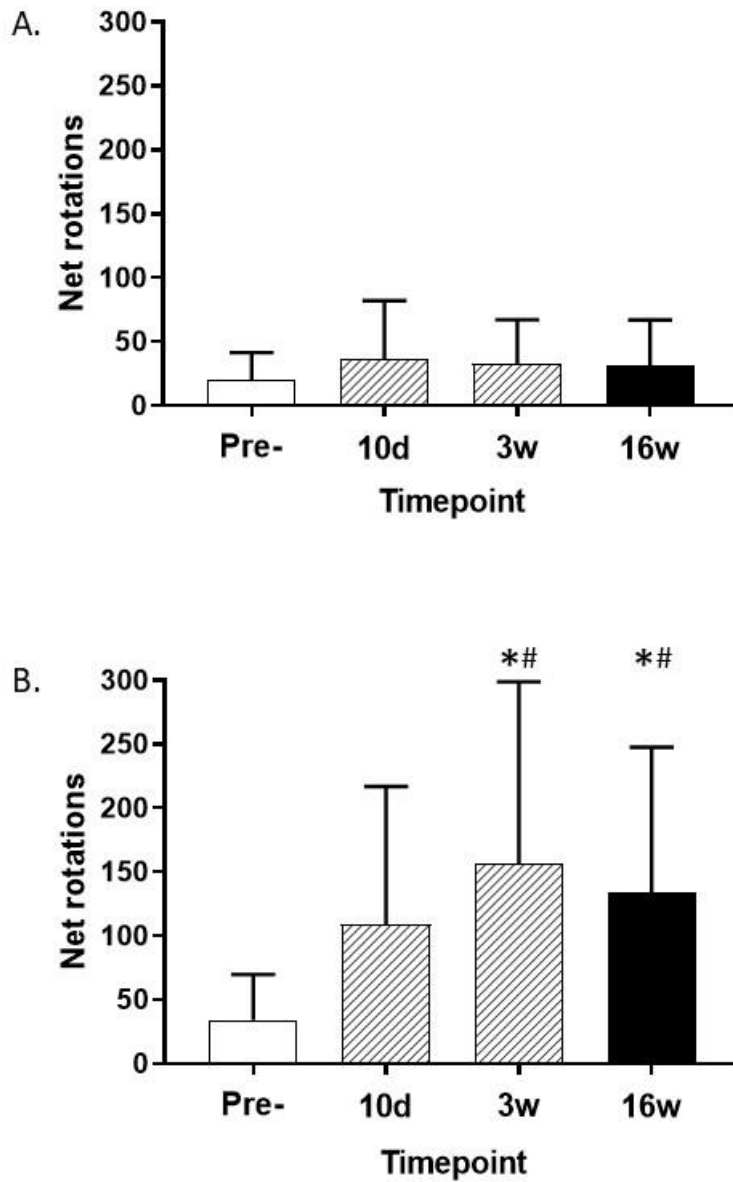
SEM = standard error of the mean







**Figure 4.1 C-D Net rotational activity in saline-treated and quinolinic acid-lesioned sheep.** Net anticlockwise rotation (ipsilateral to the first surgery) is shown as a positive, net clockwise rotation (contralateral to the first surgery) as a negative. Net rotation measured in the 60 minutes immediately prior (0) to apomorphine (Apo) administration and for 60 minutes immediately after 0.1 mg/kg apomorphine hydrochloride (+) is administered. Data are shown from testing three weeks after the first surgery (C) and sixteen weeks after the first surgery (D). Individual QA-lesioned sheep are labelled for QA +. \*  $p < 0.05$ .



**Figure 4.2 Mean net rotation in saline-treated and quinolinic acid-lesioned sheep.** Mean pre-surgical net rotation (Pre-) is compared with mean post-surgical net rotation at three time points, ten days (10d) after the first surgery, three weeks (3w) after the first surgery and sixteen weeks (16w) after the first surgery in (A) saline-treated and (B) QA-lesioned sheep. Data are mean + SD. \*  $p < 0.05$  compared to saline-control sheep, #  $p < 0.01$  compared to pre-surgical control sheep.

There was no clear relationship between the lesion location or volume (Table 4.2) and magnitude or direction of net rotation. For example, QA1, who had a large lesion of the caudate nucleus and putamen on the right side, displayed no directional bias (Fig. 4.1B-D). QA3, with a medium sized lesion of the caudate nucleus on both sides, showed little directional bias ten days after the first surgery then a large ipsilateral bias in direction three weeks after the first surgery which was maintained sixteen weeks after the first surgery (Fig. 4.1B-D). QA2, who had similar lesions, in size and placement, to QA3, showed subdued directional ipsilateral bias at three weeks after the first surgery, compared to QA3, and a smaller directional bias at sixteen weeks after the first surgery (Fig. 4.1C-D). QA6 had a small lesion of the caudate nucleus after the first surgery, yet had a larger directional bias than QA2 and QA3 at ten days and in the opposite direction, with a decrease in magnitude of net rotation at three weeks and sixteen weeks (Fig. 4.1B-D). QA4 and QA5, with a large lesion of the caudate nucleus, putamen and ventral striatum on both sides, showed modest ipsilateral rotational activity at ten days and three weeks after the first surgery (Fig. 4.1B-C). QA5 showed little directional bias at sixteen weeks after the first surgery while QA4 showed a large contralateral bias in net rotation at sixteen weeks (Fig. 4.1D). There was no difference in rotation between sheep with and without lesions of the cerebral cortex ( $p = 0.38$ ).

The primary investigator correctly predicted 5 / 8 QA-lesioned sheep and 0 / 8 of the control sheep as 'likely to be QA-lesioned' based on net rotation. Five of the eight saline-treated sheep were correctly predicted as saline-treated; however, one QA-lesioned sheep was predicted to be saline-treated. Three saline-treated sheep and two QA-lesioned sheep were unable to be subjectively classified based on their rotational data (Table 4.2).

**Table 4.2 Lesion characteristics and subjective prediction of experimental group**

<b>Animal ID</b>	<b>Side</b>	<b>Lesion location<sup>1,2</sup></b>	<b>Lesion size<sup>2,3</sup></b>	<b>Subjective prediction of experimental group<sup>4</sup></b>
QA1	Left	VS, IC, GR, Ci	n/a	Saline
	Right	CN, P, GR, Ci	Large	
QA2	Left	CN	Medium	QA
	Right	CN	Medium	
QA3	Left	CN	Medium	QA
	Right	CN	Medium	
QA4	Left	CN, P, VS	Large	QA
	Right	CN, P, VS	Large	
QA5	Left	CN, P, VS, IC, GR	Large	Unsure
	Right	CN, P, VS, IC	Large	
QA6	Left	CN	Small	Unsure
	Right	CN, P, VS, IC, GR, OF, Sy, Si	Medium	
QA7	Left	CN, P, VS, IC	Large	QA
	Right	CN, P	Large	
QA8	Left	CN, VS, IC	Small	QA
	Right	None	n/a	
Control 1	Left	None	n/a	Saline
	Right	None	n/a	
Control 2	Left	None	n/a	Saline
	Right	None	n/a	
Control 3	Left	None	n/a	Saline
	Right	None	n/a	
Control 4	Left	None	n/a	Saline
	Right	None	n/a	
Control 5	Left	None	n/a	Unsure
	Right	None	n/a	
Control 6	Left	None	n/a	Unsure
	Right	None	n/a	
Control 7	Left	None	n/a	Unsure
	Right	None	n/a	
Control 8	Left	None	n/a	Saline
	Right	None	n/a	

<sup>1</sup>CN: caudate nucleus, P: putamen, VS: ventral striatum, O: olfactory tract and bulb, IC: insular cortex, GR: gyrus rectus, Ci: cingulate gyrus, OF: orbital-frontal gyrus, Sy: sylvian gyrus, Si: syngoideus gyrus.

<sup>2</sup>Based on data detailed in Chapter 3, Table 3.2 and Section 3.3.3. <sup>3</sup>Small <100mm; Medium 100-

600mmk; Large >600mm. <sup>4</sup>Based on data in Figure 4.1.

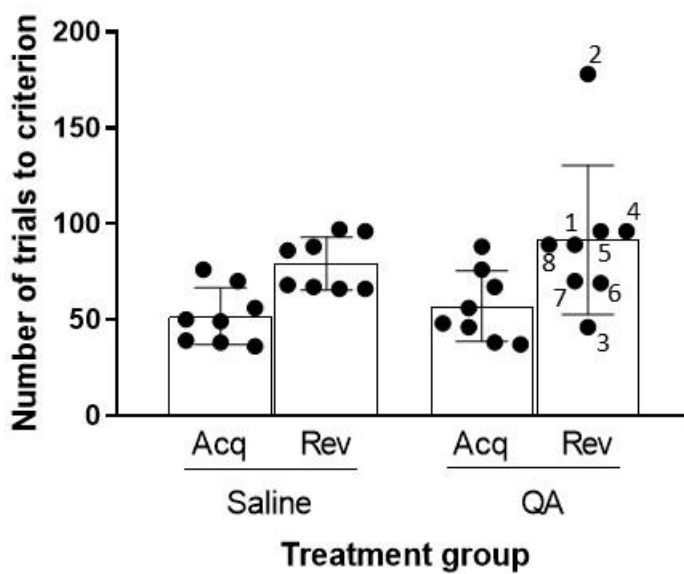
### 4.3.2 Simple two-choice discrimination learning task

All sheep learned the acquisition and reversal phases of the simple two-choice discrimination learning task. When saline-treated and QA-lesioned sheep were compared by number of sessions required to reach a criterion of two consecutive sessions of 80% or greater correct, there was no difference between saline-treated and QA-lesioned sheep for the acquisition (saline-treated cohort:  $6.6 \pm 1.9$  sessions, QA-lesioned cohort:  $7.2 \pm 2.2$  sessions,  $p = 0.55$ ) or the reversal (saline-treated cohort:  $10.1 \pm 1.6$  sessions, QA-lesioned cohort:  $10.4 \pm 4.1$  sessions,  $p = 0.88$ ). Retrospective analysis was performed using a different criterion of six discriminations correct in a row. When using this criterion, number of trials were compared instead of number of sessions. Using this criterion, there was still no significant difference for either the acquisition (saline-treated cohort:  $52 \pm 15$  trials, QA-lesioned cohort:  $57 \pm 18$  trials,  $p = 0.54$ ) or the reversal (saline-treated cohort:  $79 \pm 14$  trials, QA-lesioned cohort:  $92 \pm 37$  trials,  $p = 0.41$ : Fig. 4.3).

There was no discernible association between lesion location or volume (Table 4.2) and the ability of the sheep to learn to discriminate. For example, the first sheep to reach criterion for the reversal, QA3, had bilateral caudate nucleus lesions, while QA2, that also exhibited bilateral caudate nucleus lesions, was the slowest animal to reach reversal criterion. QA6, with a small lesion in the left striatum and medium lesion in the right striatum reached reversal criterion in 69 trials, compared with QA7, with two large striatal lesions, that reached reversal criterion in 70 trials.

Where there were sheep with concomitant cerebral cortex pathology, the cerebral cortex damage did not appear to influence the performance of the QA-lesioned sheep, when compared to the sheep with striatal lesions only, in the acquisition ( $p = 0.82$ ) or the reversal ( $p = 0.43$ ). QA2, that was much slower to achieve reversal criterion compared to any other sheep, did not exhibit any cerebral cortex pathology. In contrast both QA6 and QA7, that reached reversal criterion as quickly as the fastest saline-treated sheep, exhibited cerebral cortex pathology (Table 4.2 and Fig. 3.4).

There was no correlation between rotational behaviour and two-choice discrimination learning performance. While QA2 (the slowest sheep out of either experimental group to reach criterion in either analysis), was correctly predicted to be QA-lesioned based on rotational data, QA3 (also correctly predicted to be a QA-lesioned sheep), reached reversal criterion quickest out of both cohorts. Another sheep correctly predicted to be QA-lesioned, QA7, reached reversal criterion in the same number of trials as the fastest saline-treated sheep.



**Figure 4.3 Simple two-choice discrimination learning in saline-treated and quinolinic acid-lesioned sheep.** The mean ( $\pm$  SD) and individual number of trials required to reach a criterion of six correct choices in a row for saline-treated (Saline) and QA-lesioned sheep (QA) during acquisition (Acq) and reversal (Rev). Individual QA-lesioned sheep are labelled for the reversal.

## 4.4 Discussion

This study evaluated rotational activity and executive decision-making capability in sheep with QA-induced primary striatal and secondary cerebral cortex lesions. An experimental sheep model with bilateral striatal lesions has not been created previously. Loss of cognitive adaptability and altered motor behaviours are a feature of many neurodegenerative conditions, including HD (Roos 2010), and are associated with striatal and cortical lesions in rodents and NHPs (Roitberg et al. 2002, Clarke et al. 2008, Lindgren et al. 2013, Mishra and Kumar 2014). Results in this study indicate that while net rotation in a cohort of sheep with lesions of the striatum is significantly different to that of saline-treated sheep, there is substantial individual variation in rotational activity. Neither unequivocal identification of lesioned sheep nor characterisation of the size / locations their lesions was possible using rotation studies. Two-choice discrimination learning tasks were also unable to distinguish QA-lesioned sheep from saline-treated sheep. Sheep with excitotoxic lesions of the striatum and cerebral cortex have variable phenotypes requiring more sophisticated techniques for identification and characterisation of their lesions than those used in this study.

Apomorphine-induced rotational activity in the QA-lesioned sheep cohort after the first surgery is consistent with rodent and NHP unilateral striatum lesion studies (Jerussi and Glick 1975, Hantraye et al. 1990, Giorgetto et al. 2015). However, the marked variability in rotation is in contrast to that seen in rodents where rotation is predictable (Jerussi and Glick 1975, Antunes et al. 2013) and more similar to NHPs (Burns et al. 1995). Following infusion of QA into the striatum of rodents, there is a range of cellular, neurochemical and receptor changes that occur over an extended time course, with loss of vulnerable neurons within twenty four hours, loss of GABA<sub>A</sub> receptors at seven days and marked astrocytosis evident at one to four weeks (Brickell et al. 1999). A study which conducted longitudinal measurements of apomorphine-induced rotational activity in QA-lesioned rodents found the magnitude of the net rotational response increased until one month post-lesioning (Shemesh et al. 2010). There may have been insufficient time, at ten days after the first surgery, for the QA to



have produced cellular, neurochemical and receptor changes that would result in a significant measurable difference in net rotation.

Apomorphine-induced rotational activity in the QA-lesioned sheep after the second surgery was also significantly increased compared to saline-treated and pre-surgical control sheep. Lesion variation in this study is likely to underlie the rotation seen after the second surgery, as an imbalance in dopamine signalling between two non-identical lesions would likely exist. The sixteen weeks post-lesion rotation studies provided evidence that at least one lesion from the two surgeries produced a measurable behavioural effect. It is possible that the first surgical lesion had resolved by the sixteen week rotation study, such that the sheep was not functionally lesioned on both sides. However, evidence of motor deficits and immunohistochemical changes have been found in NHPs with chronic unilateral and bilateral QA-induced striatal lesions up-to nine months' post-surgery (Ferrante et al. 1993, Kendall et al. 2000, Roitberg et al. 2002). In the final MRI, the QA-lesioned sheep exhibited striatal atrophy and ventricular dilation on the left as well as the right side. Assuming the time-course of QA lesion resolution in sheep is similar to that of NHPs, then it is likely that the lesions from the first surgery, as well as the second surgery, are still influencing the measurement of a behavioural effect at the three-month rotation study, performed after the completion of the two-choice discrimination learning tasks.

While the magnitude of rotation in one direction was significantly greater in the QA-lesioned cohort compared to the control cohort, the direction and magnitude of individual animal rotation varied markedly amongst QA-lesioned sheep. Despite reviewing data from multiple time-points, the investigator correctly predicted the experimental group for only 5 / 8 of the sheep, which is not different to chance. Phenotypic variability between animals in response to dopaminergic agonists is also seen in NHPs with striatal lesions (Kanazawa et al. 1990, Burns et al. 1995). In those studies, the magnitude and direction of post-operative net rotation before and after dopamine agonists was affected by whether a striatal lesion was ipsilateral or contralateral to an animal's intrinsic side

preference, as well as lesion size and location within a heterogeneous striatum and the inherent propensity of an individual to rotate (Jerussi and Glick 1975, Norman et al. 1992, Hudson et al. 1993, Fricker et al. 1996, Kendall et al. 2000, Ogawa et al. 2018). In our study, no association was observed between rotation activity and lesion volume or location, which likely reflects the individual variation in propensity to rotate and the variation in lesion size and location. The lack of effect of the cerebral cortex pathology on rotation is consistent with the dopamine agonist potentiated differences in striatal dopaminergic signalling causing the rotation observed (Molochnikov and Cohen 2014).

We had predicted that the QA-lesioned sheep would have difficulty learning the reversal phase of the simple two-choice discrimination learning task. However, all sheep learnt both the acquisition and the reversal. One QA-lesioned sheep (QA2) was considerably slower than the rest of the lesioned sheep to learn the reversal, yet learned the acquisition without apparent difficulty. While this may reflect a reversal learning impairment due to the QA lesion, because it is a single animal this conclusion cannot be justified.

Discrimination learning, particularly reversal learning, is impaired in rodents (Ayalon et al. 2004, Castane et al. 2010) and NHPs (Dias et al. 1996, Clarke et al. 2008) with striatal and cerebral cortex lesions. The failure to detect a reversal learning deficit in the QA-lesioned sheep in this study does not provide conclusive evidence that sheep with caudate and cerebral cortex lesions do not develop reverse learning deficits. The QA lesions affecting the pre-frontal cortex were confined to one hemisphere. Behavioural studies in NHPs have shown that unilateral pre-frontal cortex lesions have no cognitive impact; bilateral lesions are required to initiate cognitive deficits and difficulty with reversal learning (Gaffan and Wilson 2008). Furthermore, it is possible that there was sufficient neuronal recovery in the QA-lesioned cohort at the beginning of discrimination testing to improve performance and nullify any difference between QA-lesioned and saline-treated sheep. Chronic recovery of impaired, but not dead, neurons, with a correlated improvement in behavioural tests, has been shown in QA-lesioned rodents (Shemesh et al. 2010). What is evident is that atrophy of the

striatum is consistently visible on anatomical MRI of sheep with QA lesions of the striatae, and that there is a measurable behavioural effect, using rotation studies, after discrimination testing is finished. This indicates that rotation studies, which utilise pharmacological intervention, are a more sensitive method than two-choice discrimination learning tasks for detecting striatal lesions in sheep with additional heterogeneous pathology of the cerebral cortex, but neither is adequate for assessing the consequences of striatal lesions.

## 4.5 Conclusion

In conclusion, excitotoxic lesions of the striatum can induce measurable behavioural effects in sheep, highlighting the potential usefulness of this species for studying the behavioural sequelae of neurodegeneration. More sophisticated techniques are required however, for comprehensive identification and characterisation of striatal lesions in sheep. While rotation studies are a more sensitive technique than two-choice discrimination learning tasks for the identification of striatal lesions in sheep, neither technique unmasked all individuals with lesions or provided any characterisation of a lesion. The development of variable symptomology in sheep following QA-lesioning is consistent with the variable symptomology of HD patients, however more research needs to be done to permit accurate and precise lesioning to occur and to understand the similarities and differences between species in their expression of neurodegenerative disease.

## 5 Magnetic resonance studies

---

Chapter 5 based on a manuscript currently under peer review:

O'Connell A, Kuchel TR, Perumal SR, Sherwood V, Neumann D, Finnie JW, Hemsley KM, Morton, AJ. 2019. Longitudinal magnetic resonance spectroscopy and diffusor tensor imaging in sheep (*Ovis aries*) with quinolinic acid lesions of the striatum: Time-dependent recovery of *N*-acetylaspartate and fractional anisotropy. Submitted to Journal of Neuropathology and Experimental Neurology 30<sup>th</sup> December 2019.

### Statement of authorship

Title of Paper	Longitudinal magnetic resonance spectroscopy and diffusor tensor imaging in sheep ( <i>Ovis aries</i> ) with quinolinic acid lesions of the striatum: Time-dependent recovery of <i>N</i> -acetylaspartate and fractional anisotropy.
Publication Status	<input type="checkbox"/> Published <input type="checkbox"/> Accepted for Publication <input checked="" type="checkbox"/> Submitted for Publication <input type="checkbox"/> Unpublished and Unsubmitted work written in manuscript style
Publication Details	<u>O'Connell A</u> , Kuchel TR, Perumal SR, Sherwood V, Neumann D, Finnie JW, Hemsley KM, Morton, AJ. 2019. Longitudinal magnetic resonance spectroscopy and diffusor tensor imaging in sheep ( <i>Ovis aries</i> ) with quinolinic acid lesions of the striatum: Time-dependent recovery of <i>N</i> -acetylaspartate and fractional anisotropy. Submitted to Journal of Neuropathology and Experimental Neurology 30 <sup>th</sup> December 2019.

### Principal author

Name of Principal Author (Candidate)	Adam O'Connell		
Contribution to the Paper	Concept, planning, methodological development, experimental work, analysis, writing, article submission		
Overall percentage (%)	90%		
Certification:	This paper reports on original research I conducted during the period of my Higher Degree by Research candidature and is not subject to any obligations or contractual agreements with a third party that would constrain its inclusion in this thesis. I am the primary author of this paper.		
Signature	_____	Date	15/01/2020

## Co-author contributions

By signing the Statement of Authorship, each author certifies that the candidate's stated contribution to the publication is accurate (as detailed above); and permission is granted for the candidate to include the publication in the thesis; and the sum of all co-author contributions is equal to 100% less the candidate's stated contribution.

Name of Co-Author	Tim Kuchel		
Contribution to the Paper	General advice, support and funding. <i>Dr Kuchel has passed away.</i> <i>* This is a correct record of his contribution to this paper.</i>		
Signature		Date	17/1/20

Name of Co-Author	Raj Perumal		
Contribution to the Paper	Performed MR scans.		
Signature		Date	15 / 01 / 2020

Name of Co-Author	Vicky Sherwood		
Contribution to the Paper	MR Scientist. Advice on MR capabilities, refinement of MR sequences, processing of MR data, manuscript review.		
Signature		Date	19.01.2020

Name of Co-Author	Daniel Neumann		
Contribution to the Paper	Assistance with histological processing.		
Signature		Date	15.1.20

Name of Co-Author	John Finnie		
Contribution to the Paper	Veterinary neuropathologist. Assistance with interpretation of histology. Manuscript review.		
Signature		Date	15-1-20

Name of Co-Author	Kim Hemsley		
Contribution to the Paper	Supervision, advice on all facets of the experiment, manuscript review.		
Signature		Date	17/1/20

Name of Co-Author	Jenny Morton		
Contribution to the Paper	Supervision, advice on all facets of the experiment, manuscript review.		
Signature		Date	14/1/20

## 5.1 Summary

This chapter describes the use of MRS and DTI to investigate *in vivo* metabolic and structural changes in sheep following QA-lesioning of the striatum. Sixteen sheep received a bolus infusion of QA (75  $\mu$ l, 180 mM) or saline, first into the left striatum and then four weeks later into the right striatum. MRS and DTI of the striatae was performed at four timepoints: pre-surgery, one week after the first surgery, five weeks after the first surgery and sixteen weeks after the first surgery. A linear mixed effects model was used to compare acute (one week after surgery) and chronic changes (five weeks or greater after surgery) in metabolite concentrations and FA of QA-lesioned striatae compared with unlesioned and saline-treated striatae. Compared to unlesioned or saline-treated striatae, there was a significant decrease in the neuronal marker NAA and in FA in acutely-lesioned striatae of the QA-lesioned sheep, followed by a recovery of NAA and FA in the chronically-lesioned striatae. NAA level changes indicate acute death and / or impairment of neurons immediately after surgery, with recovery of reversibly-impaired neurons over time. The change in FA values of the QA-lesioned striatae are consistent with acute structural disruption, followed by reorganisation and glial cell infiltration with time. Immunohistochemical examination of the chronic lesion supported the MRS and DTI changes, showing heterogeneous neuronal loss and gliosis visible in the QA-lesioned striatae. The study demonstrates that MRS and DTI changes in QA-sheep are consistent with HD-like pathology in other species and that the MR investigations can be performed in sheep using a clinically relevant human MRI scanner.

## 5.2 Background

A small number of QA-lesioned rodent studies have assessed lesion development with MRS and DTI, performed on very high magnetic field strength MRI scanners (Sauer et al. 1992, Strauss et al. 1997, Tkac et al. 2001, Shemesh et al. 2010). MRS is used to detect changes in the concentration of metabolites *in vivo* (Tognarelli et al. 2015). DTI is used to detect *in vivo* microstructural changes and map neural pathways by measurement of the restricted diffusion of water in tissue (Soares et al.

2013, Lope-Piedrafita 2018). FA is a measure of DTI (Alexander et al. 2007). MRS and DTI have not previously been performed in an excitotoxic large animal model. DTI and spectroscopic investigation of the normal adult sheep brain have been performed previously (Lee et al. 2015b, Gray-Edwards et al. 2018) but without a longitudinal component. Unlike *post mortem* techniques for tissue analysis, *in vivo* MR modalities, including DTI and MRS, allow the correlation of structural, functional and biochemical changes over time without having to kill study animals, or use isotopic labelling. The aim of this study was to use longitudinal MRS and DTI to assess lesion development and gross pathological change in a translational excitotoxic sheep model of HD, performed on a clinically relevant 3-Tesla MR scanner.

## 5.3 Results

### 5.3.1 Magnetic resonance spectroscopy

In the acutely-lesioned condition, there were significant decreases in NAA ( $p < 0.001$ ), TNAA ( $p < 0.001$ ) and total creatine ( $p < 0.001$ ) in the QA-lesioned compared to both the saline-treated and unlesioned striatae. An example spectrum is shown in Fig. 5.1. Additionally, there was also a significant decrease in myo-inositol ( $p = 0.028$ ) in the QA-lesioned striatae compared to the unlesioned striatae. Metabolite concentrations did not differ between the acute saline-treated striatae and unlesioned striatae (Table 5.1).

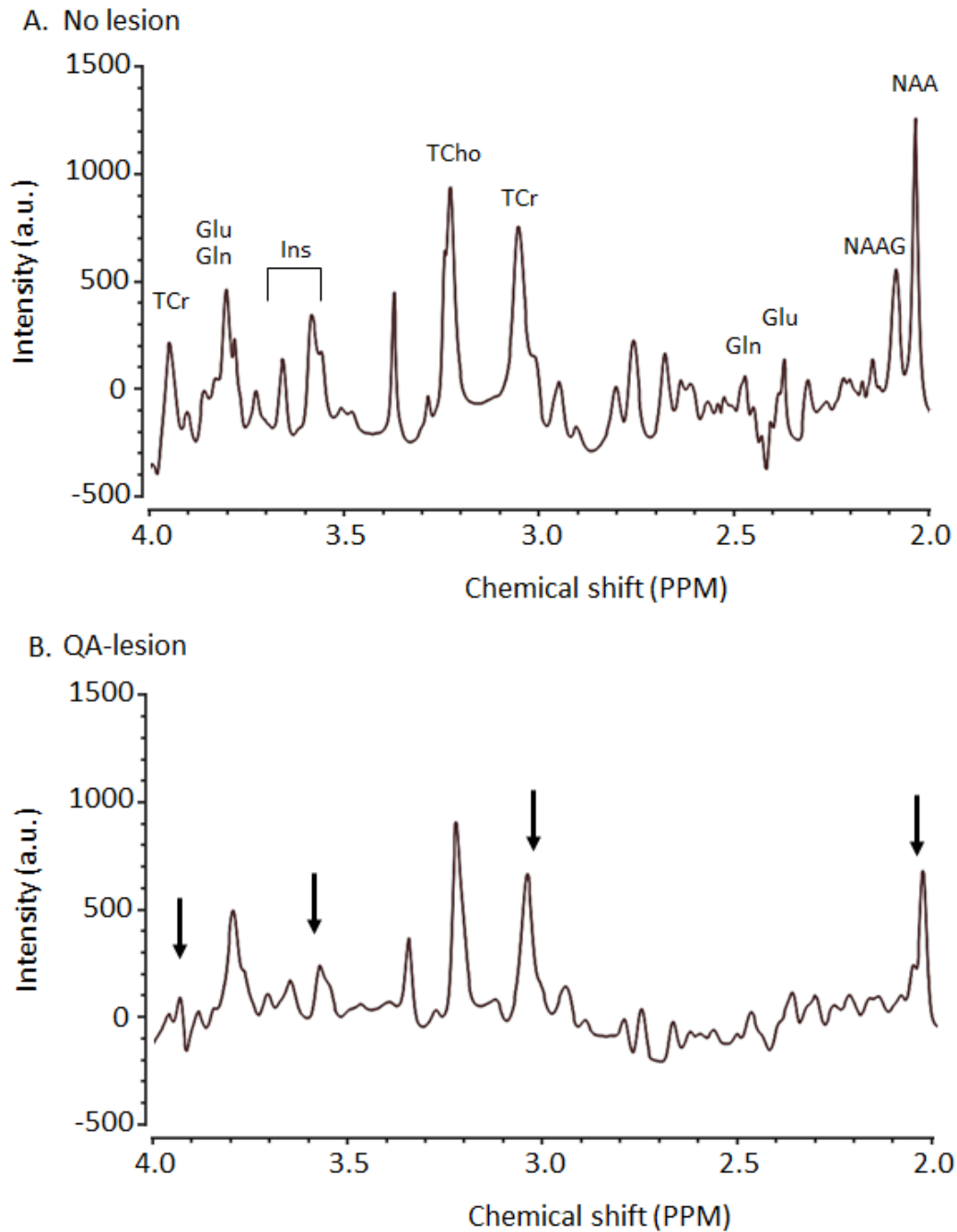
In the chronically-lesioned condition, there was no difference in metabolite concentrations between QA-lesioned and saline-treated striatae (Table 5.1). When chronic changes are compared with unlesioned striatae, NAA was significantly reduced in both saline ( $p = 0.019$ ) and QA-lesioned striatae ( $p = 0.011$ ). Myo-inositol was significantly increased in chronically lesioned QA-striatae compared to acutely lesioned QA-striatae ( $p = 0.010$ ; Table 5.1).



**Table 5.1 Mean metabolite concentration in control and quinolinic acid lesioned striatae, measured using magnetic resonance spectroscopy**

Metabolite	Metabolite concentration (mM) mean $\pm$ SEM				
	Pre-surgical	Saline		QA	
		1 week	5 - 16 weeks	1 week	5 - 16 weeks
NAA	5.52 $\pm$ 0.28	5.01 $\pm$ 0.49	4.32 $\pm$ 0.39 <sup>#</sup>	2.24 $\pm$ 0.51 <sup>#*</sup>	4.30 $\pm$ 0.39 <sup>#</sup>
TNAA	6.38 $\pm$ 0.28	6.42 $\pm$ 0.49	5.81 $\pm$ 0.36	3.44 $\pm$ 0.51 <sup>#*</sup>	6.15 $\pm$ 0.39
Gln	4.50 $\pm$ 0.55	3.31 $\pm$ 0.57	2.93 $\pm$ 0.66	3.63 $\pm$ 0.80	4.20 $\pm$ 0.67
Glu	6.62 $\pm$ 0.60	5.24 $\pm$ 0.99	5.99 $\pm$ 0.77	4.79 $\pm$ 0.95	6.89 $\pm$ 0.75
Ins	9.48 $\pm$ 0.55	8.96 $\pm$ 0.93	9.14 $\pm$ 0.70	7.03 $\pm$ 0.97 <sup>#</sup>	10.15 $\pm$ 0.76 <sup>†</sup>
TCr	7.86 $\pm$ 0.28	8.42 $\pm$ 0.50	7.63 $\pm$ 0.36	5.85 $\pm$ 0.52	8.08 $\pm$ 0.40
TCho	2.83 $\pm$ 0.14	3.10 $\pm$ 0.22	2.96 $\pm$ 0.18	2.67 $\pm$ 0.23 <sup>#*</sup>	2.79 $\pm$ 0.19

NAA: *N*-acetylaspartate, TNAA: *N*-acetylaspartate and *N*-acetylaspartylglutamate, Gln: glutamine, Glu: glutamate, Ins: myo-inositol, TCho: glycerophosphocholine and phosphocholine, TCr: creatine and phosphocreatine. <sup>#</sup> ( $p < 0.05$ ) compared to pre-surgical mean. <sup>\*</sup> ( $p < 0.05$ ) compared to saline-treated mean at the same timepoint. <sup>†</sup> ( $p < 0.05$ ) compared to QA-lesioned one week mean.



**Figure 5.1 Comparison of the magnetic resonance spectra from a representative sheep after lesioning the left striatum with quinolinic acid.** Spectra are from (A) the unlesioned right striatum and (B) the QA-lesioned left striatum one week after the first surgery. Arrows in B indicate significant changes in the corresponding metabolites labelled in A. Glutamine (Gln), glutamate (Glu), myo-inositol (Ins), *N*-acetylaspartate (NAA), *N*-acetylaspartylglutamate (NAAG), glycerophosphocholine and phosphocholine (TCho) and creatine and phosphocreatine (TCr). PPM is parts per million.

### 5.3.2 Diffusor tensor imaging and fractional anisotropy

Qualitative inspection of directional DTI maps revealed an apparent reduction in the size and integrity of fibre tracts in acute QA-lesioned (Fig. 5.2 D,F) compared to saline-treated (Fig. 5.2 C,E) or unlesioned striatae. By contrast, there was no visible difference in the fibre tracts of the chronically lesioned striatae and matching saline-treated or unlesioned striatae (Fig. 5.2 G,H).

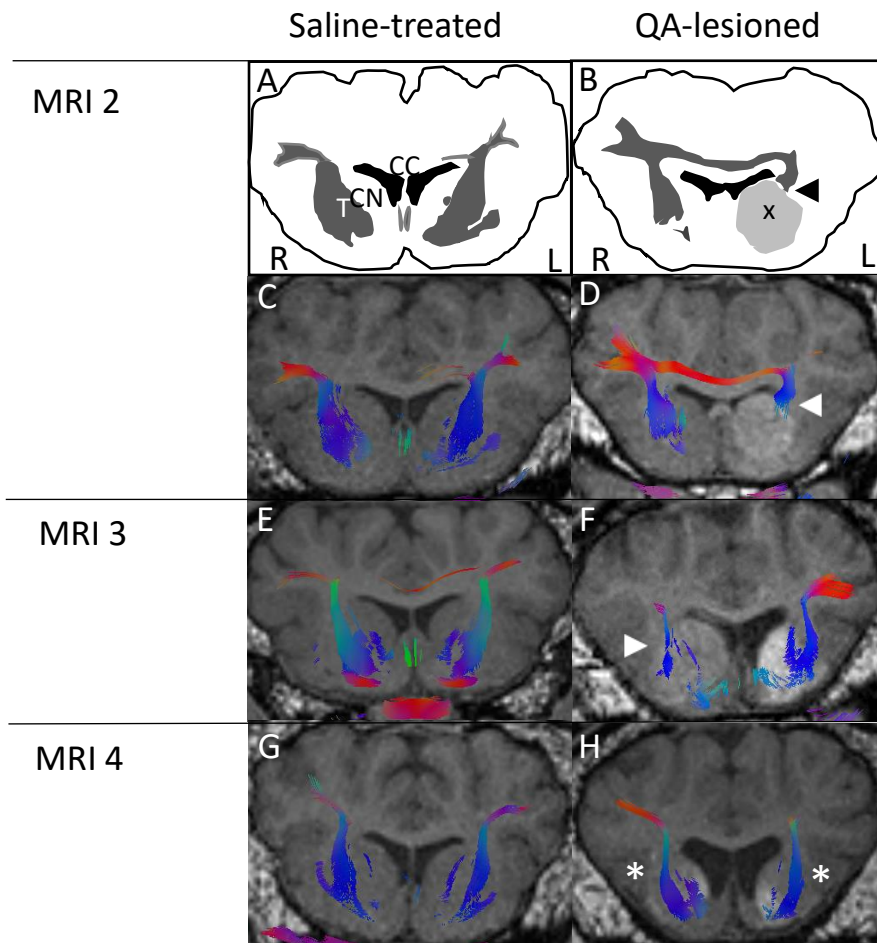
FA values were significantly decreased in acutely-lesioned compared to unlesioned ( $p < 0.001$ ) and matching saline-treated ( $p < 0.001$ ) striatae. FA values in chronically-lesioned striatae were significantly increased compared to those in unlesioned ( $p < 0.001$ ) or matching saline-treated ( $p < 0.001$ ) striatae. There was no difference between the FA values of control (unlesioned and saline-treated) striatae at any timepoint (Table 5.2).

**Table 5.2 Mean fractional anisotropy values in QA-lesioned and saline-treated sheep striatae: pre-surgery, one week after surgery (acute lesion) and five to sixteen weeks after surgery (chronic lesion)**

Experimental group (Time after lesion)	FA $\times 10^{-6}$ mm <sup>2</sup> /s		
	Mean $\pm$ SEM	95% Confidence Interval	
		Lower bound	Upper bound
Pre-surgical	320 $\pm$ 8	304	335
Saline (1 week)	327 $\pm$ 13	301	354
QA (1 week)	170 $\pm$ 11*#	144	196
Saline (5-16 weeks)	317 $\pm$ 13	296	338
QA (5-16 weeks)	396 $\pm$ 10*#	374	419

\*p < 0.05 compared to saline-treated mean

# p < 0.05 compared to pre-surgical mean



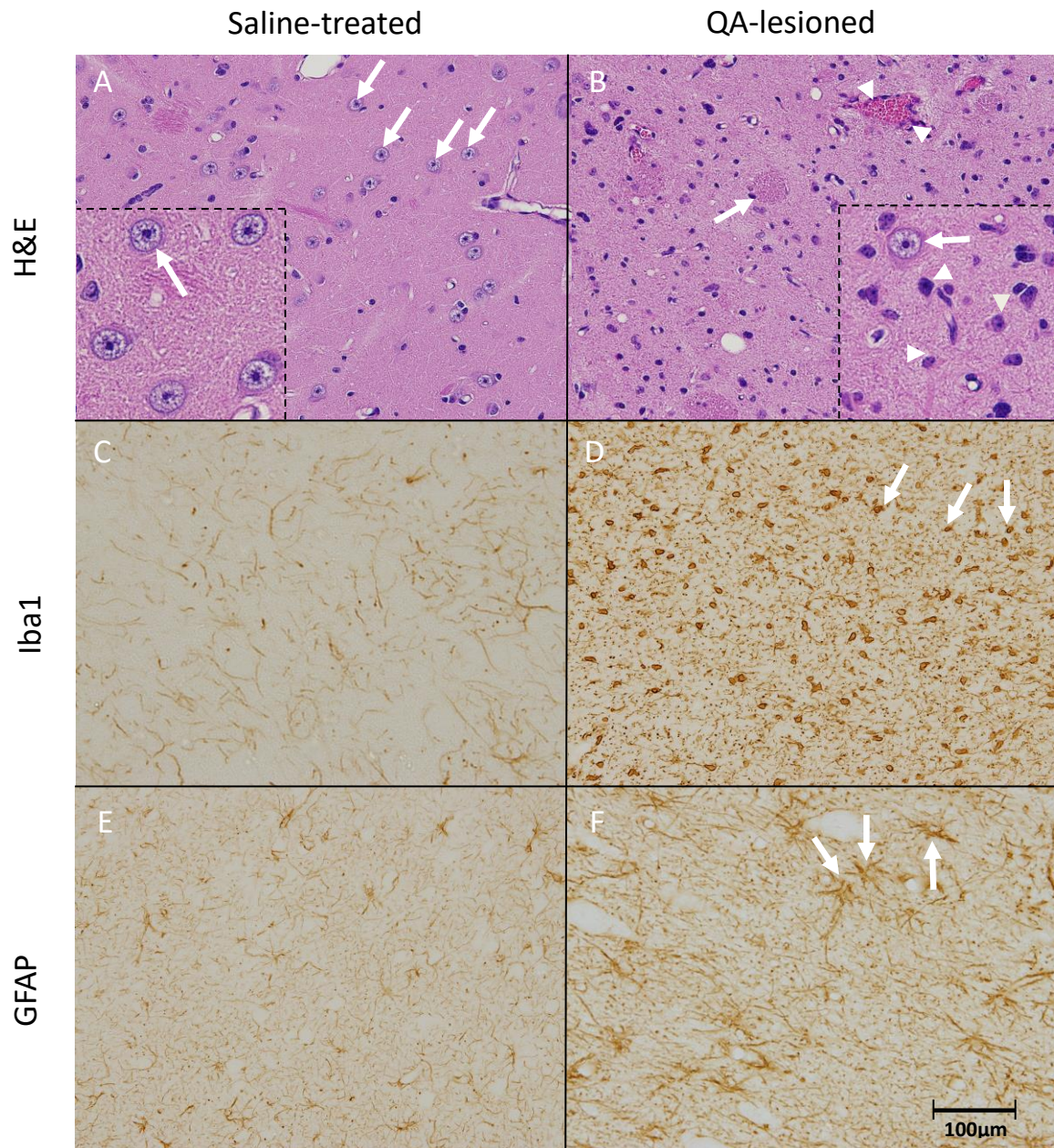
**Figure 5.2 Comparison of diffusion tracts in saline-treated and quinolinic acid-lesioned sheep after surgery.** Coronal images showing a brain slice through the caudate nucleus (CN) and putamen of two sheep. Diffusion tracts in a saline-treated (A,C,E,G) and a QA-lesioned (B,D,F,H) sheep are shown from MRI 2 (one week after the first surgery; A,B,C,D), MRI 3 (five weeks after the first surgery; E,F), and MRI 4 (sixteen weeks after the first surgery; G,H). Magnetic resonance images are T1-MPRAGE scans with diffusion tracts overlaid. Cartoons in (A) and (B) are stylized images of the scan immediately below, with the tracts shaded in dark grey. The diffusion tracts in the MRI scans are in colour (rainbow scale). The location of the caudate nucleus (CN), corpus callosum (CC) and a right-side control sheep diffusion tract (T) are indicated in (A). The QA-induced visible CN lesion is shaded in light grey (x) in (B), and a black arrowhead indicates a reduced tract on the left side. Diffusion tensor tracts are visibly disrupted (white arrowheads in D,F) in the striatae of QA-lesioned sheep on the left side in MRI 2 (D), then the right side in MRI 3 (F). By MRI 4 (H), the disruptions (\*) to the tracts are largely resolved.

### 5.3.3 Histology

Examination of the haematoxylin and eosin stained sections of the caudate nucleus of the saline-treated sheep (Fig. 5.3A) revealed an even dispersion of neurons and glial cells within the neuropil of the striatum. Neurons appeared normal, with a high nucleus to cytoplasmic ratio, nuclei being round to ovoid in shape with a prominent nucleolus and even dispersion of chromatin clumps throughout the nucleoplasm (insert in Fig. 5.3A). A variable but moderate sized, lightly basophilic to amphophilic cytoplasm surrounded the nucleus. Neurons were approximately 15  $\mu\text{m}$  in size, though an occasional neuron was disproportionately larger in size than the average neuron.

By contrast, the neuropil at the site of infusion in the caudate nucleus of each of the QA-lesioned sheep had a high density of nuclei (neuronal and glial) in the haematoxylin and eosin stained sections of the striatum (Fig. 5.3B). Traversing axons of the internal capsule were intact, as were microvessels (Fig. 5.3B). Examination of the nuclei dense region revealed a core with central necrosis of most cellular elements and occasional vacuolation of the neuropil. Immediately surrounding the necrosis was an area with marked gliosis (Fig. 5.3 B,D,F). This area was devoid of neurons. A penumbra with a gradation of heterogeneous neuronal damage and gliosis extended out from the core. A small number of neurons within the penumbra were preserved (Fig. 5.3B), however the majority displayed evidence of damage that ranged from moderate shrinkage and increased basophilic staining of the cytoplasm with a normal looking nucleus though to marked shrinkage of the cytoplasm with small hyperchromatic, pyknotic or karyolytic nuclei (Fig. 5.3B).

GFAP and Iba1 immunohistochemistry confirmed gliosis of the highly cellular regions in the QA-lesioned sheep (Fig. 5.3 D,F). QA lesions were evident as a darker stained area on gross examination of Iba1 slides, while microscopic examination revealed a large number of microglia (Fig. 5.3D). Compared to the staining observed in saline-treated sheep (Fig. 5.3E), GFAP staining of the QA-lesioned striatum (Fig. 5.3F) revealed astrogliosis with increased perinuclear staining of astrocytes and thicker processes.



**Figure 5.3 Histology of the striate in representative saline-treated and quinolinic acid-lesioned sheep.** Haematoxylin and eosin (H&E; A,B), Iba1 (C,D) and GFAP (E,F) staining of saline-treated striatae (A,C,E) and QA-lesioned striatae (B,D,F). In both (A) and the insert in (A), there are numerous neurons (examples are indicated by the white arrows) and low cellularity of the neuropil, compared to (B) which is highly cellular, with intact traversing axon bundles (white arrow) and blood vessels (white arrow heads). The insert in (B) shows a spared neuron (white arrow) amongst glial cells and degenerate neurons (white arrow heads). In contrast to (C), there are numerous microglia (examples are indicated by the white arrows) visible in (D). The astroglia in (E) are not reactive, in comparison with (F) where the astroglia have short, thick processes (examples are indicated by the white arrows). Scale bar = 100  $\mu$ m

## 5.4 Discussion

This study demonstrates for the first time with MRS and DTI, a natural history of changes that occur *in vivo* following infusion of QA in the sheep striatum to create an excitotoxic model of HD. As 3-Tesla MR scanners are routinely used for scanning human brain, demonstrating pathological changes in QA-lesioned sheep brain with this technology highlights the clinical relevance of this species for modelling neurodegenerative disease.

NAA, a nervous system-specific metabolite, is considered to be a marker of neuronal viability (Moffett et al. 2007). Decreases in NAA are thought to reflect neuronal dysfunction (Demougeot et al. 2001) and have been correlated with caudate atrophy in HD (Padowski et al. 2014). The changes in the QA-lesioned sheep striatae are consistent with those reported for QA-lesioned rodent striatae, with a reduction in NAA after QA infusion (Strauss et al. 1997, Tkac et al. 2001, Shemesh et al. 2010), followed by longer term partial recovery of NAA levels (Shemesh et al. 2010). Shemesh et al (2010) found that after lesioning the rodent striatum with QA, the majority of striatal neurons had been reversibly impaired whilst only a smaller number had undergone cell death. A similar mechanism of cell death or reversible impairment of neurons would explain the incomplete recovery of NAA in the chronically-lesioned striatae in the QA-lesioned sheep. Reduced NAA has also been observed in HD monkeys (Chan et al. 2015) and reversible impairment of striatal neurons with spontaneous partial recovery was identified in both rodents and NHPs following withdrawal of the mitochondrial toxin, 3-NP, using longitudinal MRS and immunohistochemistry (Dautry et al. 2000).

TNAA shows a similar pattern to NAA, with significant depletion in the acutely lesioned QA-striatae, followed by a longer-term recovery. Depletion of striatal TNAA has also been identified in rodents with QA lesions (Strauss et al. 1997, Tkac et al. 2001) and in HD patients (van den Bogaard et al. 2014, Sturrock et al. 2015) (Jenkins et al. 1993, Clarke et al. 1998, Jenkins et al. 1998, Sturrock et al. 2010, van den Bogaard et al. 2011). Reduction of TNAA can be explained by the significant depletion of NAA due to QA-induced neuronal impairment and loss.

The neuronal loss visible in the QA-lesioned striatae during immunohistochemical examination was consistent with the MRS-measured reduction in NAA and TNAA. Necrosis of cellular elements in the worst affected region of the epicentre with rarefaction of the neuropil is typical of QA (Beal et al. 1986, Guncova et al. 2011), while selective sparing of neurons within the heterogenous region of neuronal damage is characteristic of changes seen in both QA and HD and has been well described (Beal et al. 1986, Beal et al. 1991, Ferrante et al. 1993, Brickell et al. 1999, Ramaswamy et al. 2007).

The depletion of total creatine seen in the striatae of QA-lesioned sheep and in lesioned rodents (Strauss et al. 1997, Tkac et al. 2001) is in keeping with the findings in HD patients (Adanyeguh et al., 2018; Sanchez-Pernaute, Garcia-Segura, del Barrio Alba, Viano, & de Yebenes, 1999; Sturrock et al., 2010; van den Bogaard et al., 2014). The changes are likely to reflect impairment of energy metabolism, a consequence of both QA-induced excitotoxicity and HD (Lugo-Huitron et al. 2013). The changes in myo-inositol reflect the development of the QA-lesion with initial neuronal loss and astrocytic impairment (Ferrante et al. 1993, Feng et al. 2014), followed by the development of astrocytosis over time (Brickell et al. 1999). Immunohistochemical examination confirmed astrocytosis in the QA-lesioned striatae. Myo-inositol has been reported to be elevated in HD patients (Hoang et al. 1998, Jenkins et al. 1998, Sturrock et al. 2010), though one longitudinal study found it to decrease (van den Bogaard et al. 2014).

There is very limited, contradictory information specifically examining the cellular effect of saline injections into the brain with both localised, discrete necrosis (Robinson 1969) and neuroprotective functions described (Sabel and Stein 1982). The only significant difference in the comparison of unlesioned and saline-treated striatae was a decrease in NAA in the chronically lesioned saline-treated striatae; there was no difference in the acutely-lesioned animals, when saline-mediated necrosis would be expected. The reduction in NAA was significantly less profound than that seen in the QA-lesioned striatae, consistent with discrete localised cell death with minimal neuroinflammation, versus excitotoxic-mediated cell death in the QA-lesioned striatae. No evidence



of neuronal damage or loss was noted in the saline-treated striatae during immunohistochemical examination.

Neuron death in saline-lesioned striatae was not visible on DTI, suggesting that saline-infusion did not result in any significant loss of microstructural tissue integrity. In contrast, the acute drop in grey matter FA and disrupted DTI tracts in the QA-lesioned sheep indicate a substantial increase in the isotropic freedom of water molecules (Aung et al. 2013) which is consistent with widespread tissue disruption and central necrosis (Barbour et al. 1991, Moritani et al. 2005, Lipton 2006, Danbolt et al. 2016).

The increase in FA in the striatae of the sheep that have chronic QA lesions is consistent with the development of gliosis, as seen during immunohistochemical examination. Gliosis has been shown to be a direct cause of increased FA following a brain injury (Budde et al. 2011) while decreased freedom of water molecules has been associated with CD68 positive macrophage infiltration in rodents with QA-lesioned striatae (Shemesh et al. 2010). However, the significant increase in FA in the striatae of chronically-lesioned sheep also potentially reflects structural reorganisation and delineation of pathways due to neuronal and axonal sparing (Budde et al. 2011, Harris et al. 2016), seen histologically with the preservation of neurons in the penumbra and the sparing of the bundles of traversing axons. Neuronal and axonal sparing has also been postulated to be the cause of increased FA in the striatum of HD patients (Douaud et al. 2009, Liu et al. 2016).

## 5.5 Conclusion

This study demonstrated the feasibility of using a clinically relevant MR scanner to perform MRS and DTI on a translational excitotoxic sheep model of HD as a technique for assessing lesion development over time. There has been no longitudinal MRS or DTI examination of the diseased sheep brain previously published to our knowledge. Direct comparison with published MRS and DTI studies of rodents with QA lesions is difficult because of the differences in the MR scanners used, with small animal scanners allowing much higher resolution and sensitivity than human MR scanners.

Nevertheless, the changes shown in NAA, TNAa, total creatine and FA in the sheep are consistent with spectroscopic and DTI changes seen in QA-lesioned rodents, as well as transgenic HD NHPs and HD patients, with microstructural change due to neuronal death and gliosis. Immunohistochemical examination of the QA-lesioned sheep brain was consistent with the MRS- and DTI- detected changes, with a striatal lesion characterised by a central core devoid of neurons surrounded by a penumbra with heterogenous graded neuronal damage and gliosis. The study demonstrates the value of using sheep as a large animal model of neurodegenerative disease and illustrates the utility of using MRS and DTI at a clinically relevant field strength to examine lesion induced changes in structure and cell metabolism in sheep.

## 6 Summary

---

This is the first systematic study of unilateral or bilateral excitotoxic striatal lesions in sheep.

Lesioning the striatum with the excitotoxin QA is a well-validated HD model in rodents and NHPs (Schwarcz and Kohler 1983, Beal et al. 1986, Ferrante et al. 1993, Kendall et al. 2000) that continues to be utilised both to model striatal neurodegeneration and investigate therapeutic approaches to restoring striatal functionality (Foucault-Fruchard et al. 2018, Sánchez et al. 2018, Sumathi et al. 2018, Verma et al. 2018, Emerich et al. 2019, Lavisse et al. 2019). Other than NHPs however, no excitotoxic large animal model has been developed and assessed, despite the recognised limitations of rodent models and the need for relevant comparative animal models to improve translational success (Perlman 2016, Whitelaw et al. 2016). In order to lesion the sheep striatum, a stereotactic surgical approach was developed and is described in this thesis.

The development of the striatal lesions in the sheep brain was tracked using non-invasive longitudinal MRI. As well as anatomical MR sequences, MRS and DTI were utilised. The author is not aware of any other publication that has utilised longitudinal MRS and DTI to study neuropathology of the sheep brain. The study generated a unique set of data with over sixty 3-Tesla brain scans from sixteen sheep with unilateral and then bilateral striatal lesions.

A neurological examination specifically aimed at assessing neurological function in sheep is described. There is little published data on ruminant neurological examinations (Constable 2004, Finnie et al. 2011), and no specific description of a sheep neurological examination. The study also describes the assessment of sheep with QA-induced striatal pathology using the sheep neurological exam. In particular, the neurological exam was tested for its ability to identify striatal lesions. The QA-lesioned sheep appeared normal until interrogated. The neurological examination revealed predominantly hindlimb clinical signs that were mild in severity and, interestingly, did not correlate directly with either lesion volume or placement.

A method for quantifying rotation in sheep was developed and used to characterise striatal pathology associated with the QA lesions. There has been no previous publication of rotation studies performed in sheep with striatal lesions. Information regarding the direction of rotation in QA-lesioned sheep did not help predict the presence of a striatal lesion. The significant individual variation in rotation reduced the usefulness of rotational studies as a technique for assessing striatal lesions in sheep.

The thesis also describes the use of simple two-choice discrimination learning studies in sheep with striatal lesions. To the best of the author's knowledge, there have been no studies published describing the cognitive assessment of sheep with excitotoxic lesions of the brain. While the author expected the QA-lesioned sheep to be able to acquire the two-choice discrimination, he also predicted that the sheep would not be able to perform the reversal. However, the QA-lesioned sheep learned both components of the two-choice discrimination learning task.

## 6.1 Association between pathology and phenotype

The variable and mild phenotype in the QA-lesioned sheep may be explained by lesion variation and / or brain-repair mechanisms. The considerable inter-animal anatomical variability of sheep skulls and the lack of a brain-skull atlas meant that stereotactic placement in the striatum of the study sheep was imprecise. This was compounded by the fact that the topography of the striatum is heterogeneous with a large number of functional subdivisions (see Section 1.2; Ogawa et al. 2018). The phenotypic expression of a lesion may depend on the exact heterogeneous sub-division(s) lesioned (Norman et al. 1992, Fricker et al. 1996, Kendall et al. 2000).

As well as unpredictability of lesion placement, the left and right striatal lesions were performed one month apart to avoid adverse animal welfare effects. Brain-repair mechanisms in the first striatum to be lesioned may have influenced the functional impact of the second, bilateral, lesion. After even a mild brain injury, there is evidence of on-going structural reorganisation, functional compensation by recruitment of other brain regions and connectivity changes within the brain

continuing for at least a year (Kou and Iraj 2014, Dall'Acqua et al. 2017). Brain-repair was evident in the QA-lesioned sheep during the four month period after the first surgery when phenotypic studies were conducted. During surgical recovery, sheep that were clinically impaired showed a rapid improvement, such that they appeared functionally normal within a week of surgery.

Following acute trauma, there is an initial phase of rapid recovery associated with resolution of reversible pathological factors, including oedema related mass effects and uncontrolled neuroinflammatory factors (Chen et al. 2010, Marques et al. 2019). Proliferation of glial cells and formation of a glial scar moderates the neuroinflammatory response, restores homeostasis and creates an environment that promotes brain repair mechanisms including remodelling and plasticity (Rolls et al. 2009, Hermann and Chopp 2012). Glial cell hypertrophy is a characteristic of QA striatal lesioning (Brickell et al. 1999). Gliosis was evident *in vivo* in the QA-lesioned sheep in the MR studies described in Chapter 5. It was also evident from the immunohistochemical studies.

The restoration of NAA, a neuron marker (Moffett et al. 2007), over the four month post-surgical period, and increases in FA, a diffusion asymmetry index (Aung et al. 2013), reflect recovery of reversibly impaired neurons (Shemesh et al. 2010) and structural reorganisation, including connectivity changes and delineation of pathways (Douaud et al. 2009, Budde et al. 2011, Harris et al. 2016, Liu et al. 2016). While the final rotation study provides evidence that at least one lesion is creating a functional impact in the QA-lesioned sheep, it likely that variation and repair reduced the phenotypic impact of the lesions.

For major neurodegenerative diseases like HD, at the point at which a disease progresses from being asymptomatic to clinically evident, there is already significant neuropathology in the brains of patients. At the time of diagnosis, HD patients have significant whole-brain volume loss, ventricle expansion and striatal atrophy when compared to control patients (Tabrizi et al. 2012). Despite evidence of brain repair in the QA-lesioned sheep, there was still significant pathology evident; in the final MRI anatomical scan there is easily identifiable lateral ventricle dilation, indicating striatal

atrophy and in the *post mortem* brain, immunohistochemistry reveals widespread striatal neuron loss and gliosis (Chapter 5). What is interesting is the mismatch between the severity of the pathology and the relative paucity of detectable clinical signs in the phenotype studies described in Chapters 3 and 4. The QA-lesioned sheep appeared behaviourally to be no different from the saline-treated sheep. To provoke the mild (albeit variable) phenotype required careful veterinary neurological examination performed by experienced veterinarians and pharmacological intervention in rotation studies. However, neither technique could reliably identify QA-lesioned sheep.

Late onset neurodegenerative diseases such as HD that remain asymptomatic despite degenerative changes, illustrate the ability of the human brain to compensate for significant pathological change. Functionally normal QA-lesioned sheep illustrate the ability of the sheep brain to compensate for significant pathology, providing evidence of the value of sheep as a model of human neurodegenerative disease. Furthermore, the variability of symptoms of the QA-lesioned sheep is consistent both with HD patients as well as NHPs with striatal lesions (Hantraye et al. 1990, Burns et al. 1995). Together, these results indicate that sheep are a relevant animal model of HD.

## 6.2 Comparison with large animal quinolinic acid models

Prior to this study, NHPs were the only large animal that has been lesioned with QA to create a model of HD. Table 6.1 provides a summary of the various studies that investigated QA-lesioning of the NHPs striatum. The total number of animals in each study were very small, ranging from three (Brownell et al. 1994) to twelve (Ferrante et al. 1993, Kendall et al. 2000). Lavisse et al. (2019) utilised six QA-lesioned NHPs and up to twenty eight unlesioned NHPs in some of their cognitive tests. Eight lesioned animals and eight sham-lesion controls were utilised in the present study. Despite animal numbers being greater than all but one NHP studies, the behavioural studies described in this thesis were still underpowered. The low numbers illustrate the ethical and financial cost of large animal studies, plus the difficulty in generating significant study subjects. The majority of the NHP studies created a unilateral striatal lesion only (Ferrante et al. 1993, Brownell et al. 1994, Storey et al. 1994,

Burns et al. 1995, Kendall et al. 2000). Four studies had bilateral lesions (Burns et al. 1995, Roitberg et al. 2002, Clarke et al. 2008, Lavisse et al. 2019). Roitberg et al (2002) lesioned each striatum four weeks apart, a strategy also employed in this study.

Despite variation in species, study design and exact area targeted, there were findings across the NHP studies that were consistent with this study in sheep. In particular, both NHPs and sheep appeared functionally normal after the initial surgical recovery period. Motor abnormalities were inducible in the lesioned NHPs and sheep using a dopamine agonist, and gross anatomical lesion development in the NHPs and sheep was similar, with ventricular dilation and marked central neuronal loss and gliosis, surrounded by an area of incomplete neuron loss. The only major difference was that, unlike in this study, three NHP studies observed a decline in cognition in QA-lesioned animals (Roitberg et al. 2002, Clarke et al. 2008, Lavisse et al. 2019), though interestingly Lavisse et al (2019) found no significant difference in the simple discrimination reversal task when it was performed for the first time at six months post-surgery. The similarities provide support for functional parallels between the primate and sheep brain, and suggest that sheep can model neurodegenerative disease in a meaningful way that can be applied to humans.

**Table 6.1 Excitotoxic non-human primate models of Huntington’s disease that used quinolinic acid to lesion the striatum**

Species	Model and target	Surgical recovery	Apomorphine (motor)	Cognition	Histology / MRI
<i>Macaca mulatta</i> <sup>1</sup>	Unilateral. CN + P	Few spontaneous abnormal movements	Dyskinesia	n/a	Neuron loss, transitional zone, gliosis, ventricular dilation, axon sparing
<i>Macaca mulatta</i> and <i>fascicularis</i> <sup>2</sup>	Unilateral. CN + P	One week spontaneous dyskinesia	Dyskinesia, dystonia, rotation	n/a	Neuron loss, gliosis, axon sparing.
<i>Macaca mulatta</i> <sup>3</sup>	Unilateral. Two CN (first) + P. Three P only (one had bilateral P)	Unilateral: mild transient dyskinesia 1 week. Bilateral: marked chorea, dyskinesia for 2 days	CN: no or mild dystonia. Others: dystonia, dyskinesia, variable rotation	n/a	Lesion visible on MRI
<i>Callithrix jacchus</i> <sup>4</sup>	Unilateral. Four CN. Four P	P lesion: dystonia up to 48 hours. CN lesion: no abnormalities detected	P lesion: ipsilateral rotation, dystonia, dyskinesia. CN lesion: contralateral rotation	n/a	Neuron loss, gliosis, axon sparing, ventricular dilation
<i>Cebus apella</i> <sup>5</sup>	Bilateral, four weeks apart. CN + P	3-5 days of paresis, spontaneous rhythmic movements, poor feeding, seizures	Exacerbated posture, dyskinesia, dystonia, fine motor okay, night-time hyperactivity	Decline in object-retrieval task	Neuron loss, transitional zone, gliosis, ventricular dilation, axon sparing
<i>Callithrix jacchus</i> <sup>6</sup>	Bilateral. CN	Not discussed	n/a	Could not learn reversal task	Neuron loss, gliosis
<i>Macaca fascicularis</i> <sup>7</sup>	Bilateral. CN + P	No adverse effects	Dyskinesia (decreased motor activity)	Decline in perseverative decision making	Neuron loss, ventricular dilation

<sup>1</sup>(Ferrante et al. 1993) and (Storey et al. 1994) <sup>2</sup>(Brownell et al. 1994) <sup>3</sup>(Burns et al. 1995) <sup>4</sup>(Kendall et al. 2000) <sup>5</sup>(Roitberg et al. 2002) <sup>6</sup>(Clarke et al. 2008)

<sup>7</sup>(Lavisse et al. 2019). CN: caudate nucleus, P: putamen



### 6.3 Study limitations

As discussed in the previous section, generating a statistically well-powered sample size when conducting behavioural and surgical research studies in large animals is difficult. The present study exceeded the sample size of the other QA-lesioned large animal studies while examining motor and *in vivo* anatomical and metabolic changes in the QA-lesioned sheep and only one large animal study used more control animals during cognitive testing. The sample size in this study was also larger than that utilised in an investigation of the Tay-Sachs sheep model (Gray-Edwards et al. 2018) and larger than the sample size in two out of three of the QA-rodent MRS studies (Tkac et al. 2001, Shemesh et al. 2010). However, the sample size in the present study is still small in comparison to many rodent studies.

Under-powering of the study was compounded by the variation in the QA lesions, which was complicated by an anatomically heterogeneous striatum, though this is highly relevant when modelling the human condition. Statistically the behavioural component of the present study was under-powered. However, the anatomical MRI, DTI and MRS results were well-powered, consistent with the histological findings and often had very small p-values, therefore the author is confident of the MR results. The behavioural study data would benefit from greater power due to either larger numbers or less variable lesion placement. No relationship was found between lesion size or location and behaviour. While this may be a true result or due to the specific tests and methodology used, it is likely that more accurate lesioning or greater animal numbers would have allowed differences in the outcome of lesions made in different regions of the striatum to be apparent.

To be truly useful as an excitotoxic model, the sheep needs to be accurately lesioned. The lack of a stereotactic skull-brain atlas means that lesioning of the striatum cannot be accurately performed at the moment without the assistance of specialist imaging equipment and expertise (van der Bom et al. 2013). There are sheep brain atlases available (Ella et al. 2017, Johnson et al. 2019), however they do not provide any relationship to skull structures. Further, the sheep genotype and phenotype are

diverse, with significant variation within and between populations (Cao et al. 2015, Wang et al. 2017, Yang et al. 2018). A uniform cohort of sheep sourced from one location can still show substantial variation in the anatomy of their skulls. It is likely that any development of a skull-brain atlas in sheep will only be useful for a sub-population of sheep.

### 6.3 Future directions

One area of future experimentation is the testing of QA-lesioned sheep with more refined phenotyping procedures. The behavioural tests selected for use in this study were insensitive to significant striatal pathology. The ability to test for executive decision making ability in sheep has been extended beyond simple two-choice discrimination learning tasks, with sheep demonstrated to be capable of more complex decision making tasks, including attentional set shifting (Morton and Avanzo 2011, McBride et al. 2016). Future investigation of the decision-making capabilities of QA-lesioned sheep may reveal cognitive impairment, the caveat being to power the study appropriately.

Gait and force analysis might also prove to be more sensitive to motor deficits than the veterinary neurological examination or rotation studies used in this study. Gait analysis is established in sheep (Faria et al. 2014, Mora-Macias et al. 2015, Safayi et al. 2015). The detection of a hind limb motor deficits and increased rotation in the QA-lesioned sheep, compared to saline-treated sheep warrants further investigation. Gait analysis may detect animals with lesions of the striatum more accurately and allow the characterisation of lesions.

Hyperactivity at night has been detected in QA-lesioned rodents (Shear et al. 1998) and NHPs (Roitberg et al. 2002). Sleep disturbances are a common symptom in many neurodegenerative diseases (Cipriani et al. 2015, Ramos and Garrett 2017), while circadian rhythm disturbances have been detected in the OVT73 transgenic sheep HD model (Morton et al. 2014). An activity monitoring study was undertaken in the QA-lesioned sheep (Appendix B), however due to the difficulty of conducting the study in conjunction with other behavioural studies and data recording and download issues, the data were not of sufficient quality to warrant analysis. Activity studies in the QA-lesioned

sheep would provide further information on the capability of sheep to accurately model neurodegenerative diseases.

Finally, the traditional QA-model of HD focuses on lesioning the striatum because of the early and severe striatal pathology in HD (Vonsattel et al. 1985). However, pathological change is widespread in HD, both within and outside of the brain (Vonsattel et al. 1985). Heterogeneous cerebral cortex degeneration is a significant aspect of the HD pathology and resultant phenotype displayed by an individual (Thu et al. 2010, Waldvogel et al. 2012b, Kim et al. 2014, Nana et al. 2014) while cerebellar degeneration has been associated with the motor phenotype (Singh-Bains et al. 2019). The development of cortical pathology when lesioning the striatum with QA is consistent with NHP studies (Kendall et al. 2000, Lavisse et al. 2019) and very useful, despite the analytical complication, because it more accurately represents HD pathology. Intracerebro-ventricular infusions of QA are a well described technique for investigating whole brain excitotoxic effects (Lisy et al. 1994, Vandresen-Filho et al. 2015). Assessing the impact of intracerebro-ventricular QA infusions in combination with striatal lesions would be a potential way to extend this model and may generate a more realistic phenotypic representation.

## 6.4 Conclusion

The QA model of HD continues to be an important model for therapeutic development and studying disease mechanisms. NHPs are the gold-standard large animal neurodegenerative model due to their neuroanatomical similarity to humans, including a large brain volume and highly developed cerebral cortex (Emborg 2017). Clinical trials based only on rodent studies have poorer translational success than those that incorporated NHPs studies during pre-clinical progression (Zeiss 2017, Zeiss et al. 2017). The studies described in this thesis demonstrate that sheep have the potential to be important as large animal models of neurodegenerative disease. Sheep have large brains, that are neuroanatomically similar to primates, with a highly developed cerebral cortex and good cognitive capacity (McBride and Morton 2018, Murray et al. 2019). Sheep also provide numerous practical

advantages to NHPs, including cost, availability, ethical concern and ease of management. The experiments described here demonstrate that lesioning the sheep striatum with QA produces neuropathology that is comparable to that seen in QA-lesioned rodents and NHPs. They also show that longitudinal characterisation of QA lesions using advanced magnetic resonance modalities and phenotypic investigation of the lesioned sheep is possible. Despite its limitations, the QA-lesioned sheep represent an authentic animal model of the neurodegenerative condition, HD, that could be used for understanding disease mechanisms and evaluating therapies that modify neurodegeneration.

## 7 Appendix A: Method development

---

This appendix gives a brief overview of the method development process for the methods / studies described in the main body of the thesis. There were no applicable protocols for the methods undertaken. All methods had to be developed and optimised with a series of pilot studies.

In brief, initial surgical development was based on cadaver surgeries. Once the basic surgical method was developed, ten sheep underwent a total of nineteen surgical procedures to refine the surgical process. As well as optimisation of the stereotactic mounting position and surgical procedure, the surgical coordinates, concentration and volume of QA infusion and time between left and right striatal lesioning was adjusted after each surgery to achieve the optimal surgical method described in Chapter 2.

The first six surgical pilot study sheep were euthanised after recovery from their second surgery. Perfusion, brain removal and histological methodology was refined using these sheep. The last four surgical pilot study sheep and three non-surgical control sheep were used to develop the behavioural study methodologies.

The neurological examination utilised in Chapter 3 was developed primarily from De Lahunta's detailed canine veterinary neurological examination (de Lahunta and Glass 2009), combined with less detailed descriptions of generic (not species specific) large animal neurological examinations and the author's veterinary experience. No sheep specific veterinary neurological examination has been published previously. A two person examination was developed because it facilitated handling of the sheep as well as improved accuracy. Refinement of the location of the examination and size of the pens was very important. Because sheep are naturally flighty, larger pens were found to cause issues and potential injuries as sheep would evade handlers and become worked up. The facilities described were found to be an optimum size for keeping sheep calm and allowing procedures to be performed efficiently.

Rotation studies were developed from published rodent studies. Five pilot studies were performed with pen shape, size, location and protocol varying. The pens utilised in Chapter 4 were the optimum size pen. Circular pens were trialled, but the author was unable to construct a suitably robust circular pen. Square or rectangular pens did not appear to inhibit rotation. Pens that were too small inhibited rotation while pens that were too large made handling difficult and risked the sheep injuring themselves. For the longitudinal studies, it was important that the sheep were under cover and in a location that was free from disturbance.

The development of the discrimination study protocol and apparatus was the most time consuming and difficult of the behavioural studies described in the study. As well as fitting within existing facilities, the author needed to be able to construct the apparatus from recycled materials (due to funding constraints) and operate the discrimination studies without assistance. There were many design iterations and pilot trials performed to refine the end facility and protocol described in Chapter 4. A low stress environment, good flow and proximity of flockmates were essential. While various semi-automatic, computer based systems for symbol and reward presentation were trialled, the simple coloured bucket system was easy to use and the sheep understood the protocol faster than two dimensional symbols on computer or paper, rendering the coloured buckets the most suitable method of symbol presentation in the two-choice discrimination learning protocol. A pulley based system allowed the author to operate the maze apparatus efficiently, according to the protocol.

## 8 Appendix B: Activity monitoring

---

An activity monitoring study was undertaken on the sixteen sheep used in the main body of the thesis. Activity monitoring is a valuable tool for investigation of circadian rhythm abnormalities. Disruption of circadian rhythm with alterations in normal sleep and activity periods are clinical features of numerous neurodegenerative diseases, including Alzheimer's (Homolak et al. 2018), Parkinson's (Askenasy 2001) and Huntington's (Diago et al. 2018) disease.

Access to a scientifically valid accelerometer device (Actiwatch) used to monitor activity and provide circadian behaviour measurements was provided at the beginning of the two-choice discrimination learning study (the activity monitors were not available previously). The actiwatch had been placed inside a waterproof plastic container containing cotton wool to prevent movement of the actiwatch within the container. The plastic container was securely fixed to a large dog collar. The dog collar was placed around the neck of the sheep with the plastic container in the ventral position. The sheep were unshorn with sufficient wool growth to allow the collar to be tight around the neck, preventing artificial movement of the collar without compromising welfare. Epoch length was five minutes and recording was programmed to begin twenty four hours after the collar was placed around the neck of the sheep to prevent artificial movement recordings and allow a period of time for collar adjustments. Sheep were maintained in their group pens during recording. To prevent the influence of pen factors on activity, group pens were approximately the same size (eight by five metres) with troughs located in the same location within the pens and feed placed in the middle of the pens. Shelter was provided by trees planted in line with the border between pens. Actiwatch proprietary software was used for actogram construction. Clocklab software was available for circadian rhythm analysis.

Unfortunately, due to hardware and software issues, the data obtained was not of a sufficient quality to justify analysis.

## 9 Appendix C: Cerebrospinal fluid analysis

---

Lipidomic analysis of CSF was also performed. CSF was sampled immediately after MRI 1, MRI 2, MRI 3 and MRI 4 while the sheep were still anaesthetised. The aim was to try and identify a lipidomic marker of QA-induced striatal injury in sheep. Sixty CSF samples were collected, processed and analysed.

### 9.1.1 Cerebrospinal fluid collection

Sheep were anaesthetised according to the protocol described in Chapter 2, Section 2.5. CSF sampling was based on a standard CSF collection protocol (Scott 2010). Sheep were placed in sternal recumbency with the hind limbs projecting forwards to flex the lumbosacral region. A 10 × 10 cm area was shaved at the lumbosacral junction and aseptically prepared. Sterile surgical techniques were maintained throughout the procedure. The lumbosacral space was palpated as a midline depression between the dorsal processes of L6 and S2. A 19-gauge spinal needle was advanced perpendicular to the vertebral column, through cutaneous, subcutaneous, ligamentous and dural tissue into the subarachnoid space. Appreciation of resistance change during needle travel indicated successful location of the subarachnoid space which was confirmed by presence of CSF fluid in the needle hub. Gentle aspiration of CSF using a 2 mL syringe was performed to collect 2 – 4 mL of CSF.

### 9.1.2 Cerebrospinal fluid processing

CSF was placed on ice and transferred for immediate processing after collection, with gross appearance noted. The CSF sample was agitated for ten seconds to homogenise the CSF and 100 µl removed for RBC and WBC quantification using a haemocytometer. CSF was then centrifuged at 2,000 × g for ten minutes at 4°C to remove cells and gross appearance noted. The supernatant was transferred to a 10 mL polypropylene tube on ice and agitated for ten seconds prior to aliquoting into pre-chilled polypropylene cryovials (1.2 mL; Corning, NY, USA). Aliquoted samples were snap-frozen in liquid nitrogen and stored at –80°C.



### 9.1.3 Lipidomic analysis of cerebrospinal fluid samples

A  $-80^{\circ}\text{C}$  250  $\mu\text{l}$  aliquot of CSF was thawed, agitated and 200  $\mu\text{l}$  was aliquoted into a centrifuge tube (Eppendorf, Hamburg, Germany). 10% Methanol, 800  $\mu\text{l}$ , was added to the centrifuge tube to precipitate protein and the CSF centrifuged at 1,300 rpm for ten minutes. Supernatant was pipetted into a glass vial and placed in a  $\text{N}_2$  dryer. Once dry 100  $\mu\text{l}$  10% methanol was used to resuspend the CSF sample, the sample was agitated and 100  $\mu\text{l}$  was pipetted into centrifuge tubes. Resuspended CSF samples were centrifuged at 1,300 rpm for ten minutes. Supernatant was pipetted into a 96 well plate. A 5  $\mu\text{l}$  sample was removed from each well and placed into a collective vial. 10% Methanol, 100  $\mu\text{l}$ , was pipetted into the bottom wells of the 96 well plate. The 96 well plate was sealed with foil and stored in a  $4^{\circ}\text{C}$  fridge for analysis.

An Acquity UPLC LC system was used to separate lipids in the CSF sample (Acquity UPLC CSH column,  $\text{C}_{18}$  2.1  $\times$  100 mm, 1.7  $\mu\text{m}$ , column temperature  $55^{\circ}\text{C}$ , flow rate 400  $\mu\text{l}$  / min, mobile phase A acetonitrile / water (60 : 40) with 10 mM ammonium formate and 0.1% formic acid, mobile phase B isopropanol / acetonitrile (90 : 10) with 10 mM ammonium formate and 0.1% formic acid, injection volume 5  $\mu\text{l}$ ). A Xevo G2 XS QToF mass spectrometer was used to detect samples (acquisition mode LC/MS, ESI positive ionization mode, capillary voltage 2.0KV, cone voltage 30V, desolvation temperature  $550^{\circ}\text{C}$ , desolvation gas 900 L / hr, source temperature  $120^{\circ}\text{C}$ , acquisition range 100 – 2000  $m/z$ ). All ketoacyl subunits were identified for comparison: fatty acyls, glycerolipids (monoacylglycerols, diacylglycerols and triacylglycerols), glycerophospholipids (phosphatidylcholines, phosphatidylethanolamines, phosphatidylglycerols, phosphatidylserines, phosphatidylinositols and cardiolipins) and sphingolipids (ceramides and sphingomyelins). The sterol lipids call of isoprene subunits were also identified for comparison: cholesterol and cholesterol esters. Lipid comparisons were made using proprietary software.

Unfortunately, due to software issues, the data obtained was not of a sufficient quality to justify further analysis.

## 10 References

---

- Abudukeyoumu N, Hernandez-Flores T, Garcia-Munoz M & Arbuthnott GW (2018). Cholinergic modulation of striatal microcircuits. *Eur J Neurosci*, 49, 604-622.
- Adler A, Finkes I, Katabi S, Prut Y & Bergman H (2013). Encoding by synchronization in the primate striatum. *J Neurosci*, 33, 4854-66.
- Alarcon-Herrera N, Flores-Maya S, Bellido B, Garcia-Bores AM, Mendoza E, Avila-Acevedo G & Hernandez-Echeagaray E (2017). Protective effects of chlorogenic acid in 3-nitropropionic acid induced toxicity and genotoxicity. *Food Chem Toxicol*, 109, 1018-1025.
- Albin RL (2000). Basal ganglia neurotoxins. *Neurol Clin*, 18, 665-80.
- Albin RL, Young AB & Penney JB (1989). The functional anatomy of basal ganglia disorders. *Trends Neurosci*, 12, 366-75.
- Aldrin-Kirk P, Heuer A, Rylander Ottosson D, Davidsson M, Mattsson B & Bjorklund T (2018). Chemogenetic modulation of cholinergic interneurons reveals their regulating role on the direct and indirect output pathways from the striatum. *Neurobiol Dis*, 109, 148-162.
- Alexander AL, Lee JE, Lazar M & Field AS (2007). Diffusion tensor imaging of the brain. *Neurotherapeutics : the journal of the American Society for Experimental NeuroTherapeutics*, 4, 316-329.
- Alexander GE & Crutcher MD (1990). Functional architecture of basal ganglia circuits: neural substrates of parallel processing. *Trends Neurosci*, 13, 266-71.
- Antunes E, Ricardo C, Folharini C & Wayne C (2013). Correlations between behavioural and oxidative parameters in a rat quinolinic acid model of Huntington's disease: protective effect of melatonin. *Eur J Pharmacol*, 701, 65-72.
- Apps MA & Ramnani N (2014). The anterior cingulate gyrus signals the net value of others' rewards. *J Neurosci*, 34, 6190-200.
- Ardan T, Baxa M, Levinska B, Sedlackova M, Nguyen TD, Klima J, Juhas S, Juhasova J, Smatlikova P, Vochozkova P, Motlik J & Ellederova Z (2019). Transgenic minipig model of Huntington's disease exhibiting gradually progressing neurodegeneration. *Dis Model Mech*, 13, e041319.
- Ashkenazi A, Bento CF, Ricketts T, Vicinanza M, Siddiqi F, Pavel M, Squitieri F, Hardenberg MC, Imarisio S, Menzies FM & Rubinsztein DC (2017). Polyglutamine tracts regulate beclin 1-dependent autophagy. *Nature*, 545, 108-111.
- Askeland G, Rodinova M, Stufkova H, Dosoudilova Z, Baxa M, Smatlikova P, Bohuslavova B, Klempir J, Nguyen TD, Kusnierczyk A, Bjoras M, Klungland A, Hansikova H, Ellederova Z & Eide L (2018). A transgenic minipig model of Huntington's disease shows early signs of behavioral and molecular pathologies. *Dis Model Mech*, 11, e035949.
- Askenasy JJ (2001). Approaching disturbed sleep in late Parkinson's Disease: first step toward a proposal for a revised UPDRS. *Parkinsonism Relat Disord*, 8, 123-31.
- Aung WY, Mar S & Benzinger TL (2013). Diffusion tensor MRI as a biomarker in axonal and myelin damage. *Imaging Med*, 5, 427-440.
- Ayalon L, Doron R, Weiner I & Joel D (2004). Amelioration of behavioral deficits in a rat model of Huntington's disease by an excitotoxic lesion to the globus pallidus. *Exp Neurol*, 186, 46-58.

- Bahuguna J, Weidel P & Morrison A (2018). Exploring the role of striatal D1 and D2 medium spiny neurons in action selection using a virtual robotic framework. *Eur J Neurosci*, 49, 737-753.
- Baldwin BA (1981). Shape discrimination in sheep and calves. *Animal Behaviour*, 29, 830-834.
- Barbour B, Brew H & Attwell D (1991). Electrogenic uptake of glutamate and aspartate into glial cells isolated from the salamander (*Ambystoma*) retina. *J Physiol*, 436, 169-93.
- Bates GP, Dorsey R, Gusella JF, Hayden MR, Kay C, Leavitt BR, Nance M, Ross CA, Scahill RI, Wetzel R, Wild EJ & Tabrizi SJ (2015). Huntington disease. *Nat Rev Dis Primers*, 1, 15005.
- Baxa M, Hruska-Plochan M, Juhas S, Vodicka P, Pavlok A, Juhasova J, Miyanochara A, Nejime T, Klima J, Macakova M, Marsala S, Weiss A, Kubickova S, Musilova P, Vrtel R, Sontag EM, Thompson LM, Schier J, Hansikova H, Howland DS, Cattaneo E, Difulgia M, Marsala M & Motlik J (2013). A transgenic minipig model of Huntington's Disease. *J Huntingtons Dis*, 2, 47-68.
- Bazely DR & Ensor CV (1989). Discrimination learning in sheep with cues varying in brightness and hue. *Applied Animal Behaviour Science*, 23, 293-299.
- Bazzett TJ, Falik RC, Becker JB & Albin RL (1995). Chronic administration of malonic acid produces selective neural degeneration and transient changes in calbindin immunoreactivity in rat striatum. *Exp Neurol*, 134, 244-52.
- Beal MF, Brouillet E, Jenkins B, Henshaw R, Rosen B & Hyman BT (1993a). Age-dependent striatal excitotoxic lesions produced by the endogenous mitochondrial inhibitor malonate. *J Neurochem*, 61, 1147-50.
- Beal MF, Brouillet E, Jenkins BG, Ferrante RJ, Kowall NW, Miller JM, Storey E, Srivastava R, Rosen BR & Hyman BT (1993b). Neurochemical and histologic characterization of striatal excitotoxic lesions produced by the mitochondrial toxin 3-nitropropionic acid. *J Neurosci*, 13, 4181-92.
- Beal MF, Ferrante RJ, Swartz KJ & Kowall NW (1991). Chronic quinolinic acid lesions in rats closely resemble Huntington's disease. *J Neurosci*, 11, 1649-59.
- Beal MF, Kowall NW, Ellison DW, Mazurek MF, Swartz KJ & Martin JB (1986). Replication of the neurochemical characteristics of Huntington's disease by quinolinic acid. *Nature*, 321, 168-71.
- Benarroch EE (2016). Intrinsic circuits of the striatum: Complexity and clinical correlations. *Neurology*, 86, 1531-42.
- Beninger RJ (1983). The role of dopamine in locomotor activity and learning. *Brain Res*, 287, 173-96.
- Bergmeister KD, Hader M, Lewis S, Russold MF, Schiestl M, Manzano-Szalai K, Roche AD, Salminger S, Dietl H & Aszmann OC (2016). Prosthesis Control with an Implantable Multichannel Wireless Electromyography System for High-Level Amputees: A Large-Animal Study. *Plast Reconstr Surg*, 137, 153-62.
- Bezprozvanny I (2007). Inositol 1,4,5-triphosphate receptor, calcium signalling and Huntington's disease. *Subcell Biochem*, 45, 323-35.
- Bhattacharyya KB (2016). The story of George Huntington and his disease. *Annals of Indian Academy of Neurology*, 19, 25-28.
- Birch SM, Lenox MW, Kornegay JN, Shen L, Ai H, Ren X, Goodlett CR, Cudd TA & Washburn SE (2015). Computed tomography assessment of peripubertal craniofacial morphology in a sheep model of binge alcohol drinking in the first trimester. *Alcohol*, 49, 675-89.
- Bjorklund H, Olson L, Dahl D & Schwarcz R (1986). Short- and long-term consequences of intracranial injections of the excitotoxin, quinolinic acid, as evidenced by GFA immunohistochemistry of astrocytes. *Brain Res*, 371, 267-77.

- Bordelon YM, Chesselet MF, Nelson D, Welsh F & Erecinska M (1997). Energetic dysfunction in quinolinic acid-lesioned rat striatum. *J Neurochem*, 69, 1629-39.
- Borlongan CV, Koutouzis TK & Sanberg PR (1997). 3-Nitropropionic acid animal model and Huntington's disease. *Neurosci Biobehav Rev*, 21, 289-93.
- Boyle A & Ondo W (2015). Role of apomorphine in the treatment of Parkinson's disease. *CNS Drugs*, 29, 83-9.
- Braidy N, Brew BJ, Inestrosa NC, Chung R, Sachdev P & Guillemin GJ (2014). Changes in Cathepsin D and Beclin-1 mRNA and protein expression by the excitotoxin quinolinic acid in human astrocytes and neurons. *Metab Brain Dis*, 29, 873-83.
- Brain KL, Allison BJ, Niu Y, Cross CM, Itani N, Kane AD, Herrera EA & Giussani DA (2015). Induction of controlled hypoxic pregnancy in large mammalian species. *Physiol Rep*, 3, e12614.
- Brett AC, Rosenstock TR & Rego AC (2014). Current therapeutic advances in patients and experimental models of Huntington's disease. *Curr Drug Targets*, 15, 313-34.
- Brickell KL, Nicholson LF, Waldvogel HJ & Faull RL (1999). Chemical and anatomical changes in the striatum and substantia nigra following quinolinic acid lesions in the striatum of the rat: a detailed time course of the cellular and GABA(A) receptor changes. *J Chem Neuroanat*, 17, 75-97.
- Brimblecombe KR & Cragg SJ (2017). The striosome and matrix compartments of the striatum: A path through the labyrinth from neurochemistry toward function. *ACS Chem Neurosci*, 8, 235-242.
- Brooks SP & Dunnett SB (2015). Mouse Models of Huntington's Disease. *Curr Top Behav Neurosci*, 22, 101-33.
- Brouillet E, Hantraye P, Ferrante RJ, Dolan R, Leroy-Willig A, Kowall NW & Beal MF (1995). Chronic mitochondrial energy impairment produces selective striatal degeneration and abnormal choreiform movements in primates. *Proc Natl Acad Sci U S A*, 92, 7105-9.
- Brown VJ & Tait DS (2016). Attentional set-shifting across species. *Curr Top Behav Neurosci*, 28, 363-95.
- Brownell AL, Hantraye P, Wullner U, Hamberg L, Shoup T, Elmaleh DR, Frim DM, Madras BK, Brownell GL, Rosen BR & Et Al. (1994). PET- and MRI-based assessment of glucose utilization, dopamine receptor binding, and hemodynamic changes after lesions to the caudate-putamen in primates. *Exp Neurol*, 125, 41-51.
- Buch ER, Liew SL & Cohen LG (2017). Plasticity of sensorimotor networks: Multiple overlapping mechanisms. *Neuroscientist*, 23, 185-196.
- Budde MD, Janes L, Gold E, Turtzo LC & Frank JA (2011). The contribution of gliosis to diffusion tensor anisotropy and tractography following traumatic brain injury: validation in the rat using Fourier analysis of stained tissue sections. *Brain*, 134, 2248-60.
- Burke DA, Rotstein HG & Alvarez VA (2017). Striatal local circuitry: A new framework for lateral inhibition. *Neuron*, 96, 267-284.
- Burns LH, Pakzaban P, Deacon TW, Brownell AL, Tatter SB, Jenkins BG & Isacson O (1995). Selective putaminal excitotoxic lesions in non-human primates model the movement disorder of Huntington disease. *Neuroscience*, 64, 1007-17.
- Burton AC, Nakamura K & Roesch MR (2015). From ventral-medial to dorsal-lateral striatum: neural correlates of reward-guided decision-making. *Neurobiol Learn Mem*, 117, 51-9.
- Calabresi P, Picconi B, Tozzi A, Ghiglieri V & Di Filippo M (2014). Direct and indirect pathways of basal ganglia: a critical reappraisal. *Nat Neurosci*, 17, 1022-30.

- Cao J, Wei C, Liu D, Wang H, Wu M, Xie Z, Capellini TD, Zhang L, Zhao F, Li L, Zhong T, Wang L, Lu J, Liu R, Zhang S, Du Y, Zhang H & Du L (2015). DNA methylation Landscape of body size variation in sheep. *Sci Rep*, 5, 13950.
- Carmo C, Naia L, Lopes C & Rego AC (2018). Mitochondrial dysfunction in Huntington's disease. *Adv Exp Med Biol*, 1049, 59-83.
- Carroll JB, Bates GP, Steffan J, Saft C & Tabrizi SJ (2015). Treating the whole body in Huntington's disease. *The Lancet Neurology*, 14, 1135-1142.
- Castane A, Theobald DE & Robbins TW (2010). Selective lesions of the dorsomedial striatum impair serial spatial reversal learning in rats. *Behav Brain Res*, 210, 74-83.
- Cazorla M, Kang UJ & Kellendonk C (2015). Balancing the basal ganglia circuitry: a possible new role for dopamine D2 receptors in health and disease. *Mov Disord*, 30, 895-903.
- Chan AW, Jiang J, Chen Y, Li C, Prucha MS, Hu Y, Chi T, Moran S, Rahim T, Li S, Li X, Zola SM, Testa CM, Mao H, Villalba R, Smith Y, Zhang X & Bachevalier J (2015). Progressive cognitive deficit, motor impairment and striatal pathology in a transgenic Huntington disease monkey model from infancy to adulthood. *PLoS One*, 10, e0122335.
- Chen H, Epstein J & Stern E (2010). Neural plasticity after acquired brain injury: evidence from functional neuroimaging. *PM R*, 2, S306-12.
- Christensen J, Sørensen JC, Østergaard K & Zimmer J (1999). Early postnatal development of the rat corticostriatal pathway: an anterograde axonal tracing study using biocytin pellets. *Anatomy and Embryology*, 200, 73-80.
- Cicchetti F & Parent A (1996). Striatal interneurons in Huntington's disease: selective increase in the density of calretinin-immunoreactive medium-sized neurons. *Mov Disord*, 11, 619-26.
- Cicchetti F, Prensa L, Wu Y & Parent A (2000). Chemical anatomy of striatal interneurons in normal individuals and in patients with Huntington's disease. *Brain Res Brain Res Rev*, 34, 80-101.
- Cipriani G, Lucetti C, Danti S & Nuti A (2015). Sleep disturbances and dementia. *Psychogeriatrics*, 15, 65-74.
- Clarke CE, Lowry M & Quarrell OW (1998). No change in striatal glutamate in Huntington's disease measured by proton magnetic resonance spectroscopy. *Parkinsonism Relat Disord*, 4, 123-7.
- Clarke HF, Robbins TW & Roberts AC (2008). Lesions of the medial striatum in monkeys produce perseverative impairments during reversal learning similar to those produced by lesions of the orbitofrontal cortex. *J Neurosci*, 28, 10972-82.
- Colin E, Zala D, Liot G, Rangone H, Borrell-Pages M, Li XJ, Saudou F & Humbert S (2008). Huntingtin phosphorylation acts as a molecular switch for anterograde/retrograde transport in neurons. *EMBO J*, 27, 2124-34.
- Constable PD (2004). Clinical examination of the ruminant nervous system. *Vet Clin North Am Food Anim Pract*, 20, 185-214.
- Coulon M, Nowak R, Andanson S, Petit B, Lévy F & Boissy A (2015). Effects of prenatal stress and emotional reactivity of the mother on emotional and cognitive abilities in lambs. *Developmental Psychobiology*, 57, 626-636.
- Coyle JT, Ferkany JW & Zaczek R (1983). Kainic acid: insights from a neurotoxin into the pathophysiology of Huntington's disease. *Neurobehav Toxicol Teratol*, 5, 617-24.
- Crilly JP, Rzechorzek N & Scott P (2015). Diagnosing limb paresis and paralysis in sheep. *In Pract*, 37, 490-507.

- Crittenden JR & Graybiel AM (2011). Basal Ganglia disorders associated with imbalances in the striatal striosome and matrix compartments. *Front Neuroanat*, 5, 59.
- Crittenden JR, Tillberg PW, Riad MH, Shima Y, Gerfen CR, Curry J, Housman DE, Nelson SB, Boyden ES & Graybiel AM (2016). Striosome-dendron bouquets highlight a unique striatonigral circuit targeting dopamine-containing neurons. *Proc Natl Acad Sci U S A*, 113, 11318-11323.
- Crook ZR & Housman DE (2013). Surveying the landscape of Huntington's disease mechanisms, measurements, and medicines. *J Huntingtons Dis*, 2, 405-36.
- Cui G, Jun SB, Jin X, Pham MD, Vogel SS, Lovinger DM & Costa RM (2013). Concurrent activation of striatal direct and indirect pathways during action initiation. *Nature*, 494, 238-42.
- Cui J, Wang G, Kandhare AD, Mukherjee-Kandhare AA & Bodhankar SL (2018). Neuroprotective effect of naringin, a flavone glycoside in quinolinic acid-induced neurotoxicity: Possible role of PPAR-gamma, Bax/Bcl-2, and caspase-3. *Food Chem Toxicol*, 121, 95-108.
- Dai JX, Ma YB, Le NY, Cao J & Wang Y (2018). Large animal models of traumatic brain injury. *Int J Neurosci*, 128, 243-254.
- Dall'acqua P, Johannes S, Mica L, Simmen H-P, Glaab R, Fandino J, Schwendinger M, Meier C, Ulbrich EJ, Müller A, Baetschmann H, Jäncke L & Hänggi J (2017). Functional and Structural Network Recovery after Mild Traumatic Brain Injury: A 1-Year Longitudinal Study. *Frontiers in human neuroscience*, 11, 280-280.
- Danbolt NC, Furness DN & Zhou Y (2016). Neuronal vs glial glutamate uptake: Resolving the conundrum. *Neurochem Int*, 98, 29-45.
- Das AS & Zou WQ (2016). Prions: Beyond a Single Protein. *Clin Microbiol Rev*, 29, 633-58.
- Dautry C, Vaufray F, Brouillet E, Bizat N, Henry PG, Conde F, Bloch G & Hantraye P (2000). Early N-acetylaspartate depletion is a marker of neuronal dysfunction in rats and primates chronically treated with the mitochondrial toxin 3-nitropropionic acid. *J Cereb Blood Flow Metab*, 20, 789-99.
- Davies SW & Roberts PJ (1988). Sparing of cholinergic neurons following quinolinic acid lesions of the rat striatum. *Neuroscience*, 26, 387-93.
- Davies SW, Turmaine M, Cozens BA, Difiglia M, Sharp AH, Ross CA, Scherzinger E, Wanker EE, Mangiarini L & Bates GP (1997). Formation of neuronal intranuclear inclusions underlies the neurological dysfunction in mice transgenic for the HD mutation. *Cell*, 90, 537-48.
- Dawson TM, Golde TE & Lagier-Tourenne C (2018). Animal models of neurodegenerative diseases. *Nature neuroscience*, 21, 1370-1379.
- De Carvalho LP, Bochet P & Rossier J (1996). The endogenous agonist quinolinic acid and the non endogenous homoquinolinic acid discriminate between NMDAR2 receptor subunits. *Neurochem Int*, 28, 445-52.
- De La Monte SM, Vonsattel JP & Richardson EP, Jr. (1988). Morphometric demonstration of atrophic changes in the cerebral cortex, white matter, and neostriatum in Huntington's disease. *J Neuropathol Exp Neurol*, 47, 516-25.
- De Lahunta A & Glass E (2009). Chapter 20 - The Neurologic Examination. In: De Lahunta A & Glass E (eds.) *Veterinary Neuroanatomy and Clinical Neurology* (Third Edition). Saint Louis: W.B. Saunders.
- Demetrius L (2005). Of mice and men. When it comes to studying ageing and the means to slow it down, mice are not just small humans. *EMBO Rep*, 6 Spec No, S39-44.
- Demetrius L (2006). Aging in mouse and human systems: a comparative study. *Ann N Y Acad Sci*, 1067, 66-82.

- Demougeot C, Garnier P, Mossiat C, Bertrand N, Giroud M, Beley A & Marie C (2001). N-Acetylaspartate, a marker of both cellular dysfunction and neuronal loss: its relevance to studies of acute brain injury. *J Neurochem*, 77, 408-15.
- Deng YP, Albin RL, Penney JB, Young AB, Anderson KD & Reiner A (2004). Differential loss of striatal projection systems in Huntington's disease: a quantitative immunohistochemical study. *J Chem Neuroanat*, 27, 143-64.
- Di Cristo F, Finicelli M, Digilio FA, Paladino S, Valentino A, Scialo F, D'apolito M, Saturnino C, Galderisi U, Giordano A, Melone MaB & Peluso G (2018). Meldonium improves Huntington's disease mitochondrial dysfunction by restoring peroxisome proliferator-activated receptor gamma coactivator 1alpha expression. *J Cell Physiol*, 234, 9233-9246.
- Di Pardo A, Monyror J, Morales LC, Kadam V, Lingrell S, Maglione V, Wozniak RW & Sipione S (2019). Mutant huntingtin interacts with the sterol regulatory element-binding proteins and impairs their nuclear import. *Hum Mol Genet*, e298.
- Diago EB, Martinez-Horta S, Lasaosa SS, Alebesque AV, Perez-Perez J, Kulisevsky J & Del Val JL (2018). Circadian rhythm, cognition, and mood disorders in Huntington's disease. *J Huntingtons Dis*, 7, 193-198.
- Dias R, Robbins TW & Roberts AC (1996). Primate analogue of the Wisconsin Card Sorting Test: effects of excitotoxic lesions of the prefrontal cortex in the marmoset. *Behav Neurosci*, 110, 872-86.
- Difiglia M, Sapp E, Chase KO, Davies SW, Bates GP, Vonsattel JP & Aronin N (1997). Aggregation of huntingtin in neuronal intranuclear inclusions and dystrophic neurites in brain. *Science*, 277, 1990-3.
- Dong HW (2019). Adult mouse brain reference atlas (online). Allen Reference Atlases. Allen Institute for Brain Science. WA. <https://mouse.brain-map.org/static/atlas>.
- Dong X & Cong S (2018). Identification of differentially expressed genes and regulatory relationships in Huntington's disease by bioinformatics analysis. *Mol Med Rep*, 17, 4317-4326.
- Donoghue JP & Herkenham M (1986). Neostriatal projections from individual cortical fields conform to histochemically distinct striatal compartments in the rat. *Brain Res*, 365, 397-403.
- Douaud G, Behrens TE, Poupon C, Cointepas Y, Jbabdi S, Gaura V, Golestani N, Krystkowiak P, Verny C, Damier P, Bachoud-Levi AC, Hantraye P & Remy P (2009). In vivo evidence for the selective subcortical degeneration in Huntington's disease. *Neuroimage*, 46, 958-66.
- Doyle RE, Freire R, Cowling A, Knott SA & Lee C (2014). Performance of sheep in a spatial maze is impeded by negative stimuli. *Applied Animal Behaviour Science*, 151, 36-42.
- Dragatsis I, Levine MS & Zeitlin S (2000). Inactivation of Hdh in the brain and testis results in progressive neurodegeneration and sterility in mice. *Nat Genet*, 26, 300-6.
- Dudman JT & Krakauer JW (2016). The basal ganglia: from motor commands to the control of vigor. *Curr Opin Neurobiol*, 37, 158-166.
- Dutta S & Sengupta P (2016). Men and mice: Relating their ages. *Life Sci*, 152, 244-8.
- Duty S & Jenner P (2011). Animal models of Parkinson's disease: a source of novel treatments and clues to the cause of the disease. *Br J Pharmacol*, 164, 1357-91.
- Ella A, Delgadoillo JA, Chemineau P & Keller M (2017). Computation of a high-resolution MRI 3D stereotaxic atlas of the sheep brain. *J Comp Neurol*, 525, 676-692.
- Emborg ME (2017). Nonhuman primate models of neurodegenerative disorders. *Ilar j*, 58, 190-201.

- Emerich DF, Kordower JH, Chu Y, Thanos C, Bintz B, Paolone G & Wahlberg LU (2019). Widespread Striatal Delivery of GDNF from Encapsulated Cells Prevents the Anatomical and Functional Consequences of Excitotoxicity. *Neural Plast*, 2019, 6286197.
- Erhard HW, Boissy A, Rae MT & Rhind SM (2004). Effects of prenatal undernutrition on emotional reactivity and cognitive flexibility in adult sheep. *Behav Brain Res*, 151, 25-35.
- Erro R & Stamelou M (2017). The Motor Syndrome of Parkinson's Disease. *Int Rev Neurobiol*, 132, 25-32.
- Ertelt K, Oevermann A, Precht C, Lauper J, Henke D & Gorgas D (2016). Magnetic resonance imaging findings in small ruminants with brain disease. *Vet Radiol Ultrasound*, 57, 162-9.
- Fancellu R, Armentero MT, Nappi G & Blandini F (2003). Neuroprotective effects mediated by dopamine receptor agonists against malonate-induced lesion in the rat striatum. *Neurol Sci*, 24, 180-1.
- Faria LG, Rahal SC, Agostinho FS, Minto BW, Matsubara LM, Kano WT, Castilho MS & Mesquita LR (2014). Kinematic analysis of forelimb and hind limb joints in clinically healthy sheep. *BMC Vet Res*, 10, 294.
- Fecteau G, Parent J & George LW (2017). Neurologic Examination of the Ruminant. *Vet Clin North Am Food Anim Pract*, 33, 1-8.
- Feng Q, Ma Y, Mu S, Wu J, Chen S, Ouyang L & Lei W (2014). Specific reactions of different striatal neuron types in morphology induced by quinolinic acid in rats. *PLoS One*, 9, e91512.
- Ferrante RJ, Beal MF, Kowall NW, Richardson EP, Jr. & Martin JB (1987). Sparing of acetylcholinesterase-containing striatal neurons in Huntington's disease. *Brain Res*, 411, 162-6.
- Ferrante RJ, Kowall NW, Cipolloni PB, Storey E & Beal MF (1993). Excitotoxin lesions in primates as a model for Huntington's disease: histopathologic and neurochemical characterization. *Exp Neurol*, 119, 46-71.
- Ferreira G, Keller M, Saint-Dizier H, Perrin G & Levy F (2004). Transfer between views of conspecific faces at different ages or in different orientations by sheep. *Behav Processes*, 67, 491-9.
- Finnie JW, Blumbergs PC, Manavis J, Turner RJ, Helps S, Vink R, Byard RW, Chidlow G, Sandoz B, Dutschke J & Anderson RW (2012). Neuropathological changes in a lamb model of non-accidental head injury (the shaken baby syndrome). *J Clin Neurosci*, 19, 1159-64.
- Finnie JW, Windsor PA & Kessell AE (2011). Neurological diseases of ruminant livestock in Australia. I: general neurological examination, necropsy procedures and neurological manifestations of systemic disease, trauma and neoplasia. *Aust Vet J*, 89, 243-6.
- Fisher EMC & Bannerman DM (2019). Mouse models of neurodegeneration: Know your question, know your mouse. *Science Translational Medicine*, 11, eaaq1818.
- Florio TM, Scarnati E, Rosa I, Di Censo D, Ranieri B, Cimini A, Galante A & Alecci M (2018). The Basal Ganglia: More than just a switching device. *CNS Neurosci Ther*, 24, 677-684.
- Foucault-Fruchard L, Tronel C, Bodard S, Gulhan Z, Busson J, Chalon S & Antier D (2018). Alpha-7 nicotinic acetylcholine receptor agonist treatment in a rat model of Huntington's disease and involvement of heme oxygenase-1. *Neural Regen Res*, 13, 737-741.
- Fox LM, Kim K, Johnson CW, Chen S, Croce KR, Victor MB, Eenjes E, Bosco JR, Randolph LK, Dragatsis I, Dragich JM, Yoo AS & Yamamoto A (2019). Huntington's disease pathogenesis is modified in vivo by *Alfy/Wdfy3* and selective macroautophagy. *Neuron*, 19, e31045.
- Francelle L, Galvan L & Brouillet E (2014). Possible involvement of self-defense mechanisms in the preferential vulnerability of the striatum in Huntington's disease. *Front Cell Neurosci*, 8, 295.



- Fricker RA, Annett LE, Torres EM & Dunnett SB (1996). The placement of a striatal ibotenic acid lesion affects skilled forelimb use and the direction of drug-induced rotation. *Brain Res Bull*, 41, 409-16.
- Fujiyama F, Unzai T & Karube F (2019). Thalamostriatal projections and striosome-matrix compartments. *Neurochem Int*, 125, 67-73.
- Gaffan D & Wilson CR (2008). Medial temporal and prefrontal function: recent behavioural disconnection studies in the macaque monkey. *Cortex*, 44, 928-35.
- Gahm JK & Shi Y (2017). Holistic Mapping of Striatum Surfaces in the Laplace-Beltrami Embedding Space. *Med Image Comput Comput Assist Interv*, 10433, 21-30.
- Gantert M, Kreczmanski P, Kuypers E, Jellema R, Strackx E, Bastian N, Gavilanes AW, Zimmermann LJ, Garnier Y, Schmitz C & Kramer BW (2012). Effects of in utero endotoxemia on the ovine fetal brain: a model for schizophrenia? *Front Biosci (Elite Ed)*, 4, 2845-53.
- Garas FN, Kormann E, Shah RS, Vinciati F, Smith Y, Magill PJ & Sharott A (2018). Structural and molecular heterogeneity of calretinin-expressing interneurons in the rodent and primate striatum. *J Comp Neurol*, 526, 877-898.
- Gerfen CR (1984). The neostriatal mosaic: compartmentalization of corticostriatal input and striatonigral output systems. *Nature*, 311, 461-4.
- Gerfen CR (1992). The neostriatal mosaic: multiple levels of compartmental organization. *Trends Neurosci*, 15, 133-9.
- Gerfen CR, Baimbridge KG & Miller JJ (1985). The neostriatal mosaic: compartmental distribution of calcium-binding protein and parvalbumin in the basal ganglia of the rat and monkey. *Proc Natl Acad Sci U S A*, 82, 8780-4.
- Gerfen CR & Bolam JP (2016). Chapter 1 - The Neuroanatomical Organization of the Basal Ganglia. In: Steiner H & Tseng KY (eds.) *Handbook of Behavioral Neuroscience*. Elsevier.
- Gerfen CR, Engber TM, Mahan LC, Susel Z, Chase TN, Monsma FJ, Jr. & Sibley DR (1990). D1 and D2 dopamine receptor-regulated gene expression of striatonigral and striatopallidal neurons. *Science*, 250, 1429-32.
- Ghosh R & Tabrizi SJ (2018). Clinical features of Huntington's disease. *Adv Exp Med Biol*, 1049, 1-28.
- Gill JS, Jamwal S, Kumar P & Deshmukh R (2017). Sertraline and venlafaxine improves motor performance and neurobehavioral deficit in quinolinic acid induced Huntington's like symptoms in rats: Possible neurotransmitters modulation. *Pharmacol Rep*, 69, 306-313.
- Giorgetto C, Silva EC, Kitabatake TT, Bertolino G & De Araujo JE (2015). Behavioural profile of Wistar rats with unilateral striatal lesion by quinolinic acid (animal model of Huntington disease) post-injection of apomorphine and exposure to static magnetic field. *Exp Brain Res*, 233, 1455-62.
- Giorgini F, Moller T, Kwan W, Zwilling D, Wacker JL, Hong S, Tsai LC, Cheah CS, Schwarcz R, Guidetti P & Muchowski PJ (2008). Histone deacetylase inhibition modulates kynurenine pathway activation in yeast, microglia, and mice expressing a mutant huntingtin fragment. *J Biol Chem*, 283, 7390-400.
- Glaser T, Arnaud Sampaio VF, Lameu C & Ulrich H (2018). Calcium signalling: A common target in neurological disorders and neurogenesis. *Semin Cell Dev Biol*, 95, 25-33.
- Glick SD, Zimmerberg B & Jerussi TP (1977). Adaptive significance of laterality in the rodent. *Ann N Y Acad Sci*, 299, 180-5.
- Gogolla N (2017). The insular cortex. *Curr Biol*, 27, R580-R586.

- Gonzales KK, Pare JF, Wichmann T & Smith Y (2013). GABAergic inputs from direct and indirect striatal projection neurons onto cholinergic interneurons in the primate putamen. *J Comp Neurol*, 521, 2502-22.
- Graveland GA & Difiglia M (1985). The frequency and distribution of medium-sized neurons with indented nuclei in the primate and rodent neostriatum. *Brain Res*, 327, 307-11.
- Gray-Edwards HL, Randle AN, Maitland SA, Benatti HR, Hubbard SM, Canning PF, Vogel MB, Brunson BL, Hwang M, Ellis LE, Bradbury AM, Gentry AS, Taylor AR, Wooldridge AA, Wilhite DR, Winter RL, Whitlock BK, Johnson JA, Holland M, Salibi N, Beyers RJ, Sartin JL, Denney TS, Cox NR, Sena-Esteves M & Martin DR (2018). Adeno-associated virus gene therapy in a sheep model of tay-sachs disease. *Hum Gene Ther*, 29, 312-326.
- Gray M, Shirasaki DI, Cepeda C, Andre VM, Wilburn B, Lu XH, Tao J, Yamazaki I, Li SH, Sun YE, Li XJ, Levine MS & Yang XW (2008). Full-length human mutant huntingtin with a stable polyglutamine repeat can elicit progressive and selective neuropathogenesis in BACHD mice. *J Neurosci*, 28, 6182-95.
- Graybiel AM & Grafton ST (2015). The striatum: where skills and habits meet. *Cold Spring Harb Perspect Biol*, 7, a021691.
- Graybiel AM & Ragsdale CW, Jr. (1978). Histochemically distinct compartments in the striatum of human, monkeys, and cat demonstrated by acetylthiocholinesterase staining. *Proc Natl Acad Sci U S A*, 75, 5723-6.
- Graybiel AM, Ragsdale CW, Jr., Yoneoka ES & Elde RP (1981). An immunohistochemical study of enkephalins and other neuropeptides in the striatum of the cat with evidence that the opiate peptides are arranged to form mosaic patterns in register with the striosomal compartments visible by acetylcholinesterase staining. *Neuroscience*, 6, 377-97.
- Griffiths SK, Pierson LL, Gerhardt KJ, Abrams RM & Peters AJ (1996). Auditory brainstem response in sheep. Part II: Postnatal development. *Dev Psychobiol*, 29, 53-68.
- Grillner S & Robertson B (2016). The Basal Ganglia Over 500 Million Years. *Curr Biol*, 26, R1088-R1100.
- Guidetti P & Schwarcz R (2003). 3-Hydroxykynurenine and quinolinate: pathogenic synergism in early grade Huntington's disease? *Adv Exp Med Biol*, 527, 137-45.
- Guilbaud L, Garabedian C, Di Rocco F, Fallet-Bianco C, Friszer S, Zerah M & Jouannic JM (2014). Limits of the surgically induced model of myelomeningocele in the fetal sheep. *Childs Nerv Syst*, 30, 1425-9.
- Guillemin GJ, Wang L & Brew BJ (2005). Quinolinic acid selectively induces apoptosis of human astrocytes: potential role in AIDS dementia complex. *J Neuroinflammation*, 2, 16.
- Guncova I, Latr I & Mazurova Y (2011). The neurodegenerative process in a neurotoxic rat model and in patients with Huntington's disease: histopathological parallels and differences. *Acta Histochem*, 113, 783-92.
- Guo Q, Wang D, He X, Feng Q, Lin R, Xu F, Fu L & Luo M (2015). Whole-brain mapping of inputs to projection neurons and cholinergic interneurons in the dorsal striatum. *PLoS One*, 10, e0123381.
- Ha AD & Fung VS (2012). Huntington's disease. *Curr Opin Neurol*, 25, 491-8.
- Haber SN (2016). Corticostriatal circuitry. *Dialogues in clinical neuroscience*, 18, 7-21.
- Hantraye P, Riche D, Maziere M & Isacson O (1990). A primate model of Huntington's disease: behavioral and anatomical studies of unilateral excitotoxic lesions of the caudate-putamen in the baboon. *Exp Neurol*, 108, 91-104.

- Harper PA, Duncan DW, Plant JW & Smeal MG (1986). Cerebellar abiotrophy and segmental axonopathy: two syndromes of progressive ataxia of Merino sheep. *Aust Vet J*, 63, 18-21.
- Harris NG, Verley DR, Gutman BA & Sutton RL (2016). Bi-directional changes in fractional anisotropy after experiment TBI: Disorganization and reorganization? *Neuroimage*, 133, 129-143.
- Hazrati LN & Parent A (1991). Contralateral pallidothalamic and pallidotegmental projections in primates: an anterograde and retrograde labeling study. *Brain Res*, 567, 212-23.
- Heemskerk A-W & Roos RaC (2010). E04 causes of death in Huntington's disease. *Journal of Neurology, Neurosurgery & Psychiatry*, 81, A22-A22.
- Heemskerk A-W & Roos RaC (2012). Aspiration pneumonia and death in Huntington's disease. *PLoS currents*, 4, RRN1293-RRN1293.
- Heisler JM, Morales J, Donegan JJ, Jett JD, Redus L & O'connor JC (2015). The attentional set shifting task: a measure of cognitive flexibility in mice. *J Vis Exp*, 96, 51944.
- Herkenham M & Pert CB (1981). Mosaic distribution of opiate receptors, parafascicular projections and acetylcholinesterase in rat striatum. *Nature*, 291, 415-8.
- Hermann DM & Chopp M (2012). Promoting brain remodelling and plasticity for stroke recovery: therapeutic promise and potential pitfalls of clinical translation. *The Lancet. Neurology*, 11, 369-380.
- Herrmann AM, Meckel S, Gounis MJ, Kringe L, Motschall E, Mulling C & Boltze J (2019). Large animals in neurointerventional research: A systematic review on models, techniques and their application in endovascular procedures for stroke, aneurysms and vascular malformations. *J Cereb Blood Flow Metab*, 39, 375-394.
- Hoang TQ, Bluml S, Dubowitz DJ, Moats R, Kopyov O, Jacques D & Ross BD (1998). Quantitative proton-decoupled 31P MRS and 1H MRS in the evaluation of Huntington's and Parkinson's diseases. *Neurology*, 50, 1033-40.
- Hodges A, Strand AD, Aragaki AK, Kuhn A, Sengstag T, Hughes G, Elliston LA, Hartog C, Goldstein DR, Thu D, Hollingsworth ZR, Collin F, Synek B, Holmans PA, Young AB, Wexler NS, Delorenzi M, Kooperberg C, Augood SJ, Faull RL, Olson JM, Jones L & Luthi-Carter R (2006). Regional and cellular gene expression changes in human Huntington's disease brain. *Hum Mol Genet*, 15, 965-77.
- Hogan-Cann AD & Anderson CM (2016). Physiological roles of non-neuronal NMDA receptors. *Trends Pharmacol Sci*, 37, 750-767.
- Homolak J, Mudrovic M, Vukic B & Toljan K (2018). Circadian rhythm and Alzheimer's disease. *Med Sci (Basel)*, 6, e52.
- Howland DS & Munoz-Sanjuan I (2014). Mind the gap: models in multiple species needed for therapeutic development in Huntington's disease. *Mov Disord*, 29, 1397-403.
- Hudson JL, Van Horne CG, Stromberg I, Brock S, Clayton J, Masserano J, Hoffer BJ & Gerhardt GA (1993). Correlation of apomorphine- and amphetamine-induced turning with nigrostriatal dopamine content in unilateral 6-hydroxydopamine lesioned rats. *Brain Res*, 626, 167-74.
- Hugenholtz F & De Vos WM (2018). Mouse models for human intestinal microbiota research: a critical evaluation. *Cell Mol Life Sci*, 75, 149-160.
- Hunter DS, Hazel SJ, Kind KL, Liu H, Marini D, Owens JA, Pitcher JB & Gatford KL (2015). Do I turn left or right? Effects of sex, age, experience and exit route on maze test performance in sheep. *Physiology and Behavior*, 139, 244-253.
- Izquierdo A, Brigman JL, Radke AK, Rudebeck PH & Holmes A (2017). The neural basis of reversal learning: An updated perspective. *Neuroscience*, 345, 12-26.

- Jacobsen JC, Bawden CS, Rudiger SR, Mclaughlan CJ, Reid SJ, Waldvogel HJ, Macdonald ME, Gusella JF, Walker SK, Kelly JM, Webb GC, Faull RL, Rees MI & Snell RG (2010). An ovine transgenic Huntington's disease model. *Hum Mol Genet*, 19, 1873-82.
- Jenkins BG, Koroshetz WJ, Beal MF & Rosen BR (1993). Evidence for impairment of energy metabolism in vivo in Huntington's disease using localized <sup>1</sup>H NMR spectroscopy. *Neurology*, 43, 2689-95.
- Jenkins BG, Rosas HD, Chen YC, Makabe T, Myers R, Macdonald M, Rosen BR, Beal MF & Koroshetz WJ (1998). <sup>1</sup>H NMR spectroscopy studies of Huntington's disease: correlations with CAG repeat numbers. *Neurology*, 50, 1357-65.
- Jerussi TP & Glick SD (1975). Apomorphine-induced rotation in normal rats and interaction with unilateral caudate lesions. *Psychopharmacologia*, 40, 329-34.
- Joag H, Ghatpande V, Desai M, Sarkar M, Raina A, Shinde M, Chitale R, Deo A, Bose T & Majumdar A (2019). A role of cellular translation regulation associated with toxic Huntingtin protein. *Cell Mol Life Sci*, e03392.
- John SE, Lovell TJH, Opie NL, Wilson S, Scordas TC, Wong YT, Rind GS, Ronayne S, Bauquier SH, May CN, Grayden DB, O'brien TJ & Oxley TJ (2017). The ovine motor cortex: A review of functional mapping and cytoarchitecture. *Neuroscience & Biobehavioral Reviews*, 80, 306-315.
- Johns P (2014). Chapter 3 - Functional neuroanatomy. In: Johns P (ed.) *Clinical Neuroscience*. Churchill Livingstone. 27-47.
- Johnson J, Sudheimer K, Davis K & Winn B (2019). The sheep brain atlas (online). Brain Biodiversity Bank. Michigan State University, East Lansing, MI. <http://www.msu.edu/user/brains/sheepatlas/>.
- Jolly RD, Arthur DG, Kay GW & Palmer DN (2002). Neuronal ceroid-lipofuscinosis in Borderdale sheep. *N Z Vet J*, 50, 199-202.
- Jolly RD & West DM (1976). Blindness in South Hampshire sheep: a neuronal ceroidlipofuscinosis. *N Z Vet J*, 24, 123.
- Jorgensen K & Olesen PT (2018). Kainic acid in the seaweed *Palmaria palmata* (dulse). *Food Addit Contam Part B Surveill*, 11, 198-200.
- Kalia LV & Lang AE (2015). Parkinson's disease. *Lancet*, 386, 896-912.
- Kanazawa I, Kimura M, Murata M, Tanaka Y & Cho F (1990). Choreic movements in the macaque monkey induced by kainic acid lesions of the striatum combined with L-dopa. *Pharmacological, biochemical and physiological studies on neural mechanisms*. *Brain*, 113 (Pt 2), 509-35.
- Kanazawa I, Tanaka Y & Cho F (1986). 'Choreic' movement induced by unilateral kainate lesion of the striatum and L-DOPA administration in monkey. *Neurosci Lett*, 71, 241-6.
- Karageorgos L, Lancaster MJ, Nimmo JS & Hopwood JJ (2011). Gaucher disease in sheep. *J Inherit Metab Dis*, 34, 209-15.
- Kellinghaus C, Montgomery E, Neme S, Ruggieri P & Luders HO (2003). Unilateral absence of the basal ganglia plus epilepsy without motor symptoms. *Neurology*, 60, 870-3.
- Kendall AL, David F, Rayment G, Torres EM, Annett LE & Dunnett SB (2000). The influence of excitotoxic basal ganglia lesions on motor performance in the common marmoset. *Brain*, 123 (Pt 7), 1442-58.
- Kendrick KM & Baldwin BA (1987). Cells in temporal cortex of conscious sheep can respond preferentially to the sight of faces. *Science*, 236, 448-50.

- Kendrick KM, Da Costa AP, Leigh AE, Hinton MR & Peirce JW (2001). Sheep don't forget a face. *Nature*, 414, 165-6.
- Keryer G, Pineda JR, Liot G, Kim J, Dietrich P, Benstaali C, Smith K, Cordelieres FP, Spassky N, Ferrante RJ, Dragatsis I & Saudou F (2011). Ciliogenesis is regulated by a huntingtin-HAP1-PCM1 pathway and is altered in Huntington disease. *J Clin Invest*, 121, 4372-82.
- Kessell AE, Finnie JW, Manavis J, Cheetham GD & Blumbergs PC (2012). A Rosenthal fiber encephalomyelopathy resembling Alexander's disease in 3 sheep. *Vet Pathol*, 49, 248-54.
- Kim EH, Thu DC, Tippett LJ, Oorschot DE, Hogg VM, Roxburgh R, Synek BJ, Waldvogel HJ & Faull RL (2014). Cortical interneuron loss and symptom heterogeneity in Huntington disease. *Ann Neurol*, 75, 717-27.
- Kincaid AE & Wilson CJ (1996). Corticostriatal innervation of the patch and matrix in the rat neostriatum. *J Comp Neurol*, 374, 578-92.
- Kita H & Kitai ST (1988). Glutamate decarboxylase immunoreactive neurons in rat neostriatum: their morphological types and populations. *Brain Res*, 447, 346-52.
- Klein A, Lane EL & Dunnett SB (2013). Brain repair in a unilateral rat model of Huntington's disease: new insights into impairment and restoration of forelimb movement patterns. *Cell Transplant*, 22, 1735-51.
- Klug JR, Engelhardt MD, Cadman CN, Li H, Smith JB, Ayala S, Williams EW, Hoffman H & Jin X (2018). Differential inputs to striatal cholinergic and parvalbumin interneurons imply functional distinctions. *Elife*, 7, e35657.
- Knolle F, Goncalves RP & Morton AJ (2017a). Sheep recognize familiar and unfamiliar human faces from two-dimensional images. *R Soc Open Sci*, 4, 171228.
- Knolle F, McBride SD, Stewart JE, Goncalves RP & Morton AJ (2017b). A stop-signal task for sheep: introduction and validation of a direct measure for the stop-signal reaction time. *Anim Cogn*, 20, 615-626.
- Knowlton BJ & Patterson TK (2018). Habit Formation and the Striatum. *Curr Top Behav Neurosci*, 37, 275-295.
- Konold T & Phelan L (2014). Clinical examination protocol to detect atypical and classical scrapie in sheep. *J Vis Exp*, e51101.
- Kou Z & Iraj A (2014). Imaging brain plasticity after trauma. *Neural Regen Res*, 9, 693-700.
- Kowall NW, Ferrante RJ & Martin JB (1987). Patterns of cell loss in Huntington's disease. *Trends in Neurosciences*, 10, 24-29.
- Kravitz AV, Freeze BS, Parker PR, Kay K, Thwin MT, Deisseroth K & Kreitzer AC (2010). Regulation of parkinsonian motor behaviours by optogenetic control of basal ganglia circuitry. *Nature*, 466, 622-6.
- Kreiman G, Koch C & Fried I (2000). Imagery neurons in the human brain. *Nature*, 408, 357-61.
- Kumar A, Kumar Singh S, Kumar V, Kumar D, Agarwal S & Rana MK (2015). Huntington's disease: an update of therapeutic strategies. *Gene*, 556, 91-7.
- Kumar A, Sharma N, Mishra J & Kalonia H (2013). Synergistical neuroprotection of rofecoxib and statins against malonic acid induced Huntington's disease like symptoms and related cognitive dysfunction in rats. *Eur J Pharmacol*, 709, 1-12.
- Kumar P, Kalonia H & Kumar A (2010). Huntington's disease: pathogenesis to animal models. *Pharmacol Rep*, 62, 1-14.

- Labbadia J & Morimoto RI (2013). Huntington's disease: underlying molecular mechanisms and emerging concepts. *Trends Biochem Sci*, 38, 378-85.
- Lanciego JL, Luquin N & Obeso JA (2012). Functional neuroanatomy of the basal ganglia. *Cold Spring Harb Perspect Med*, 2, a009621.
- Lanciego JL & Vázquez A (2012). The basal ganglia and thalamus of the long-tailed macaque in stereotaxic coordinates. A template atlas based on coronal, sagittal and horizontal brain sections. *Brain Structure and Function*, 217, 613-666.
- Lavisse S, Williams S, Lecourtois S, Van Camp N, Guillermier M, Gipchtein P, Jan C, Goutal S, Eymin L, Valette J, Delzescaux T, Perrier AL, Hantraye P & Aron Badin R (2019). Longitudinal characterization of cognitive and motor deficits in an excitotoxic lesion model of striatal dysfunction in non-human primates. *Neurobiol Dis*, 130, 104484.
- Lazarov O & Marr RA (2013). Of mice and men: neurogenesis, cognition and Alzheimer's disease. *Front Aging Neurosci*, 5, 43.
- Le Gras S, Keime C, Anthony A, Lotz C, De Longprez L, Brouillet E, Cassel JC, Boutillier AL & Merienne K (2017). Altered enhancer transcription underlies Huntington's disease striatal transcriptional signature. *Sci Rep*, 7, 42875.
- Le Heron C, Holroyd CB, Salamone J & Husain M (2018). Brain mechanisms underlying apathy. *J Neurol Neurosurg Psychiatry*, 90, 302-312.
- Lee C, Colegate S & Fisher AD (2006). Development of a maze test and its application to assess spatial learning and memory in Merino sheep. *Applied Animal Behaviour Science*, 96, 43-51.
- Lee J-M, Wheeler Vanessa c, Chao Michael j, Vonsattel Jean paul g, Pinto Ricardo m, Lucente D, Abu-Elneel K, Ramos Eliana m, Mysore Jayalakshmi s, Gillis T, Macdonald Marcy e, Gusella James f, Harold D, Stone Timothy c, Escott-Price V, Han J, Vedernikov A, Holmans P, Jones L, Kwak S, Mahmoudi M, Orth M, Landwehrmeyer GB, Paulsen Jane s, Dorsey ER, Shoulson I & Myers Richard h (2015a). Identification of genetic factors that modify clinical onset of Huntington's disease. *Cell*, 162, 516-526.
- Lee JM, Ramos EM, Lee JH, Gillis T, Mysore JS, Hayden MR, Warby SC, Morrison P, Nance M, Ross CA, Margolis RL, Squitieri F, Orobello S, Di Donato S, Gomez-Tortosa E, Ayuso C, Suchowersky O, Trent RJ, Mccusker E, Novelletto A, Frontali M, Jones R, Ashizawa T, Frank S, Saint-Hilaire MH, Hersch SM, Rosas HD, Lucente D, Harrison MB, Zanko A, Abramson RK, Marder K, Sequeiros J, Paulsen JS, Landwehrmeyer GB, Myers RH, Macdonald ME & Gusella JF (2012). CAG repeat expansion in Huntington disease determines age at onset in a fully dominant fashion. *Neurology*, 78, 690-5.
- Lee W, Lee SD, Park MY, Foley L, Purcell-Estabrook E, Kim H & Yoo SS (2015b). Functional and diffusion tensor magnetic resonance imaging of the sheep brain. *BMC Vet Res*, 11, 262.
- Lelos MJ & Dunnett SB (2018). Generating Excitotoxic Lesion Models of Huntington's Disease. *Methods Mol Biol*, 1780, 209-220.
- Lentz L, Zhao Y, Kelly MT, Schindeldecker W, Goetz S, Nelson DE & Raibe RS (2015). Motor behaviors in the sheep evoked by electrical stimulation of the subthalamic nucleus. *Exp Neurol*, 273, 69-82.
- Leonard MK, Cai R, Babiak MC, Ren A & Chang EF (2016). The peri-Sylvian cortical network underlying single word repetition revealed by electrocortical stimulation and direct neural recordings. *Brain Lang*, 193.
- Levesque M & Parent A (2005). The striatofugal fiber system in primates: a reevaluation of its organization based on single-axon tracing studies. *Proc Natl Acad Sci U S A*, 102, 11888-93.

- Li SH, Schilling G, Young WS, 3rd, Li XJ, Margolis RL, Stine OC, Wagster MV, Abbott MH, Franz ML, Ranen NG & Et Al. (1993). Huntington's disease gene (IT15) is widely expressed in human and rat tissues. *Neuron*, 11, 985-93.
- Li XJ & Li S (2012). Influence of species differences on the neuropathology of transgenic Huntington's disease animal models. *J Genet Genomics*, 39, 239-45.
- Li XJ & Li S (2015). Large animal models of Huntington's disease. *Curr Top Behav Neurosci*, 22, 149-60.
- Libby P (2015). Murine "model" monotheism: an iconoclast at the altar of mouse. *Circ Res*, 117, 921-5.
- Liebelt F & Vertegaal AC (2016). Ubiquitin-dependent and independent roles of SUMO in proteostasis. *Am J Physiol Cell Physiol*, 311, C284-96.
- Lin CC, Chen KS, Lin YL & Chan JP (2015). Multiple subluxations and comminuted fracture of the cervical spine in a sheep. *Tierarztl Prax Ausg G Grosstiere Nutztiere*, 43, 44-8.
- Lin JH (2008). Applications and limitations of genetically modified mouse models in drug discovery and development. *Curr Drug Metab*, 9, 419-38.
- Lin L, Jin Z, Tan H, Xu Q, Peng T & Li H (2016). Atypical ubiquitination by E3 ligase WWP1 inhibits the proteasome-mediated degradation of mutant huntingtin. *Brain Res*, 1643, 103-12.
- Lindgren HS, Wickens R, Tait DS, Brown VJ & Dunnett SB (2013). Lesions of the dorsomedial striatum impair formation of attentional set in rats. *Neuropharmacology*, 71, 148-53.
- Lipton SA (2006). Paradigm shift in neuroprotection by NMDA receptor blockade: memantine and beyond. *Nat Rev Drug Discov*, 5, 160-70.
- Lisy V, Dvorakova L & Stastny F (1994). Altered glutamate binding following quinolinate lesions in developing rat brain. *Exp Neurol*, 125, 82-6.
- Liu JP & Zeitlin SO (2017). Is Huntingtin Dispensable in the Adult Brain? *J Huntingtons Dis*, 6, 1-17.
- Liu W, Yang J, Burgunder J, Cheng B & Shang H (2016). Diffusion imaging studies of Huntington's disease: A meta-analysis. *Parkinsonism Relat Disord*, 32, 94-101.
- Lollgen S & Weiher H (2015). The role of the Mpv17 protein mutations of which cause mitochondrial DNA depletion syndrome (MDDS): lessons from homologs in different species. *Biol Chem*, 396, 13-25.
- Lope-Piedrafita S (2018). Diffusion tensor imaging (DTI). *Methods Mol Biol*, 1718, 103-116.
- Lugo-Huitron R, Ugalde Muniz P, Pineda B, Pedraza-Chaverri J, Rios C & Perez-De La Cruz V (2013). Quinolinic acid: an endogenous neurotoxin with multiple targets. *Oxid Med Cell Longev*, 2013, 104024.
- Macdonald ME, Ambrose CM, Duyao MP, Myers RH, Lin C, Srinidhi L, Barnes G, Taylor SA, James M, Groot N, Macfarlane H, Jenkins B, Anderson MA, Wexler NS, Gusella JF, Bates GP, Baxendale S, Hummerich H, Kirby S, North M, Youngman S, Mott R, Zehetner G, Sedlacek Z, Poustka A, Frischauf A-M, Lehrach H, Buckler AJ, Church D, Doucette-Stamm L, O'donovan MC, Riba-Ramirez L, Shah M, Stanton VP, Strobel SA, Draths KM, Wales JL, Dervan P, Housman DE, Altherr M, Shiang R, Thompson L, Fielder T, Wasmuth JJ, Tagle D, Valdes J, Elmer L, Allard M, Castilla L, Swaroop M, Blanchard K, Collins FS, Snell R, Holloway T, Gillespie K, Datson N, Shaw D & Harper PS (1993). A novel gene containing a trinucleotide repeat that is expanded and unstable on Huntington's disease chromosomes. *Cell*, 72, 971-983.

- Mageed M, Ionita JC, Ludewig E, Brehm W & Gerlach K (2014). Morphometrical analysis of the thoracolumbar dural sac in sheep using computed assisted myelography. *Vet Comp Orthop Traumatol*, 27, 124-9.
- Mahajan V, Demissie E, Mattoo H, Viswanadham V, Varki A, Morris R & Pillai S (2016). Striking immune phenotypes in gene-targeted mice are driven by a copy-number variant originating from a commercially available C57BL/6 strain. *Cell Reports*, 15, 1901-1909.
- Mailly P, Aliane V, Groenewegen HJ, Haber SN & Deniau JM (2013). The rat prefrontostriatal system analyzed in 3D: evidence for multiple interacting functional units. *J Neurosci*, 33, 5718-27.
- Mangiarini L, Sathasivam K, Seller M, Cozens B, Harper A, Hetherington C, Lawton M, Trottier Y, Lehrach H, Davies SW & Bates GP (1996). Exon 1 of the HD gene with an expanded CAG repeat is sufficient to cause a progressive neurological phenotype in transgenic mice. *Cell*, 87, 493-506.
- Marques BL, Carvalho GA, Freitas EMM, Chiareli RA, Barbosa TG, Di Araujo AGP, Nogueira YL, Ribeiro RI, Parreira RC, Vieira MS, Resende RR, Gomez RS, Oliveira-Lima OC & Pinto MCX (2019). The role of neurogenesis in neurorepair after ischemic stroke. *Semin Cell Dev Biol*, 95, 98-110.
- Marques S & Humbert S (2013). Huntingtin: here, there, everywhere! *J Huntingtons Dis*, 2, 395-403.
- Marshall PE, Landis DM & Zalzneraitis EL (1983). Immunocytochemical studies of substance P and leucine-enkephalin in Huntington's disease. *Brain Res*, 289, 11-26.
- Martin DD, Ladha S, Ehrnhoefer DE & Hayden MR (2015). Autophagy in Huntington disease and huntingtin in autophagy. *Trends Neurosci*, 38, 26-35.
- Mason S & Barker RA (2015). Progress in Huntington's disease: the search for markers of disease onset and progression. *J Neurol*, 262, 1990-5.
- Mason SL, Daws RE, Soreq E, Johnson EB, Scahill RI, Tabrizi SJ, Barker RA & Hampshire A (2018). Predicting clinical diagnosis in Huntington's disease: An imaging polymarker. *Ann Neurol*, 83, 532-543.
- Matamales M, Bertran-Gonzalez J, Salomon L, Degos B, Deniau JM, Valjent E, Herve D & Girault JA (2009). Striatal medium-sized spiny neurons: identification by nuclear staining and study of neuronal subpopulations in BAC transgenic mice. *PLoS One*, 4, e4770.
- Mcbride SD & Morton AJ (2018). Indices of comparative cognition: assessing animal models of human brain function. *Exp Brain Res*, 236, 3379-3390.
- Mcbride SD, Perentos N & Morton AJ (2015). Understanding the concept of a reflective surface: Can sheep improve navigational ability through the use of a mirror? *Animal Cognition*, 18, 361-371.
- Mcbride SD, Perentos N & Morton AJ (2016). A mobile, high-throughput semi-automated system for testing cognition in large non-primate animal models of Huntington disease. *J Neurosci Methods*, 265, 25-33.
- Mccolgan P & Tabrizi SJ (2018). Huntington's disease: a clinical review. *Eur J Neurol*, 25, 24-34.
- Mehler MF, Petronglo JR, Arteaga-Bracho EE, Gulinello M, Winchester ML, Pichamoorthy N, Young SK, Dejesus CD, Ishtiaq H, Gokhan S & Molero AE (2019). Loss-of-huntingtin in medial and lateral ganglionic lineages differentially disrupts regional interneuron and projection neuron subtypes and promotes Huntington's disease-associated behavioral, cellular and pathological hallmarks. *J Neurosci*, 39, 1892-1909.
- Menalled L & Brunner D (2014). Animal models of Huntington's disease for translation to the clinic: best practices. *Mov Disord*, 29, 1375-90.



- Menalled LB, Sison JD, Dragatsis I, Zeitlin S & Chesselet MF (2003). Time course of early motor and neuropathological anomalies in a knock-in mouse model of Huntington's disease with 140 CAG repeats. *J Comp Neurol*, 465, 11-26.
- Mestas J & Hughes CC (2004). Of mice and not men: differences between mouse and human immunology. *J Immunol*, 172, 2731-8.
- Meyer M, Zysset S, Von Cramon DY & Alter K (2005). Distinct fMRI responses to laughter, speech, and sounds along the human peri-sylvian cortex. *Brain Res Cogn Brain Res*, 24, 291-306.
- Mielcarek M (2015). Huntington's disease is a multi-system disorder. *Rare Dis*, 3, e1058464.
- Miller J, Arrasate M, Shaby BA, Mitra S, Masliah E & Finkbeiner S (2010). Quantitative relationships between huntingtin levels, polyglutamine length, inclusion body formation, and neuronal death provide novel insight into huntington's disease molecular pathogenesis. *J Neurosci*, 30, 10541-50.
- Mishra J & Kumar A (2014). Improvement of mitochondrial NAD(+)/FAD(+)-linked state-3 respiration by caffeine attenuates quinolinic acid induced motor impairment in rats: implications in Huntington's disease. *Pharmacol Rep*, 66, 1148-55.
- Moffett JR, Ross B, Arun P, Madhavarao CN & Namboodiri AM (2007). N-Acetylaspartate in the CNS: from neurodiagnostics to neurobiology. *Prog Neurobiol*, 81, 89-131.
- Molochnikov I & Cohen D (2014). Hemispheric differences in the mesostriatal dopaminergic system. *Front Syst Neurosci*, 8, 110.
- Monaco G, Van Dam S, Casal Novo Ribeiro JL, Larbi A & De Magalhães JP (2015). A comparison of human and mouse gene co-expression networks reveals conservation and divergence at the tissue, pathway and disease levels. *BMC evolutionary biology*, 15, 259-259.
- Mora-Macias J, Reina-Romo E, Morgaz J & Dominguez J (2015). In vivo gait analysis during bone transport. *Ann Biomed Eng*, 43, 2090-100.
- Morales-Martinez A, Sanchez-Mendoza A, Martinez-Lazcano JC, Pineda-Farias JB, Montes S, El-Hafidi M, Martinez-Gopar PE, Tristan-Lopez L, Perez-Neri I, Zamorano-Carrillo A, Castro N, Rios C & Perez-Severiano F (2017). Essential fatty acid-rich diets protect against striatal oxidative damage induced by quinolinic acid in rats. *Nutr Neurosci*, 20, 388-395.
- Morigaki R & Goto S (2017). Striatal vulnerability in Huntington's disease: Neuroprotection versus neurotoxicity. *Brain Sciences*, 7, 63.
- Moritani T, Smoker WR, Sato Y, Numaguchi Y & Westesson PL (2005). Diffusion-weighted imaging of acute excitotoxic brain injury. *AJNR Am J Neuroradiol*, 26, 216-28.
- Moroni F, Lombardi G, Moneti G & Aldinio C (1984). The excitotoxin quinolinic acid is present in the brain of several mammals and its cortical content increases during the aging process. *Neuroscience Letters*, 47, 51-55.
- Morris JE, Fisher AD, Doyle RE & Bush RD (2010). Determination of sheep learning responses to a directional audio cue. *Journal of Applied Animal Welfare Science*, 13, 347-360.
- Morton AJ (2018). Large-brained animal models of Huntington's disease: Sheep. *Methods Mol Biol*, 1780, 221-239.
- Morton AJ & Avanzo L (2011). Executive decision-making in the domestic sheep. *PLoS One*, 6, e15752.
- Morton AJ & Howland DS (2013). Large genetic animal models of Huntington's disease. *J Huntingtons Dis*, 2, 3-19.

- Morton AJ, Middleton B, Rudiger S, Bawden CS, Kuchel TR & Skene DJ (2019). Increased plasma melatonin in presymptomatic Huntington disease sheep (*Ovis aries*): Compensatory neuroprotection in a neurodegenerative disease? *J Pineal Res*, e12624.
- Morton AJ, Rudiger SR, Wood NI, Sawiak SJ, Brown GC, Mclaughlan CJ, Kuchel TR, Snell RG, Faull RL & Bawden CS (2014). Early and progressive circadian abnormalities in Huntington's disease sheep are unmasked by social environment. *Hum Mol Genet*, 23, 3375-83.
- Murray SJ, Black BL, Reid SJ, Rudiger SR, Simon Bawden C, Snell RG, Waldvogel HJ & Faull RLM (2019). Chemical neuroanatomy of the substantia nigra in the ovine brain. *J Chem Neuroanat*, 97, 43-56.
- Nagy DW (2017). Diagnostics and ancillary tests of neurologic dysfunction in the ruminant. *Vet Clin North Am Food Anim Pract*, 33, 9-18.
- Nakanishi S (1992). Molecular diversity of glutamate receptors and implications for brain function. *Science*, 258, 597-603.
- Nam HY, Na EJ, Lee E, Kwon Y & Kim HJ (2017). Antiepileptic and neuroprotective effects of oleamide in rat striatum on kainate-induced behavioral seizure and excitotoxic damage via calpain inhibition. *Front Pharmacol*, 8, 817.
- Nana AL, Kim EH, Thu DC, Oorschot DE, Tippett LJ, Hogg VM, Synek BJ, Roxburgh R, Waldvogel HJ & Faull RL (2014). Widespread heterogeneous neuronal loss across the cerebral cortex in Huntington's disease. *J Huntingtons Dis*, 3, 45-64.
- Nanetti L, Contarino VE, Castaldo A, Sarro L, Bachoud-Levi AC, Giavazzi M, Frittoli S, Ciammola A, Rizzo E, Gellera C, Bruzzone MG, Taroni F, Grisoli M & Mariotti C (2018). Cortical thickness, stance control, and arithmetic skill: An exploratory study in premanifest Huntington disease. *Parkinsonism Relat Disord*, 51, 17-23.
- Nasir J, Floresco SB, O'kusky JR, Diewert VM, Richman JM, Zeisler J, Borowski A, Marth JD, Phillips AG & Hayden MR (1995). Targeted disruption of the Huntington's disease gene results in embryonic lethality and behavioral and morphological changes in heterozygotes. *Cell*, 81, 811-23.
- Nelson AB & Kreitzer AC (2014). Reassessing models of basal ganglia function and dysfunction. *Annu Rev Neurosci*, 37, 117-35.
- Neto JL, Lee JM, Afridi A, Gillis T, Guide JR, Dempsey S, Lager B, Alonso I, Wheeler VC & Pinto RM (2017). Genetic contributors to intergenerational CAG repeat instability in Huntington's disease knock-in mice. *Genetics*, 205, 503-516.
- Nonomura S, Nishizawa K, Sakai Y, Kawaguchi Y, Kato S, Uchigashima M, Watanabe M, Yamanaka K, Enomoto K, Chiken S, Sano H, Soma S, Yoshida J, Samejima K, Ogawa M, Kobayashi K, Nambu A, Isomura Y & Kimura M (2018). Monitoring and updating of action selection for goal-directed behavior through the striatal direct and indirect pathways. *Neuron*, 99, 1302-1314.
- Norman AB, Norgren RB, Wyatt LM, Hildebrand JP & Sanberg PR (1992). The direction of apomorphine-induced rotation behavior is dependent on the location of excitotoxin lesions in the rat basal ganglia. *Brain Res*, 569, 169-72.
- O'Kusky JR, Nasir J, Cicchetti F, Parent A & Hayden MR (1999). Neuronal degeneration in the basal ganglia and loss of pallido-subthalamic synapses in mice with targeted disruption of the Huntington's disease gene. *Brain Res*, 818, 468-79.
- Ogawa A, Osada T, Tanaka M, Hori M, Aoki S, Nikolaidis A, Milham MP & Konishi S (2018). Striatal subdivisions that coherently interact with multiple cerebrocortical networks. *Hum Brain Mapp*, 39, 4349-4359.
- Olson L, Seiger A & Fuxe K (1972). Heterogeneity of striatal and limbic dopamine innervation: highly fluorescent islands in developing and adult rats. *Brain Res*, 44, 283-8.

- Oxley TJ, Opie NL, John SE, Rind GS, Ronayne SM, Wheeler TL, Judy JW, McDonald AJ, Dornom A, Lovell TJ, Steward C, Garrett DJ, Moffat BA, Lui EH, Yassi N, Campbell BC, Wong YT, Fox KE, Nurse ES, Bennett IE, Bauquier SH, Liyanage KA, Van Der Nagel NR, Perucca P, Ahnood A, Gill KP, Yan B, Churilov L, French CR, Desmond PM, Horne MK, Kiers L, Prawer S, Davis SM, Burkitt AN, Mitchell PJ, Grayden DB, May CN & O'Brien TJ (2016). Minimally invasive endovascular stent-electrode array for high-fidelity, chronic recordings of cortical neural activity. *Nat Biotechnol*, 34, 320-7.
- Padowski JM, Weaver KE, Richards TL, Laurino MY, Samii A, Aylward EH & Conley KE (2014). Neurochemical correlates of caudate atrophy in Huntington's disease. *Mov Disord*, 29, 327-35.
- Palfi S, Ferrante RJ, Brouillet E, Beal MF, Dolan R, Guyot MC, Peschanski M & Hantraye P (1996). Chronic 3-nitropropionic acid treatment in baboons replicates the cognitive and motor deficits of Huntington's disease. *J Neurosci*, 16, 3019-25.
- Patassini S, Begley P, Xu J, Church SJ, Kureishy N, Reid SJ, Waldvogel HJ, Faull RLM, Snell RG, Unwin RD & Cooper GJS (2019). Cerebral vitamin B5 (D-Pantothenic Acid) deficiency as a potential cause of metabolic perturbation and neurodegeneration in Huntington's disease. *Metabolites*, 9, 113.
- Patassini S, Begley P, Xu J, Church SJ, Reid SJ, Kim EH, Curtis MA, Dragunow M, Waldvogel HJ, Snell RG, Unwin RD, Faull RL & Cooper GJ (2016). Metabolite mapping reveals severe widespread perturbation of multiple metabolic processes in Huntington's disease human brain. *Biochim Biophys Acta*, 1862, 1650-62.
- Perentos N, Martins AQ, Cumming RJ, Mitchell NL, Palmer DN, Sawiak SJ & Morton AJ (2016). An EEG investigation of sleep homeostasis in healthy and CLN5 Batten disease affected sheep. *J Neurosci*, 36, 8238-49.
- Perentos N, Martins AQ, Watson TC, Bartsch U, Mitchell NL, Palmer DN, Jones MW & Morton AJ (2015). Translational neurophysiology in sheep: measuring sleep and neurological dysfunction in CLN5 Batten disease affected sheep. *Brain*, 138, 862-74.
- Perez V, Suarez-Vega A, Fuertes M, Benavides J, Delgado L, Ferreras MC & Arranz JJ (2013). Hereditary lissencephaly and cerebellar hypoplasia in Churra lambs. *BMC Vet Res*, 9, 156.
- Perez XA, Zhang D, Bordia T & Quik M (2017). Striatal D1 medium spiny neuron activation induces dyskinesias in parkinsonian mice. *Mov Disord*, 32, 538-548.
- Perlman RL (2016). Mouse models of human disease: An evolutionary perspective. *Evolution, medicine, and public health*, 2016, 170-176.
- Pert CB, Kuhar MJ & Snyder SH (1976). Opiate receptor: autoradiographic localization in rat brain. *Proc Natl Acad Sci U S A*, 73, 3729-33.
- Pfister EL, Dinardo N, Mondo E, Borel F, Conroy F, Fraser C, Gernoux G, Han X, Hu D, Johnson E, Kennington L, Liu P, Reid SJ, Sapp E, Vodicka P, Kuchel T, Morton AJ, Howland D, Moser R, Sena-Esteves M, Gao G, Mueller C, DiFiglia M & Aronin N (2018). Artificial miRNAs reduce human mutant Huntingtin throughout the striatum in a transgenic sheep model of Huntington's disease. *Hum Gene Ther*, 29, 663-673.
- Pickrell AM, Fukui H, Wang X, Pinto M & Moraes CT (2011). The striatum is highly susceptible to mitochondrial oxidative phosphorylation dysfunctions. *J Neurosci*, 31, 9895-904.
- Pierozan P, Zamoner A, Soska AK, Silvestrin RB, Loureiro SO, Heimfarth L, Mello E Souza T, Wajner M & Pessoa-Pureur R (2010). Acute intrastriatal administration of quinolinic acid provokes hyperphosphorylation of cytoskeletal intermediate filament proteins in astrocytes and neurons of rats. *Exp Neurol*, 224, 188-96.
- Pierson LL, Gerhardt KJ, Griffiths SK & Abrams RM (1995). Auditory brainstem response in sheep. Part I: Fetal development. *Dev Psychobiol*, 28, 293-305.

- Popoli P, Pezzola A, Domenici MR, Sagratella S, Diana G, Caporali MG, Bronzetti E, Vega J & Scotti De Carolis A (1994). Behavioral and electrophysiological correlates of the quinolinic acid rat model of Huntington's disease in rats. *Brain Res Bull*, 35, 329-35.
- Pouladi MA, Morton AJ & Hayden MR (2013). Choosing an animal model for the study of Huntington's disease. *Nat Rev Neurosci*, 14, 708-21.
- Prensa L, Gimenez-Amaya JM & Parent A (1998). Morphological features of neurons containing calcium-binding proteins in the human striatum. *J Comp Neurol*, 390, 552-63.
- Provost JS, Hanganu A & Monchi O (2015). Neuroimaging studies of the striatum in cognition Part I: healthy individuals. *Front Syst Neurosci*, 9, 140.
- Ramaswamy S, McBride JL & Kordower JH (2007). Animal models of Huntington's disease. *Ilar j*, 48, 356-73.
- Ramos ARS & Garrett C (2017). Huntington's disease: Premotor phase. *Neurodegener Dis*, 17, 313-322.
- Reddy PH & Shirendeb UP (2012). Mutant huntingtin, abnormal mitochondrial dynamics, defective axonal transport of mitochondria, and selective synaptic degeneration in Huntington's disease. *Biochim Biophys Acta*, 1822, 101-10.
- Regnier A, Andreoletti O, Albaric O, Gruson DC, Schelcher F & Toutain PL (2011). Clinical, electroretinographic and histomorphometric evaluation of the retina in sheep with natural scrapie. *BMC Vet Res*, 7, 25.
- Reid SJ, Patassini S, Handley RR, Rudiger SR, Mclaughlan CJ, Osmand A, Jacobsen JC, Morton AJ, Weiss A, Waldvogel HJ, Macdonald ME, Gusella JF, Bawden CS, Faull RL & Snell RG (2013). Further molecular characterisation of the OVT73 transgenic sheep model of Huntington's disease identifies cortical aggregates. *J Huntingtons Dis*, 2, 279-95.
- Reiner A, Albin RL, Anderson KD, D'Amato CJ, Penney JB & Young AB (1988). Differential loss of striatal projection neurons in Huntington disease. *Proc Natl Acad Sci U S A*, 85, 5733-7.
- Reiner A & Deng YP (2018). Disrupted striatal neuron inputs and outputs in Huntington's disease. *CNS Neurosci Ther*, 24, 250-280.
- Reiner A, Dragatsis I & Dietrich P (2011). Genetics and neuropathology of Huntington's disease. *International review of neurobiology*, 98, 325-372.
- Reiner A, Shelby E, Wang H, Demarch Z, Deng Y, Guley NH, Hogg V, Roxburgh R, Tippett LJ, Waldvogel HJ & Faull RL (2013). Striatal parvalbuminergic neurons are lost in Huntington's disease: implications for dystonia. *Mov Disord*, 28, 1691-9.
- Rios C & Santamaria A (1991). Quinolinic acid is a potent lipid peroxidant in rat brain homogenates. *Neurochem Res*, 16, 1139-43.
- Robbe D (2018). To move or to sense? Incorporating somatosensory representation into striatal functions. *Curr Opin Neurobiol*, 52, 123-130.
- Robinson N (1969). Histochemical changes in neocortex and corpus callosum after intracranial injection. *J Neurol Neurosurg Psychiatry*, 32, 317-23.
- Rodrigues FB, Abreu D, Damásio J, Goncalves N, Correia-Guedes L, Coelho M, Ferreira JJ & Network RIOTEHSD (2017). Survival, mortality, causes and places of death in a European Huntington's disease prospective cohort. *Movement Disorders Clinical Practice*, 4, 737-742.
- Rogers CS (2016). Genetically engineered livestock for biomedical models. *Transgenic Res*, 25, 345-359.

- Rohlfing T, Zahr NM, Sullivan EV & Pfefferbaum A (2010). The SRI24 multichannel atlas of normal adult human brain structure. *Human brain mapping*, 31, 798-819.
- Roitberg BZ, Emborg ME, Sramek JG, Palfi S & Kordower JH (2002). Behavioral and morphological comparison of two nonhuman primate models of Huntington's disease. *Neurosurgery*, 50, 137-45; discussion 145-6.
- Rolls A, Shechter R & Schwartz M (2009). The bright side of the glial scar in CNS repair. *Nat Rev Neurosci*, 10, 235-41.
- Roos RA (2010). Huntington's disease: a clinical review. *Orphanet J Rare Dis*, 5, 40.
- Roshchupkin GV, Gutman BA, Vernooij MW, Jahanshad N, Martin NG, Hofman A, McMahon KL, Van Der Lee SJ, Van Duijn CM, De Zubicaray GI, Uitterlinden AG, Wright MJ, Niessen WJ, Thompson PM, Ikram MA & Adams HH (2016). Heritability of the shape of subcortical brain structures in the general population. *Nat Commun*, 7, 13738.
- Rothman AH & Glick SD (1976). Differential effects of unilateral and bilateral caudate lesions on side preference and passive avoidance behavior in rats. *Brain Res*, 118, 361-9.
- Rub U, Seidel K, Heinsen H, Vonsattel JP, Den Dunnen WF & Korf HW (2016). Huntington's disease (HD): The neuropathology of a multisystem neurodegenerative disorder of the human brain. *Brain Pathol*, 26, 726-740.
- Rudebeck PH, Ripple JA, Mitz AR, Averbeck BB & Murray EA (2017). Amygdala contributions to stimulus-reward encoding in the macaque medial and orbital frontal cortex during learning. *J Neurosci*, 37, 2186-2202.
- Sabel BA & Stein DG (1982). Intracerebral injections of isotonic saline prevent behavioral deficits from brain damage. *Physiol Behav*, 28, 1017-23.
- Safayi S, Jeffery ND, Shivapour SK, Zamanighomi M, Zylstra TJ, Bratsch-Prince J, Wilson S, Reddy CG, Fredericks DC, Gillies GT & Howard MA, 3rd (2015). Kinematic analysis of the gait of adult sheep during treadmill locomotion: Parameter values, allowable total error, and potential for use in evaluating spinal cord injury. *J Neurol Sci*, 358, 107-12.
- Safayi S, Miller JW, Wilson S, Shivapour SK, Oelfke TF, Ford AL, Klarmann Staudt A, Abode-Iyamah K, Reddy CG, Jeffery ND, Fredericks DC, Gillies GT & Howard MA, 3rd (2016). Treadmill measures of ambulation rates in ovine models of spinal cord injury and neuropathic pain. *J Med Eng Technol*, 40, 72-9.
- Sagredo O, Gonzalez S, Aroyo I, Pazos MR, Benito C, Lastres-Becker I, Romero JP, Tolon RM, Mechoulam R, Brouillet E, Romero J & Fernandez-Ruiz J (2009). Cannabinoid CB2 receptor agonists protect the striatum against malonate toxicity: relevance for Huntington's disease. *Glia*, 57, 1154-67.
- Sahoo B, Arduini I, Drombosky KW, Kodali R, Sanders LH, Greenamyre JT & Wetzel R (2016). Folding landscape of mutant huntingtin exon1: Diffusible multimers, oligomers and fibrils, and no detectable monomer. *PLoS One*, 11, e0155747.
- Salomonczyk D, Panzera R, Pirogovosky E, Goldstein J, Corey-Bloom J, Simmons R & Gilbert PE (2010). Impaired postural stability as a marker of premanifest Huntington's disease. *Mov Disord*, 25, 2428-33.
- Sánchez T, Fraguera M, Lezcano L, Amador E, Fernández B, Agramonte M, Pedre L & Rosado J (2018). Rotating and neurochemical activity of rats lesioned with quinolinic acid and transplanted with bone marrow mononuclear cells. *Behavioral sciences (Basel, Switzerland)*, 8, 87.

- Saudou F, Finkbeiner S, Devys D & Greenberg ME (1998). Huntingtin acts in the nucleus to induce apoptosis but death does not correlate with the formation of intranuclear inclusions. *Cell*, 95, 55-66.
- Saudou F & Humbert S (2016). The biology of huntingtin. *Neuron*, 89, 910-26.
- Sauer D, Allegrini PR, Thedinga KH, Massieu L, Amacker H & Fagg GE (1992). Evaluation of quinolinic acid induced excitotoxic neurodegeneration in rat striatum by quantitative magnetic resonance imaging in vivo. *J Neurosci Methods*, 42, 69-74.
- Schliebs R, Roßner S & Bigl V (1996). Chapter 25 Immunolesion by 192IgG-saporin of rat basal forebrain cholinergic system: a useful tool to produce cortical cholinergic dysfunction. In: Klein J & Löffelholz K (eds.) *Progress in Brain Research*. Elsevier. 253-264.
- Schneider B & Koenigs M (2017). Human lesion studies of ventromedial prefrontal cortex. *Neuropsychologia*, 107, 84-93.
- Schwarcz R, Guidetti P, Sathyaikumar KV & Muchowski PJ (2010). Of mice, rats and men: Revisiting the quinolinic acid hypothesis of Huntington's disease. *Prog Neurobiol*, 90, 230-45.
- Schwarcz R, Hokfelt T, Fuxe K, Jonsson G, Goldstein M & Terenius L (1979). Ibotenic acid-induced neuronal degeneration: a morphological and neurochemical study. *Exp Brain Res*, 37, 199-216.
- Schwarcz R & Kohler C (1983). Differential vulnerability of central neurons of the rat to quinolinic acid. *Neurosci Lett*, 38, 85-90.
- Scott PR (1995). The collection and analysis of cerebrospinal fluid as an aid to diagnosis in ruminant neurological disease. *Br Vet J*, 151, 603-14.
- Scott PR (2010). Cerebrospinal fluid collection and analysis in suspected sheep neurological disease. *Small Ruminant Research*, 92, 96-103.
- Selvaraj K, Manickam N, Kumaran E, Thangadurai K, Elumalai G, Sekar A, Radhakrishnan RK & Kandasamy M (2020). Deterioration of neuroregenerative plasticity in association with testicular atrophy and dysregulation of the hypothalamic-pituitary-gonadal (HPG) axis in Huntington's disease: A putative role of the huntingtin gene in steroidogenesis. *The Journal of Steroid Biochemistry and Molecular Biology*, 197, 105526.
- Seok J, Warren HS, Cuenca AG, Mindrinos MN, Baker HV, Xu W, Richards DR, McDonald-Smith GP, Gao H, Hennessy L, Finnerty CC, Lopez CM, Honari S, Moore EE, Minei JP, Cuschieri J, Bankey PE, Johnson JL, Sperry J, Nathens AB, Billiar TR, West MA, Jeschke MG, Klein MB, Gamelli RL, Gibran NS, Brownstein BH, Miller-Graziano C, Calvano SE, Mason PH, Cobb JP, Rahme LG, Lowry SF, Maier RV, Moldawer LL, Herndon DN, Davis RW, Xiao W & Tompkins RG (2013). Genomic responses in mouse models poorly mimic human inflammatory diseases. *Proc Natl Acad Sci U S A*, 110, 3507-12.
- Sharma S & Taliyan R (2015). Transcriptional dysregulation in Huntington's disease: The role of histone deacetylases. *Pharmacol Res*, 100, 157-69.
- Shear DA, Dong J, Gundy CD, Haik-Creguer KL & Dunbar GL (1998). Comparison of intrastriatal injections of quinolinic acid and 3-nitropropionic acid for use in animal models of Huntington's disease. *Progress in Neuro-Psychopharmacology and Biological Psychiatry*, 22, 1217-1240.
- Shemesh N, Sadan O, Melamed E, Offen D & Cohen Y (2010). Longitudinal MRI and MRSI characterization of the quinolinic acid rat model for excitotoxicity: peculiar apparent diffusion coefficients and recovery of N-acetyl aspartate levels. *NMR Biomed*, 23, 196-206.
- Shipp S (2016). The functional logic of corticostriatal connections. *Brain Struct Funct*, 222, 669-706.

- Singh-Bains MK, Mehrabi NF, Sehji T, Austria MDR, Tan AYS, Tippet LJ, Dragunow M, Waldvogel HJ & Faull RLM (2019). Cerebellar degeneration correlates with motor symptoms in Huntington disease. *Ann Neurol*, 85, 396-405.
- Skiold B, Wu Q, Hooper SB, Davis PG, McIntyre R, Tolcos M, Pearson J, Vreys R, Egan GF, Barton SK, Cheong JL & Polglase GR (2014). Early detection of ventilation-induced brain injury using magnetic resonance spectroscopy and diffusion tensor imaging: an in vivo study in preterm lambs. *PLoS One*, 9, e95804.
- Slow EJ, Van Raamsdonk J, Rogers D, Coleman SH, Graham RK, Deng Y, Oh R, Bissada N, Hossain SM, Yang YZ, Li XJ, Simpson EM, Gutekunst CA, Leavitt BR & Hayden MR (2003). Selective striatal neuronal loss in a YAC128 mouse model of Huntington disease. *Hum Mol Genet*, 12, 1555-67.
- Smith Y, Bevan MD, Shink E & Bolam JP (1998). Microcircuitry of the direct and indirect pathways of the basal ganglia. *Neuroscience*, 86, 353-87.
- Snell RS (2010). Chapter 10: Clinical neuroanatomy. 7th ed.: Wolters Kluwer Health/Lippincott Williams & Wilkins. 528-549.
- Soares JM, Marques P, Alves V & Sousa N (2013). A hitchhiker's guide to diffusion tensor imaging. *Frontiers in neuroscience*, 7, 31-31.
- Southwell AL, Skotte NH, Villanueva EB, Ostergaard ME, Gu X, Kordasiewicz HB, Kay C, Cheung D, Xie Y, Waltl S, Dal Cengio L, Findlay-Black H, Doty CN, Petoukhov E, Iworima D, Slama R, Ooi J, Pouladi MA, Yang XW, Swayze EE, Seth PP & Hayden MR (2017). A novel humanized mouse model of Huntington disease for preclinical development of therapeutics targeting mutant huntingtin alleles. *Hum Mol Genet*, 26, 1115-1132.
- Storey E, Cipolloni PB, Ferrante RJ, Kowall NW & Beal MF (1994). Movement disorder following excitotoxin lesions in primates. *Neuroreport*, 5, 1259-61.
- Stout JC, Paulsen JS, Queller S, Solomon AC, Whitlock KB, Campbell JC, Carlozzi N, Duff K, Beglinger LJ, Langbehn DR, Johnson SA, Biglan KM & Aylward EH (2011). Neurocognitive signs in prodromal Huntington disease. *Neuropsychology*, 25, 1-14.
- Strauss I, Williamson JM, Bertram EH, Lothman EW & Fernandez EJ (1997). Histological and 1H magnetic resonance spectroscopic imaging analysis of quinolinic acid-induced damage to the rat striatum. *Magn Reson Med*, 37, 24-33.
- Strong TV, Tagle DA, Valdes JM, Elmer LW, Boehm K, Swaroop M, Kaatz KW, Collins FS & Albin RL (1993). Widespread expression of the human and rat Huntington's disease gene in brain and nonneural tissues. *Nat Genet*, 5, 259-65.
- Sturrock A, Laule C, Decolongon J, Dar Santos R, Coleman AJ, Creighton S, Bechtel N, Reilmann R, Hayden MR, Tabrizi SJ, Mackay AL & Leavitt BR (2010). Magnetic resonance spectroscopy biomarkers in premanifest and early Huntington disease. *Neurology*, 75, 1702-10.
- Sturrock A, Laule C, Wyper K, Milner RA, Decolongon J, Dar Santos R, Coleman AJ, Carter K, Creighton S, Bechtel N, Bohlen S, Reilmann R, Johnson HJ, Hayden MR, Tabrizi SJ, Mackay AL & Leavitt BR (2015). A longitudinal study of magnetic resonance spectroscopy Huntington's disease biomarkers. *Mov Disord*, 30, 393-401.
- Sudheimer K, Winn B, Kerndt G, Shoaps J, Davis K, Fobbs Jr. A & Johnson J (2019). The human brain atlas (online). Brain Biodiversity Bank. Michigan State University. <https://msu.edu/~brains/brains/human/index.html>.
- Sugnaseelan S, Prescott NB, Broom DM, Wathes CM & Phillips CJC (2013). Visual discrimination learning and spatial acuity in sheep. *Applied Animal Behaviour Science*, 147, 104-111.

- Sumathi T, Vedagiri A, Ramachandran S & Purushothaman B (2018). Quinolinic Acid-Induced Huntington Disease-Like Symptoms Mitigated by Potent Free Radical Scavenger Edaravone-a Pilot Study on Neurobehavioral, Biochemical, and Histological Approach in Male Wistar Rats. *J Mol Neurosci*, 66, 322-341.
- Swanson LW (2018). Brain maps 4.0-Structure of the rat brain: An open access atlas with global nervous system nomenclature ontology and flatmaps. *The Journal of comparative neurology*, 526, 935-943.
- Tabrizi SJ, Reilmann R, Roos RaC, Durr A, Leavitt B, Owen G, Jones R, Johnson H, Craufurd D, Hicks SL, Kennard C, Landwehrmeyer B, Stout JC, Borowsky B, Scahill RI, Frost C & Langbehn DR (2012). Potential endpoints for clinical trials in premanifest and early Huntington's disease in the TRACK-HD study: analysis of 24 month observational data. *The Lancet Neurology*, 11, 42-53.
- Tabrizi SJ, Scahill RI, Owen G, Durr A, Leavitt BR, Roos RA, Borowsky B, Landwehrmeyer B, Frost C, Johnson H, Craufurd D, Reilmann R, Stout JC & Langbehn DR (2013). Predictors of phenotypic progression and disease onset in premanifest and early-stage Huntington's disease in the TRACK-HD study: analysis of 36-month observational data. *Lancet Neurol*, 12, 637-49.
- Taft RA, Davisson M & Wiles MV (2006). Know thy mouse. *Trends Genet*, 22, 649-53.
- Tang X, Luo Y, Chen Z, Huang N, Johnson HJ, Paulsen JS & Miller MI (2018a). A Fully-Automated Subcortical and Ventricular Shape Generation Pipeline Preserving Smoothness and Anatomical Topology. *Front Neurosci*, 12, 321.
- Tang X, Ross CA, Johnson H, Paulsen JS, Younes L, Albin RL, Ratnanather JT & Miller MI (2018b). Regional subcortical shape analysis in premanifest Huntington's disease. *Hum Brain Mapp*, 40, 1419-1433.
- Tavares RG, Tasca CI, Santos CE, Alves LB, Porciuncula LO, Emanuelli T & Souza DO (2002). Quinolinic acid stimulates synaptosomal glutamate release and inhibits glutamate uptake into astrocytes. *Neurochem Int*, 40, 621-7.
- Tepper JM, Koos T, Ibanez-Sandoval O, Tecuapetla F, Faust TW & Assous M (2018). Heterogeneity and diversity of striatal GABAergic interneurons: Update 2018. *Front Neuroanat*, 12, 91.
- Thu DC, Oorschot DE, Tippett LJ, Nana AL, Hogg VM, Synek BJ, Luthi-Carter R, Waldvogel HJ & Faull RL (2010). Cell loss in the motor and cingulate cortex correlates with symptomatology in Huntington's disease. *Brain*, 133, 1094-110.
- Tinterri A, Menardy F, Diana MA, Lokmane L, Keita M, Couplier F, Lemoine S, Mailhes C, Mathieu B, Merchan-Sala P, Campbell K, Gyory I, Grosschedl R, Popa D & Garel S (2018). Active intermixing of indirect and direct neurons builds the striatal mosaic. *Nat Commun*, 9, 4725.
- Tippett LJ, Waldvogel HJ, Thomas SJ, Hogg VM, Van Roon-Mom W, Synek BJ, Graybiel AM & Faull RL (2007). Striosomes and mood dysfunction in Huntington's disease. *Brain*, 130, 206-21.
- Tkac I, Keene CD, Pfeuffer J, Low WC & Gruetter R (2001). Metabolic changes in quinolinic acid-lesioned rat striatum detected non-invasively by in vivo (1)H NMR spectroscopy. *J Neurosci Res*, 66, 891-8.
- Tognarelli JM, Dawood M, Shariff MIF, Grover VPB, Crossey MME, Cox IJ, Taylor-Robinson SD & Mcphail MJW (2015). Magnetic resonance spectroscopy: Principles and techniques: Lessons for clinicians. *Journal of clinical and experimental hepatology*, 5, 320-328.
- Torres PA, Zeng BJ, Porter BF, Alroy J, Horak F, Horak J & Kolodny EH (2010). Tay-Sachs disease in Jacob sheep. *Mol Genet Metab*, 101, 357-63.
- Trager U, Andre R, Lahiri N, Magnusson-Lind A, Weiss A, Grueninger S, Mckinnon C, Sirinathsinghi E, Kahlon S, Pfister EL, Moser R, Hummerich H, Antoniou M, Bates GP, Luthi-Carter R, Lowdell MW,



- Bjorkqvist M, Ostroff GR, Aronin N & Tabrizi SJ (2014). HTT-lowering reverses Huntington's disease immune dysfunction caused by NFkappaB pathway dysregulation. *Brain*, 137, 819-33.
- Tuney I, Tasset I, Perez-De La Cruz V & Santamaria A (2010). 3-Nitropropionic acid as a tool to study the mechanisms involved in Huntington's disease: past, present and future. *Molecules*, 15, 878-916.
- Tyynela J, Sohar I, Sleat DE, Gin RM, Donnelly RJ, Baumann M, Haltia M & Lobel P (2001). Congenital ovine neuronal ceroid lipofuscinosis--a cathepsin D deficiency with increased levels of the inactive enzyme. *Eur J Paediatr Neurol*, 5 Suppl A, 43-5.
- Ungerstedt U & Arbuthnott GW (1970). Quantitative recording of rotational behavior in rats after 6-hydroxy-dopamine lesions of the nigrostriatal dopamine system. *Brain Res*, 24, 485-93.
- Valor LM (2015). Transcription, epigenetics and ameliorative strategies in Huntington's Disease: a genome-wide perspective. *Mol Neurobiol*, 51, 406-23.
- Van Den Bogaard SJ, Dumas EM, Teeuwisse WM, Kan HE, Webb A, Roos RA & Van Der Grond J (2011). Exploratory 7-Tesla magnetic resonance spectroscopy in Huntington's disease provides in vivo evidence for impaired energy metabolism. *J Neurol*, 258, 2230-9.
- Van Den Bogaard SJ, Dumas EM, Teeuwisse WM, Kan HE, Webb A, Van Buchem MA, Roos RA & Van Der Grond J (2014). Longitudinal metabolite changes in Huntington's disease during disease onset. *J Huntingtons Dis*, 3, 377-86.
- Van Der Bom IM, Moser RP, Gao G, Mondo E, O'Connell D, Gounis MJ, McGowan S, Chaurette J, Bishop N, Sena-Esteves MS, Mueller C & Aronin N (2013). Finding the striatum in sheep: use of a multi-modal guided approach for convection enhanced delivery. *J Huntingtons Dis*, 2, 41-5.
- Van Der Burg JM, Bjorkqvist M & Brundin P (2009). Beyond the brain: widespread pathology in Huntington's disease. *Lancet Neurol*, 8, 765-74.
- Vandresen-Filho S, Martins WC, Bertoldo DB, Mancini G, De Bem AF & Tasca CI (2015). Cerebral cortex, hippocampus, striatum and cerebellum show differential susceptibility to quinolinic acid-induced oxidative stress. *Neurol Sci*, 36, 1449-56.
- Verma MK, Goel R, Nandakumar K & Nemmani KVS (2018). Bilateral quinolinic acid-induced lipid peroxidation, decreased striatal monoamine levels and neurobehavioral deficits are ameliorated by GIP receptor agonist D-Ala(2)GIP in rat model of Huntington's disease. *Eur J Pharmacol*, 828, 31-41.
- Vink R (2018). Large animal models of traumatic brain injury. *Journal of Neuroscience Research*, 96, 527-535.
- Vonsattel JP, Myers RH, Stevens TJ, Ferrante RJ, Bird ED & Richardson EP, Jr. (1985). Neuropathological classification of Huntington's disease. *J Neuropathol Exp Neurol*, 44, 559-77.
- Waelter S, Scherzinger E, Hasenbank R, Nordhoff E, Lurz R, Goehler H, Gauss C, Sathasivam K, Bates GP, Lehrach H & Wanker EE (2001). The huntingtin interacting protein HIP1 is a clathrin and alpha-adaptin-binding protein involved in receptor-mediated endocytosis. *Hum Mol Genet*, 10, 1807-17.
- Waldvogel HJ, Kim EH, Thu DC, Tippett LJ & Faull RL (2012a). New perspectives on the neuropathology in Huntington's disease in the human brain and its relation to symptom variation. *J Huntingtons Dis*, 1, 143-53.
- Waldvogel HJ, Kim EH, Tippett LJ, Vonsattel JP & Faull RL (2015). The neuropathology of Huntington's disease. *Curr Top Behav Neurosci*, 22, 33-80.
- Waldvogel HJ, Thu D, Hogg V, Tippett L & Faull RL (2012b). Selective neurodegeneration, neuropathology and symptom profiles in Huntington's disease. *Adv Exp Med Biol*, 769, 141-52.

- Wall NR, De La Parra M, Callaway EM & Kreitzer AC (2013). Differential innervation of direct- and indirect-pathway striatal projection neurons. *Neuron*, 79, 347-60.
- Wang G, Liu X, Gaertig MA, Li S & Li X-J (2016). Ablation of huntingtin in adult neurons is nondeleterious but its depletion in young mice causes acute pancreatitis. *Proceedings of the National Academy of Sciences of the United States of America*, 113, 3359-3364.
- Wang J, Zhou H, Forrest RHJ, Hu J, Liu X, Li S, Luo Y & Hickford JGH (2017). Variation in the ovine MYF5 gene and its effect on carcass lean meat yield in New Zealand Romney sheep. *Meat Sci*, 131, 146-151.
- Wasle K, Pospischil A, Hassig M, Gerspach C & Hilbe M (2017). The Post-mortem Examination in Ruminants and its Possible Benefit to Ruminant Clinical Medicine. *J Comp Pathol*, 156, 202-216.
- Watabe-Uchida M, Zhu L, Ogawa SK, Vamanrao A & Uchida N (2012). Whole-brain mapping of direct inputs to midbrain dopamine neurons. *Neuron*, 74, 858-73.
- Wells AJ, Vink R, Blumbergs PC, Brophy BP, Helps SC, Knox SJ & Turner RJ (2012). A surgical model of permanent and transient middle cerebral artery stroke in the sheep. *PLoS One*, 7, e42157.
- Wexler NS, Lorimer J, Porter J, Gomez F, Moskowitz C, Shackell E, Marder K, Penchaszadeh G, Roberts SA, Gayan J, Brocklebank D, Cherny SS, Cardon LR, Gray J, Dlouhy SR, Wiktorski S, Hodes ME, Conneally PM, Penney JB, Gusella J, Cha JH, Irizarry M, Rosas D, Hersch S, Hollingsworth Z, Macdonald M, Young AB, Andresen JM, Housman DE, De Young MM, Bonilla E, Stillings T, Negrette A, Snodgrass SR, Martinez-Jaurrieta MD, Ramos-Arroyo MA, Bickham J, Ramos JS, Marshall F, Shoulson I, Rey GJ, Feigin A, Arnheim N, Acevedo-Cruz A, Acosta L, Alvir J, Fischbeck K, Thompson LM, Young A, Dure L, O'brien CJ, Paulsen J, Brickman A, Krch D, Peery S, Hogarth P, Higgins DS, Jr. & Landwehrmeyer B (2004). Venezuelan kindreds reveal that genetic and environmental factors modulate Huntington's disease age of onset. *Proc Natl Acad Sci U S A*, 101, 3498-503.
- Wheeler VC, Persichetti F, Mcneil SM, Mysore JS, Mysore SS, Macdonald ME, Myers RH, Gusella JF & Wexler NS (2007). Factors associated with HD CAG repeat instability in Huntington disease. *J Med Genet*, 44, 695-701.
- Whetsell WO, Jr. & Schwarcz R (1989). Prolonged exposure to submicromolar concentrations of quinolinic acid causes excitotoxic damage in organotypic cultures of rat corticostriatal system. *Neurosci Lett*, 97, 271-5.
- Whishaw IQ, Zeeb F, Erickson C & Mcdonald RJ (2007). Neurotoxic lesions of the caudate-putamen on a reaching for food task in the rat: acute sensorimotor neglect and chronic qualitative motor impairment follow lateral lesions and improved success follows medial lesions. *Neuroscience*, 146, 86-97.
- White J, Weinstein SA, De Haro L, Bedry R, Schaper A, Rumack BH & Zilker T (2019). Mushroom poisoning: A proposed new clinical classification. *Toxicol*, 157, 53-65.
- Whitelaw CB, Sheets TP, Lilloco SG & Telugu BP (2016). Engineering large animal models of human disease. *J Pathol*, 238, 247-56.
- Wijeratne PA, Young AL, Oxtoby NP, Marinescu RV, Firth NC, Johnson EB, Mohan A, Sampaio C, Scahill RI, Tabrizi SJ & Alexander DC (2018). An image-based model of brain volume biomarker changes in Huntington's disease. *Ann Clin Transl Neurol*, 5, 570-582.
- Wilson M, Reynolds G, Kauppinen RA, Arvanitis TN & Peet AC (2011). A constrained least-squares approach to the automated quantitation of in vivo (1)H magnetic resonance spectroscopy data. *Magn Reson Med*, 65, 1-12.

- Wu Y & Parent A (2000). Striatal interneurons expressing calretinin, parvalbumin or NADPH-diaphorase: a comparative study in the rat, monkey and human. *Brain Res*, 863, 182-91.
- Yan S, Li S & Li XJ (2019). Use of large animal models to investigate Huntington's diseases. *Cell Regen (Lond)*, 8, 9-11.
- Yan S, Tu Z, Liu Z, Fan N, Yang H, Yang S, Yang W, Zhao Y, Ouyang Z, Lai C, Yang H, Li L, Liu Q, Shi H, Xu G, Zhao H, Wei H, Pei Z, Li S, Lai L & Li XJ (2018). A Huntingtin Knockin Pig Model Recapitulates Features of Selective Neurodegeneration in Huntington's Disease. *Cell*, 173, 989-1002.e13.
- Yang D, Wang CE, Zhao B, Li W, Ouyang Z, Liu Z, Yang H, Fan P, O'Neill A, Gu W, Yi H, Li S, Lai L & Li XJ (2010). Expression of Huntington's disease protein results in apoptotic neurons in the brains of cloned transgenic pigs. *Hum Mol Genet*, 19, 3983-94.
- Yang L, Xu L, Zhou Y, Liu M, Wang L, Kijas JW, Zhang H, Li L & Liu GE (2018). Diversity of copy number variation in a worldwide population of sheep. *Genomics*, 110, 143-148.
- Yang SH, Cheng PH, Banta H, Piotrowska-Nitsche K, Yang JJ, Cheng EC, Snyder B, Larkin K, Liu J, Orkin J, Fang ZH, Smith Y, Bachevalier J, Zola SM, Li SH, Li XJ & Chan AW (2008). Towards a transgenic model of Huntington's disease in a non-human primate. *Nature*, 453, 921-4.
- Yapo C, Nair AG, Clement L, Castro LR, Hellgren Kotaleski J & Vincent P (2017). Detection of phasic dopamine by D1 and D2 striatal medium spiny neurons. *J Physiol*, 595, 7451-7475.
- Yin HH (2016). The basal ganglia in action. *Neuroscientist*, 23, 299-313.
- Yushkevich PA, Piven J, Hazlett HC, Smith RG, Ho S, Gee JC & Gerig G (2006). User-guided 3D active contour segmentation of anatomical structures: significantly improved efficiency and reliability. *Neuroimage*, 31, 1116-28.
- Zala D, Hinckelmann MV & Saudou F (2013). Huntingtin's function in axonal transport is conserved in *Drosophila melanogaster*. *PLoS One*, 8, e60162.
- Zeiss CJ (2017). From Reproducibility to Translation in Neurodegenerative Disease. *Ilar j*, 58, 106-114.
- Zeiss CJ, Allore HG & Beck AP (2017). Established patterns of animal study design undermine translation of disease-modifying therapies for Parkinson's disease. *PLoS One*, 12, e0171790.
- Zeitlin S, Liu JP, Chapman DL, Papaioannou VE & Efstratiadis A (1995). Increased apoptosis and early embryonic lethality in mice nullizygous for the Huntington's disease gene homologue. *Nat Genet*, 11, 155-63.
- Zhang J, Han Y, Zhao Y, Li QR, Jin HF, Du JB & Qin J (2019). Role of endoplasmic reticulum stress-associated gene TRIB3 in rats following kainic acid-induced seizures. *Int J Clin Exp Pathol*, 12, 599-605.
- Zhao X, Chen XQ, Han E, Hu Y, Paik P, Ding Z, Overman J, Lau AL, Shahmoradian SH, Chiu W, Thompson LM, Wu C & Mobley WC (2016). TRiC subunits enhance BDNF axonal transport and rescue striatal atrophy in Huntington's disease. *Proc Natl Acad Sci U S A*, 113, E5655-64.
- Zimmerberg B, Glick SD & Jerussi TP (1974). Neurochemical correlate of a spatial preference in rats. *Science*, 185, 623-5.
- Zuhlke C, Riess O, Bockel B, Lange H & Thies U (1993). Mitotic stability and meiotic variability of the (CAG)<sub>n</sub> repeat in the Huntington disease gene. *Hum Mol Genet*, 2, 2063-7.